

# **CMOS-Chip Based Printing System for Combinatorial Synthesis**

Vom Fachbereich Maschinenbau  
an der Technischen Universität Darmstadt  
zur  
Erlangung des akademischen Grades eines Doktor-Ingenieurs (Dr.-Ing.)  
genehmigte

**Dissertation**

vorgelegt von  
Master of Science Yun-Chien Cheng  
aus Taiwan

Berichterstatter: Prof. Dr.-Ing. Edgar Dörsam  
Mitberichterstatter: Prof. Dr. Katja Schmitz

Datum der Einreichung: 30.04.2012  
Datum der mündlichen Prüfung: 04.07.2012

Darmstadt August 2012  
D17



## **CMOS-Chip Based Printing System for Combinatorial Synthesis**

Peptide arrays, produced through combinatorial synthesis from amino-acid monomers, are an important tool for proteomic research. The arrays enable high throughput screening by exposing a large number of different peptide spots to a solution of target molecules. In particle based synthesis, the monomers are encapsulated into solid particles and deposited on the synthesis spots. The resulting spot density can be much higher than that of liquid based on-spot peptide synthesis.

This dissertation presents the construction of a CMOS-chip based "printing system" that automatically prints monomer particles onto a glass slide for combinatorial synthesis of high-density arrays. The monomer particles ( $\sim 4 \mu\text{m}$ ) are addressed onto the electrode pixels of a CMOS chip, and then printed onto a glass slide by using an electrical field. Afterwards, the particles are melted to release monomers for peptide synthesis.

The printing system should print particles onto the slide with high reproducibility and homogeneity. This is achieved with high precision ( $\mu\text{m}$ ) motors, a slide holder and 3 electrical contact sensors. For ideal printing result, the parameters including particle size, printing voltage, and printing distance are discussed. With printed particles, a peptide synthesis is performed, resulting in an array with 10,000 spots per  $\text{cm}^2$ , which is 100 times more than with conventional method. Additionally, the advantage of the printing system is that the synthesis is not performed on the CMOS chip but on the regular glass slide, which is more chemically robust and suitable for biological applications.

## **CMOS-Chip basiertes Drucksystem für die kombinatorische Synthese**

Peptidarrays sind ein wichtiges Werkzeug für die Proteomikforschung. Sie ermöglichen Hochdurchsatz Screenings, in denen eine große Zahl von Peptiden parallel einer Lösung mit Zielmolekülen ausgesetzt wird. Bei der partikelbasierten Synthese werden die Monomere in festen Partikeln eingebettet und auf den Synthesespots abgelagert. Dies erlaubt eine Erhöhung der Spotdichte verglichen mit flüssigkeitsbasierten Systemen.

Diese Dissertation beschreibt den Bau eines CMOS-Chip basierten "Drucksystems", das automatisch Monomerpartikel für die kombinatorische Synthese von hochdichten Arrays auf einen Objektträger druckt. Die Monomerpartikel ( $\sim 4 \mu\text{m}$ ) werden auf den Pixeln des CMOS-Chips abgelagert und dann mittels eines elektrischen Feldes auf den Objektträger gedruckt. Anschließend werden die Partikel aufgeschmolzen, um die Monomere für die Synthese freizugeben.

Das Drucksystem soll mit guter Wiederholgenauigkeit und Homogenität Partikel auf Objektträger drucken. Dies wird mit hochpräzisen ( $\mu\text{m}$ ) Antrieben, einer Trägerhalterung und 3 elektrischen Kontaktsensoren erreicht. Das optimale Druckergebnis wird anhand von Parametern wie der Partikelgröße, der angelegten elektrischen Spannung und dem Abstand zwischen Chip und Objektträger diskutiert. Mit den gedruckten Partikeln wird eine kombinatorische Synthese durchgeführt und somit ein Array mit 10.000 Spots pro  $\text{cm}^2$  hergestellt, das ist 100-mal mehr als mit herkömmlichen flüssigkeitsbasierten Systemen. Zusätzlich hat das Drucksystem den Vorteil, dass die Synthese nicht direkt auf dem CMOS-Chip durchgeführt wird, sondern auf Glasobjektträgern, die chemikalienbeständiger sind und sich besser für biologische Anwendungen eignen.



# Acknowledgements

I am very grateful to Prof. Dr. Edgar Dösam for the supportive engineering supervision of this work, for all the technical support of the system construction, for teaching me the skills for successful collaboration, and for the discussion and encouragement.

I am equally grateful to PD. Dr. Alexander Nesterov for the supportive physics and biochemistry supervision of this work, for the inspiring discussion, and for all the practical suggestions.

I am indebted to PD. Dr. Frank Breitling for biochemistry supervision, for offering the opportunity to work on this project, for the research funding, and for the great working environment.

I am also very grateful to Prof. Dr. Katja Schmitz for the biochemistry comments and all the very detailed and helpful suggestions in my dissertation.

I am very thankful to PD. Dr. Ralf Bischoff for the biology suggestions and discussion. I am also grateful to Dr. Volker Stadler for the working environment in DKFZ.

Mr. Manfred Jakobi, Michael Desch, Dr. Martin Hass, and Dr. Alfred Neudörfer have my gratitude for providing the great engineering discussion, including drawing specification, controlling the motors, and Labview programming, etc. I am also grateful to Elias Chaloub, who has made excellent 3D UniGraphics drawings for the system.

I thank Felix Löffler for constructing the aerosol generation system, for the physics discussion, and for the Tischkicker tutorial. I also thank Frieder Märkle, Dr. Lothar Hahn, and Sebastian Schillo for the helpful discussions about system calibration and aerosol generation, etc.

I am indebted to Dr. Fanny Liu and Christopher Schirwitz for the chemistry knowledge, Bastian Münster for making the particles, and Jakob Striffler for preparing the slide coating.

My gratitude also goes to all my other colleagues at DKFZ group “Chip-based Peptide Libraries,” Darmstadt University of Technology, and Karlsruhe Institute of Technology.

Thank DAAD and Ministry of Education, Taiwan for the financial support.

Thanks to ManJung. I can not hang on even till the second year without your support. I am also very grateful to my friends and family for their support and encouragement.

Heidelberg, April 2012



# Table of Contents

<b>1. Introduction</b>	<b>1</b>
1.1 Motivation	1
1.2 Objectives	3
1.3 Methodology	3
1.4 Overview of each chapters	3
<b>2. Background</b>	<b>5</b>
2.1 From Peptide Synthesis to Combinatorial Synthesis	5
2.1.1 Application of Peptide	5
2.1.2 Solid Phase Peptide Synthesis	6
2.1.3 Peptide Array and Combinatorial Synthesis	8
2.2 Current Techniques for Peptide Array Synthesis	9
2.2.1 Challenges in Peptide Arrays	9
2.2.1.1 Maximizing the Spot Density and Minimizing the Cost per Spot	9
2.2.1.2 Length of Peptide Chain and Yield Rate	10
2.2.1.3 Time Needed for Amino-acid Deposition	10
2.2.1.4 Enhancing the Detection Sensitivity	10
2.2.2 SPOT Synthesis	11
2.2.3 Photolithographic Synthesis	12
2.2.4 Solid-particle Based Synthesis	13
2.2.4.1 Solid Amino-acid Particles	13
2.2.4.2 Solid-particle Based Synthesis with Laser-printer	14
2.2.4.3 Solid-particle Based Synthesis with CMOS-chip	16
2.3 On-slide Synthesis by Means of CMOS Chip	18
<b>3. CMOS-chip Based Printing System</b>	<b>20</b>
3.1 Requirements and Limitations of the System	20
3.1.1 CMOS Chip for Particle Deposition	20
3.1.2 Aerosol Generation System	22
3.1.3 Requirements of the Printing System	24
3.2 Homogeneity and Reproducibility of Particle Printing	25
3.2.1 Methods for the Homogeneity of Particle Printing	25
3.2.2 Methods for the Reproducibility of Particle Printing	28
3.2.3 Design for Homogeneous and Reproducible Printing	30
3.2.3.1 Design of the Devices	30
3.2.3.2 Contact Sensor	34
3.3 Construction of the Chip-printing System	36

3.3.1	Frame Design . . . . .	37
3.3.2	Particle Confining and Recycling System . . . . .	39
3.3.2.1	Fume Hood . . . . .	40
3.3.2.2	Particle Suction and Recycling System . . . . .	41
3.3.2.3	Chip Cleaner . . . . .	42
3.3.3	High Voltage for Particle Transfer and Aerosol System . . . . .	43
3.3.4	Control Software . . . . .	44
3.3.5	Quality Control of Particle Deposition . . . . .	47
3.4	Discussion . . . . .	49
3.4.1	System Automation . . . . .	49
3.4.2	Theoretical Reproducibility and Homogeneity of Printing . . . . .	50
3.4.3	Geometry Design and Particle Recycling . . . . .	50
3.4.4	Time Needed for Printing onto Glass Slide . . . . .	51
<b>4.</b>	<b>CMOS-chip Based Particle Printing . . . . .</b>	<b>52</b>
4.1	Particle Composition and Manufacture . . . . .	52
4.2	Particle Characteristics for Deposition . . . . .	54
4.2.1	Particle Size . . . . .	54
4.2.2	Humidity Influence on Particles . . . . .	58
4.3	Particle Printing from CMOS Chip onto Glass Slide . . . . .	60
4.3.1	Reproducibility of Printing . . . . .	60
4.3.2	Homogeneity of Printing . . . . .	64
4.3.3	Voltage and Space between Chip and Slide . . . . .	65
4.3.4	Cross Contamination of Printing Result . . . . .	67
4.4	Discussion . . . . .	68
<b>5</b>	<b>Combinatorial Synthesis with Chip-printing System . . . . .</b>	<b>70</b>
5.1	Synthesis with Amino Acids and Biotin . . . . .	70
5.2	Chemical Synthesis and Staining . . . . .	71
5.2.1	Materials . . . . .	72
5.2.2	Printing and Melting of Biotin, Alanine, and Glycine Particles . . . . .	72
5.2.3	Protocols of Synthesis and Staining . . . . .	74
5.2.3.1	Coupling the Monomers . . . . .	75
5.2.3.2	Capping the Free Amino groups and Washing the Residue . . . . .	75
5.2.3.3	Fmoc Deprotection . . . . .	76
5.2.3.4	HA Coupling . . . . .	77
5.2.3.5	Side-chain Deprotection . . . . .	78
5.2.3.6	Blocking the Surface with BSA . . . . .	79
5.2.3.7	Staining with Anti-HA Antibody and Streptavidin . . . . .	79
5.3	Coating on Slide . . . . .	80



5.4	Discussion . . . . .	85
<b>6</b>	<b>Conclusion . . . . .</b>	<b>86</b>
6.1	Discussion of Results . . . . .	86
6.1.1	System Construction . . . . .	86
6.1.2	Quality of Particle Deposition . . . . .	86
6.1.3	Combinatorial Synthesis Result . . . . .	87
6.2	Application . . . . .	87
6.3	Next Generation of the Chip-printing System . . . . .	88
	<b>References . . . . .</b>	<b>90</b>
	<b>Appendices . . . . .</b>	<b>93</b>
A1.	Amino Acids . . . . .	95
A2.	LabVIEW Program . . . . .	97
A3.	3D UniGraphics Drawing of the System . . . . .	103
A4.	Motor Control Interface . . . . .	107
A5.	Production of Particles . . . . .	108
A6.	Synthesis and Staining Steps of Biotin and Amino-acids . . . . .	109

## Abbreviations

AEG <sub>3</sub>	Amino(ethyleneglycol) <sub>3</sub>
APTES	(3-aminopropyl)triethoxysilane
β-Ala	β-Alanine
CMOS	Complementary metal-oxide-semiconductor
DCM	Dichloromethane
DIPEA	N,N-Diisopropylethylamine
DMF	N,N-Dimethylformamid
DPF	Diphenyl formamide
DPSO	Diphenyl sulfoxide
ESA	Acetic anhydride
EtOH	Ethanol
Fmoc	Fluorenylmethyloxycarbonyl chloride
HOBT	N-Hydroxybenzotriazole
HBTU	O-Benzotriazole-N,N,N',N'-tetramethyl-uronium-hexafluoro-phosphate
OPfp	Ortho-pentafluorophenyl
OPC	Organic photoconducting
PCB	Printed circuit board
PMMA	Poly(methyl methacrylate)
PEGMA	Poly(ethyleneglycol)methylmethacrylat
PTES	Propyltriethoxysilan
SCP	Side chain protection
TBS-T	Tris-buffered saline with Tween 20
TFA	Trifluoroacetic acid
TIBS	Triisobutylsilane

Amino acids	Three letter code	One letter code
Alanine	Ala	A
Arginine	Arg	R
Asparagine	Asn	N
Aspartic acid	Asp	D
Cysteine	Cys	C
Glutamic acid	Glu	E
Glutamine	Gln	Q
Glycine	Gly	G
Histidine	His	H
Isoleucine	Ile	I
Leucine	Leu	L
Lysine	Lys	K
Methionine	Met	M
Phenylalanine	Phe	F
Proline	Pro	P
Serine	Ser	S
Threonine	Thr	T
Tryptophan	Trp	W
Tyrosine	Tyr	Y
Valine	Val	V

Table 1: Three and one letter code of proteinogenic amino acids.



# 1. Introduction

## 1.1 Motivation

The proteomic research is important for understanding the biochemistry function in human body. In proteomic research, peptide arrays enable the screening of hundreds to thousands of proteins at the same time [EIC05, FRA02-1, LIU03], since the peptide arrays have 96 – 16,000 different peptide spots on a single substrate [BRE08, BEI08]. When the arrays are exposed to the fluorescently labeled protein, only the specific peptides can bind to the protein. Therefore, the specific peptide can be pinned out by fluorescence scanning. Because the peptide spots are exposed to proteins at the same time, the reagents consumption can be few. The peptide arrays can be applied to:

- characterize antibodies in medical diagnosis or immunological research [REI02],
- analyze the peptide interaction with other proteins, DNA or metal ions [UTT08],
- design sequences for new peptides which can mimic the function of catalytic proteins [ALB08, KNO99, EIC04].

In solid phase synthesis, the linear heteropolymers (such as DNA or peptides) are synthesized by adding monomers onto the sequences one by one. Amino acid monomers or nucleotide monomers are added on to the substrate for peptide or DNA synthesis, respectively. During synthesis, side chain protecting groups are used to ensure that there will not be additional monomers coupled to the sequences [MER64-1, MER64-2].

Once the array is synthesized, it can be experimentally used by exposing the array with target molecules in solution. The specific sequences will then bind to the target molecules. This binding event can be detected by labeling the target molecules with fluorescent dye.

High density microarrays based on combinatorial synthesis are widely used in biological and medical field, since microarrays can be used to analyze thousands of different peptides or nucleotides at the same time. The spot density of the microarray is a very important parameter for the related applications. Because the time and reagents used for one slide is similar, so a higher spot density means lower cost per peptide spot. Hence, enhancing the spot density of the microarray is a key point in microarray research [BRE08].

Conventionally, the monomer droplets are deposited onto the substrate by pipette array [FRA02-2]. Two problems limit the spot density of the pipette deposition. One is the droplet spread on the substrate surface. The other is that the solvent in the solution evaporate, so the monomer concentration from beginning to the end of deposition will be different.

To increase the spot density, an innovative method for combinatorial synthesis was developed with photolithography. The surface is protected by photolabile material, so the monomers can only couple to the spots which are exposed to the light. This method can achieve very high spot density (10,000 spots / cm<sup>2</sup>) since the density is limited by the resolution of light mask [FOD91]. However, the problem of this method is that only one kind of monomer can couple to the surface in one coupling cycle. That is, the peptide array, which has 20 standard amino acids, needs 20 coupling cycles for a monolayer, so synthesizing peptide array with photolithographic method is time consuming.

The particle based synthesis method is faster than the photolithographic method. The particle based combinatorial synthesis replaces the liquid droplet with solid particles. The particles containing the monomers can be printed onto the glass substrate with laser printer and then melted at once for coupling. That is, one monolayer synthesis needs only one coupling cycle, so the time needed is about 20 times less than the photolithographic method [BEY07, STA08-1].

The laser printer based particle deposition method adopts the organic photoconducting drum technique and successfully prints particles for combinatorial synthesis [STA08-1]. The method reduces the time needed by melting the particles for monolayer synthesis at the same time.

The CMOS-chip based particle deposition has higher spot density than the laser printer method (10,000 spots / cm<sup>2</sup> vs. 400 spots / cm<sup>2</sup>.) The CMOS-chip method addresses the particles onto the pixels on chip by electrical fields. Then the particles are melted to release the monomers and the solid phase synthesis is carried out on the chip surface at the same time [BEY07].

The CMOS-chip method enables higher spot density than laser printer and is 20 times faster than photolithographic method. However, this method suffers from the fragility of the CMOS chip. The chip can be easily damaged during the chemical process. Hence, the

particles should be transferred from chip onto glass slide, which is well adapted for chemical process, and melted for combinatorial synthesis on the slide.

The aim of my work is to develop a system to print the particles from the CMOS chip onto the glass slide for array synthesis. This dissertation describes the development of this printing-from-chip-onto-slide technique. The system is built in a collaboration between the German Cancer Research Center (DKFZ) and Darmstadt University of Technology (TUD).

## **1.2 Objectives**

This dissertation focuses on how to print the particles from the CMOS chip onto the glass slide, so that the combinatorial synthesis can be done on the slide surface instead of the CMOS chip. A system was constructed for high-precision particle printing and to automate the particle deposition and printing process. Since the CMOS chip and the method of particle deposition on chip were already developed, a main challenge of the construction was integrating the chip and deposition method into the system. Another challenge was how to print the particles onto slide with high reproducibility and homogeneity.

## **1.3 Methodology**

The demands of the CMOS-chip based printing system were first described and considered in the first phase of this work. The demands included the printing homogeneity, printing reproducibility and geometry design. Then the solutions for these demands were listed and discussed to find the optimal solution combination. Afterwards, the system was constructed based on the chosen solutions.

The constructed system was tested with commercial toner particles. For ideal printing results, the system was calibrated and several parameters, including the particle size, printing voltage and printing distance, were discussed.

At last, the system was used to print amino-acid and biotin particles on the slide, and combinatorial synthesis was conducted with the particles.

## **1.4 Overview of Each Chapter**

In Chapter 2, this dissertation describes the concept of peptide arrays, combinatorial synthesis, different methods for peptide array synthesis, and the advantage of CMOS-chip based printing method.

In chapter 3, the design concepts, solutions, and construction of the CMOS-chip based printing system are described.

The particle printing issues, including particle characteristics, deposition quality, and printing quality are discussed in chapter 4.

Based on this printing system, the combinatorial synthesis and staining results are described in the course of chapter 5.

Chapter 6 discusses and concludes the results and achievements of this PhD work.

The References and Appendixes, including the amino-acid structures, the LabVIEW programs, the 3D drawing of the system components, and the protocols for synthesis, are listed at last.



## 2. Background

Solid phase synthesis can synthesize large amounts of molecules which have similar structure. These molecules can be applied in several aspects: peptide arrays can be used to analyze proteins from living organisms; surfaces can be functionalized. The solid phase peptide synthesis is used to synthesize large amount of structural related molecules. In this chapter, current combinatorial synthesis techniques for peptides are introduced and compared.

### 2.1 From Peptide Synthesis to Combinatorial Synthesis

#### 2.1.1 Application of Peptides

Proteins are also called polypeptide and peptides are sequences consisting of amino acids. In living organisms, most biochemical functions relate to proteins. For example, the reactions catalyzed by enzyme, binding partners of the inter-/intra- cellular communication, and the receptors of antibodies are all protein, and peptides can be used to investigate these processes in proteomics research.

Many biological and medical researchers try to identify the protein-protein, protein-peptide, protein-DNA, protein-RNA, or protein-metal interactions. The interacting regions (epitopes) can be presented by short peptide chains (starting from 8 amino acids) [ALB08, KNO99]. On the other hand, some binding sites on protein can be mimicked by peptide sequences (mimotopes) [EIC04]. These proteomic studies are usually performed by synthetic peptides [UTT08].

In addition, the complex protein network in human body can be activated or inhibited by protein to maintain a balanced environment in varying circumstances. Short peptides can also stimulate the protein as well [EIC05, BIA03]. These interactions are in the main focus of pharmaceutical research.

Furthermore, peptides can be used as artificial recognition sequences of specific receptors and, hence, to develop new peptide-based drugs [VLI10]. These specific receptors can also be used to detect the target molecules in serum or other solutions [REI02].

### 2.1.2 Solid Phase Peptide Synthesis

Conventionally, scientists can get proteins and also peptides by artificial cloning method. The genetically modified cells are incubated, broken up, and then recombinant isolated. However, the artificial cloning method is laborious and resource consuming, because for each peptide a clone should be generated and purified. Therefore, chemical synthesis is more preferable in several applications. This method uses essential cell extracts and synthesizes peptide from mRNA or DNA. It can even synthesize complete protein. The problem of both methods is that scientists cannot design any sequences with non-standard amino acids and other monomers at will, while such sequences can be very useful. In living organisms, peptide with non-standard amino acids has longer half-life than peptides with standard amino acids, which can be quickly degenerated by peptidases [OTV08, NES09]. Some peptides with non-amino-acid monomers can even be used as electron transferring material in solar cells [EGB].

The main method for chemically synthesizing peptides in lab is called solid phase peptide synthesis (SPPS) or Merrifield synthesis technique [MER 63, MER 64-1, MER 64-2]. This method can synthesize peptide with amino acids from C- to N-terminal, and enables researchers to synthesize peptides with non-standard amino acids.

The basic process of Fmoc peptide synthesis is shown in Figure 2.1[ATH89]. This technique is based on small, insoluble, porous resin beads. The resin beads are functionalized so they can form covalent bonds with the COOH-terminals (carboxyl groups) of amino acids. . The COOH-terminals are activated by reagents before so they can couple to the linker groups on the resin. After the amino acids couple to the beads, the synthesis residues, such as excess amino acids and reagents, are washed away. The amino acids are immobilized on the resin beads, so they will not be washed away together with the synthesis residues during the filtration process. Then the protecting groups (Fmoc or Boc) are removed from the coupled amino acids, so the NH<sub>2</sub>-terminals (amino groups) of amino acids are released for next coupling reaction with activated amino acids. Again, the residues are washed away but the peptides are still immobilized on the resin beads. This “coupling-washing-deprotecting-washing” cycle is repeated to couple amino acids till the whole peptides are synthesized. Then, the peptides are cleaved from the resin beads with anhydrous hydrogen fluoride or trifluoroacetic acid (TFA).

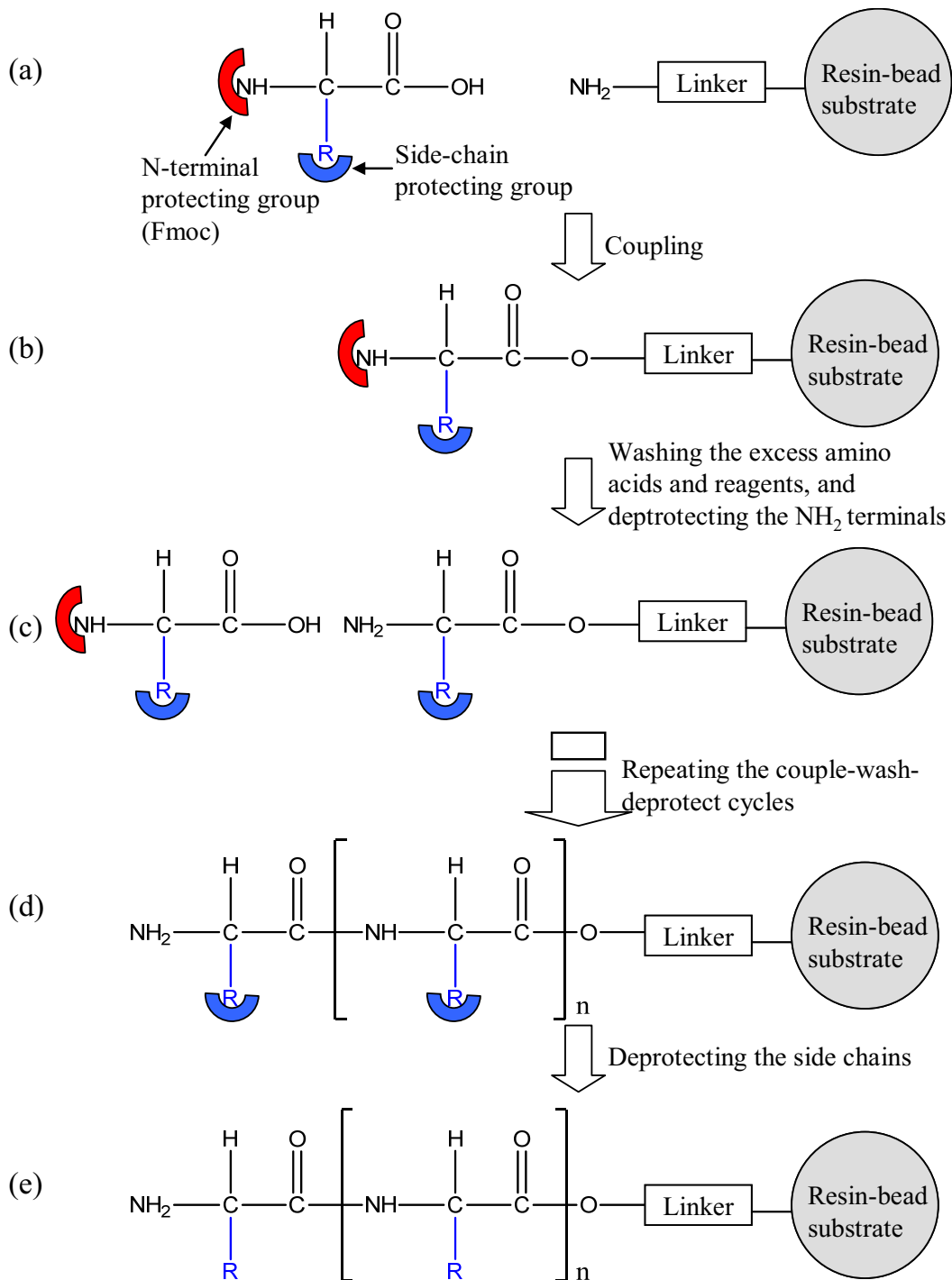


Figure 2.1: Fmoc peptide synthesis. (a): The resin beads are functionalized with linker, so the beads can react with COOH-terminal. (b): The  $\text{NH}_2$ -terminal couples to the carboxyl group of the amino acid. (c): After coupling, the unused chemicals are washed away, and then the Fmoc protecting group is removed. The next amino acid couples to the  $\text{NH}_2$  group of the previous amino acid. (d): The couple-wash-deprotect-wash cycle repeats till the whole amino-acid sequence is synthesized. (e): The side-chain protecting groups are removed from the synthesized sequence [ATH89].

The advantage of this SPPS method is that the growing peptides can be washed to remove the synthesis residue after each coupling reaction. It is because the growing peptides are immobilized on the resin beads. A high excess of each building block can be used so that the yield in each step can be very high. The yield is extremely important for peptide synthesis. For example, if the yield is 99% in one coupling step, the final yield of a 26-mer peptide will be  $(99\%)^{26} = 77\%$  or even lower. If the yield is 95% in one coupling step, the final yield of a 26-mer peptide will be only  $(95\%)^{26} = 25\%$ . Therefore, the high yield of SPPS is an important advantage of peptide synthesis.

### **2.1.3 Peptide Array and Combinatorial Synthesis**

The SPPS method enables the scientists to synthesize a large amount of same peptides. However, there are huge amount of different peptides. For example, a 10-mer peptide can have at least  $20^{10}$  combinations of amino-acid sequence. If the other monomers, such as unnatural amino acids, are considered, the combinations will be even more. In addition, the analysis of one peptide at one time is time and resource consuming. Therefore, the peptide array technique has been invented to analyze many different peptides at the same time [EIC05, FRA02-1, LIU03].

The peptide array has different peptide spots on substrates such as glass slide or petridish, and the spots are immobilized on the functionalized surfaces. The fluorescently labeled probes (target molecules) will hybridize with the array and only specific peptides will be stained with the probes. The scanning results of the fluorescently labeled spots will then be analyzed.

Based on the peptide array synthesis technique, the solid phase synthesis uses some other monomers, in addition to standard amino acids, as long as the monomers have carboxyl group (COOH-terminal) and amino group (NH<sub>2</sub>-terminal) for the coupling reaction. Hence, the sequences can not only be used as peptides but also have other possible applications like light harvesting intermediate (i.e. solar cell) [EGB].

## **2.2 Current Technique for Peptide Array Synthesis**

As described in section 2.1, the peptides play an important role in proteomic and human biochemistry research. Some peptide researches, such as peptide-sequence design, should test hundreds to millions different peptides. Therefore, a technique for analyzing large

amount of peptides at the same time is necessary. One of the techniques is coupling different peptides onto one substrate, and it is called peptide array. The peptide array can be used to analyze 96-768 peptides at one time [INT], so it is more time and resource saving than one-by-one peptide analysis [EIC05, FRA02-1, LIU03]. However, 768 spots on one slide are still not enough for current needs. A 10-mer has  $20^{10}$  possible combinations, which is far more than the current spot number on one slide. In addition, the yield of the peptides on spot should also be improved for the spot-detection accuracy. To solve these challenges, especially the cost, many techniques were invented for peptide synthesis. These challenges and solutions are described and discussed in this section.

## 2.2.1 Challenges in Peptide Arrays

### 2.2.1.1 Maximizing the Spot Density and Minimizing the Cost per Spot

As mentioned before, some peptide researches should test large amount of different peptides. A 10-mer peptide, which is synthesized with 20 kinds of natural amino acids, has about  $10^{13}$  possible combinations. The conventional peptide arrays have 96-768 spots per slide, so the cost per peptide spot becomes a bottleneck for peptide research. Since the expensive chemicals and amino-acid monomers needed are the same for same area, increasing the spot density can decrease the cost of each peptide spot.

For conventional SPOT synthesis technique, the amino acids are deposited onto the substrate in droplets [FRA02] and the spot density is limited by the liquid characteristics, like evaporation and spreading. The details of SPOT synthesis are described in section 2.2.2 and the new techniques invented to enhance the spot density are described in the following sections.

### 2.2.1.2 Length of Peptide Chain and Yield

While the peptides produced by artificial cell cloning have thousands of amino acids, the length of synthesized peptide is limited by the coupling efficiency. The yield of peptide is defined as the number of desired peptides divided by the number of total peptides synthesized in one spot. Equation 2.1 shows the relationship between coupling efficiency ( $E$ ) of amino acid and yield ( $Y$ ) of resulting peptides.  $Y$  is the product of  $E_i$  of each step  $i$ .

$$Y = \prod_i E_i \quad (\text{Eq. 2.1})$$

For example, if the coupling efficiency is 95%, the yield for a 26-mer peptide is only  $(95\%)^{26} = 25\%$ . If the coupling efficiency is 99%, yield for a 26-mer peptide can be  $(99\%)^{26} = 77\%$ . The yield and peptide length become a tradeoff because of the non-perfect coupling efficiency. Therefore, enhancing the coupling efficiency is also a critical issue for enhancing the length of peptide sequence.

### *2.2.1.3 Time Needed for Amino-acid Deposition*

Depositing the amino acids onto the assigned spots quickly is also important. If the activated amino acids can not couple to the desired  $\text{NH}_2$ -terminals in few minutes, they will couple the other compounds in solution and become useless.

Besides, if the droplet deposition process takes too long, the solvent evaporates. Eventually, the concentration of amino-acid droplets will be different throughout the whole substrate surface [FRA 92, FRA 02].

### *2.2.1.4 Enhancing the Detection Sensitivity*

The quality of peptide spots and the substrate background influences the spot detection and analysis. Some issues can be considered for the spots and substrate. First, the number of correct peptides on one spot should be maximized, so that the scanner can even detect the signals from low binding ratios. Second, the peptide amount per spot should be homogeneous all over the slide, or the binding efficiency between different peptides can not be compared. Third, the substrate surface should be blocked to prevent non-specific binding, so the background will not have misleading background signals.

## **2.2.2 SPOT Synthesis**

SPOT synthesis is the most commonly used technique for peptide-array synthesis. In SPOT synthesis, the droplets of amino-acid solution are dispensed onto the planar surface of a porous membrane (Figure 2.2). When the amino acids have been deposited on to the substrate, the coupling reaction is carried out for monolayer synthesis [FRA 92, FRA 02]. To ensure most activated terminals can be coupled with amino acids, excessive amount of amino acids are added for reaction in the hemispherical droplet on the substrate. The SPOT synthesis has several advantages: (1) reliable and easy experimental procedure with automation system, (2) inexpensive equipment needs and (3) flexible array.

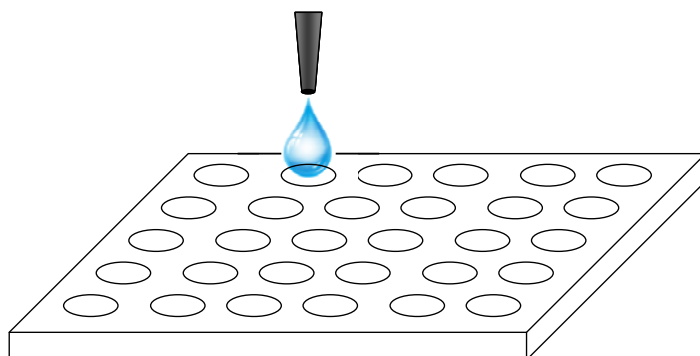


Figure 2.2: The SPOT technique for depositing amino-acid onto substrate. The pipette or jet is used to drop amino-acid solution on to different spots on the surface for synthesis.

The disadvantage of SPOT technique is low spot density. The spot density is limited because the liquid droplets spread on the substrate surface. When two droplets are too close to each other, they will merge and mix with each other. Thus, the distance between spots should be sufficient, and the maximum spot density of SPOT technique cannot be higher than 25 spots / cm<sup>2</sup>. The liquid spreading relates to the dispensed volume, absorptive capacity of the surface and the surface tension property between surface and liquid.

The evaporation of amino-acid solvent is another problem. The solvent evaporates during the whole deposition process, so the solution concentration of former droplets is higher than the later droplets. The evaporation problem becomes more critical for small volume droplet, which is necessary for high spot density. Hence, the spot density and homogeneity of droplet deposition becomes another trade-off owing to the droplet volume.

### 2.2.3 Photolithographic Synthesis

A breakthrough on the spot density of combinatorial synthesis was made by photolithographic method, and density of 10<sup>4</sup> spots / cm<sup>2</sup> is reported [FOD91]. The concept of the photolithographic synthesis is described in Figure 2.3. The NH<sub>2</sub>-terminals are protected by photolabile protecting group, so the NH<sub>2</sub>-terminals can be activated by the light, which is already patterned by lithographic mask. Then, the activated area will couple with amino acids protected by photolabile groups. Following that, another area will be activated by light and couple to next amino acids. The light activation-coupling cycles continue till all the monomers are coupled.

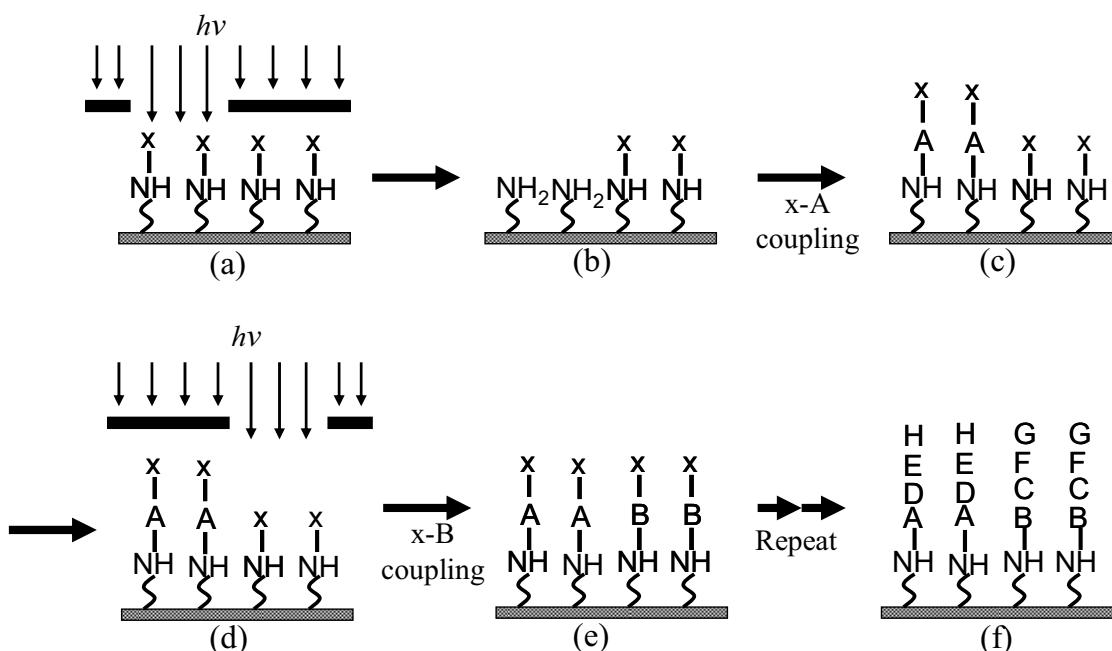


Figure 2.3 (a): The NH<sub>2</sub>-terminal on substrate is protected with a photolabile protecting group x. The photodeprotection is caused by light, which shines through the transparent patterns of a lithographic mask. (b): The NH<sub>2</sub>-terminals on the exposed sector are deprotected for coupling. (c): The amino acid A with photolabile protecting group x couples with the deprotected NH<sub>2</sub>-terminal. (d): Another sector is exposed to the light with another mask for photodeprotection. (e): Amino acid B with protecting group x couples with the deprotected NH<sub>2</sub>-terminal. (f): Additional photodeprotection and coupling are executed to complete the whole synthesis. [FOD91]

The array pattern of photolithographic method can reach 100-nm scale, so the synthesized peptide spot can be much smaller than the spot of SPOT technique. A spot density of  $10^4$  spots / cm<sup>2</sup> was reported by Fodor.

However photolithographic method needs excessive coupling cycles for peptide array synthesis. For one monomer synthesis, this method needs one coupling cycle, so 20 coupling cycles are needed for one monolayer synthesis. That is, an array with 20-mer peptides needs 20 (mer) × 20 (amino acids) = 400 (coupling cycles). Such large number of coupling cycles results in many side reaction and long synthesis time. In addition, 400 expensive lithographic masks are necessary to allow for combinatorial synthesis. Because of the excessive-coupling disadvantage, this photolithographic method is mainly used in synthesis with nucleotides, which have only 4 building blocks [BRE11].



## 2.2.4 Solid-particle Based Synthesis

To solve the problem of excessive coupling cycles from photolithographic method and density limitation of SPOT method, solid-particle synthesis was developed. In solid-particle method, the amino acids can be released at the same time for monolayer synthesis, so the coupling cycles can be 20 times less than the photolithographic method. The spot density of solid-particle method can also be  $10^4$  spots /  $\text{cm}^2$  [BEY07].

### 2.2.4.1 Solid Amino-acid Particles

In solid amino-acid particle method, the amino acids are encapsulated into solid particles and then deposited onto substrate for synthesis. The resulting spot density (400 to 10,000 spots /  $\text{cm}^2$ ) can be much higher than that of SPOT synthesis (25 spots /  $\text{cm}^2$ ) and the coupling cycles can be 20 times less than photolithographic synthesis.

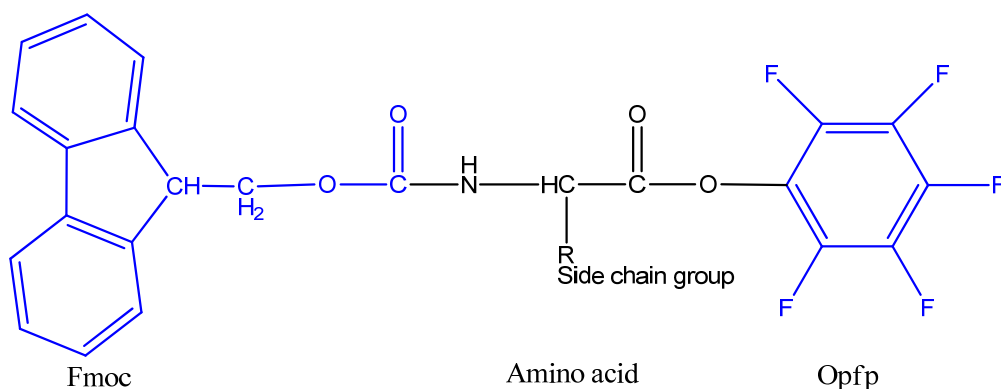


Figure 2.4: Fmoc-amino acid-Opfp, the  $\text{NH}_2$ -terminal is protected by Fmoc group and the carboxyl group is activated by Opfp group [BEY07].

As shown in Figure 2.4, the amino acids are protected in Fmoc (9-fluorenylmethoxycarbonyl) and OPfp (pentafluorophenyl) ester compound, like SPPS synthesis. Then this Fmoc-amino acid-OPfp compound (10% w/w), resin (60% w/w) and other constituent parts are dissolved in acetone. Afterwards, the whole solution is dried and the dried matrices are milled into particles with winnower (100 MZR, Hosokawa Alpine AG) and air mill (Hosokawa alpine 50AS). These solid particles with amino acids will then be deposited onto substrate for peptide synthesis [BEY07][STA08-1].

When all the 20 kinds of amino-acid particles are deposited onto the substrate, the particles are melted to release the amino acids for coupling (Figure 2.5). The melting point of particles is designed to be between  $69\text{ }^\circ\text{C}$  to  $73\text{ }^\circ\text{C}$  so that the particles will not melt at room temperature and the amino acid will not be destroyed during melting.

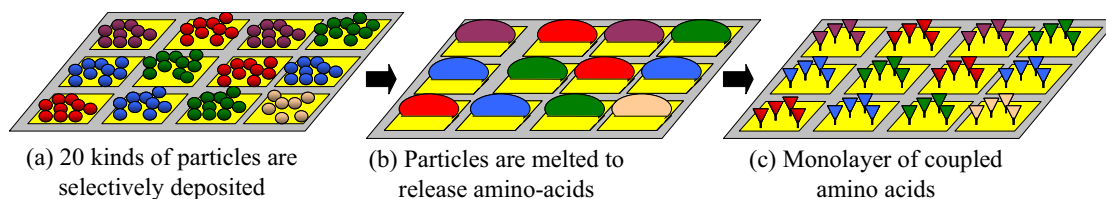


Figure 2.5 (a): The amino-acid particles are deposited onto substrate and then (b): melted to release amino acids for coupling. (c): The unused residues will be washed away.

Comparing with SPOT synthesis, the solid amino-acid particle technique is superior in spot density and physical characteristics. For the spot density, the minimum size of liquid droplet is about 5 pL [STA08-1], while the size of solid particle can be 0.1 pL. That is, the size of solid particle is about 500 times smaller than liquid droplet. In addition, the melted particles will shrink on the surface while the droplets spread. Hence, with proper deposition technique, the spot size of solid-particle method can be significantly smaller than that of SPOT method. For the physical characteristics, the droplet used by SPOT synthesis will evaporate and result in inhomogeneous amino-acid deposition throughout the surface. Because of evaporation, the amino-acid solution will become sticky and block the jet.

Comparing with photolithographic synthesis, the cycles needed for solid-particle method are 20 times less than photolithographic method. 20 kinds of amino-acid particles can be melted to synthesize a monolayer at the same time, while photolithographic method need one cycle for each monomer coupling. Therefore, solid-particle method needs much less time and has less side reactions than lithographic method.

Unlike SPOT method, solid amino-acid particles cannot be deposited with pipette or jet, so new methods are developed to address the particles onto the substrate. These new methods include laser printing method and electrode pixels on CMOS chip.

#### 2.2.4.2 Solid-particle Based Synthesis with Laser-printer

The solid amino-acid particles can be deposited onto glass slide by laser printing technique, which is used to print toner particles onto paper [STA08-1]. The spot density of laser printer (400 spots / cm<sup>2</sup>) is 16 times higher than conventional SPOT technique (25 spots / cm<sup>2</sup>).

Figure 2.6 shows the basic concept of laser printing. The printer design was based on the OKI C7400 commercial printer [OKI]. The surface of the organic photoconducting (OPC)

drum is uniformly charged by the corona. Then, selected charged areas are illuminated and neutralized by light, so the triboelectrically charged particles can deposit on the neutralized area. The charged particles are transferred onto the glass substrate with strong electrical field (4 kV/mm), and will be melted to release amino acids for coupling.

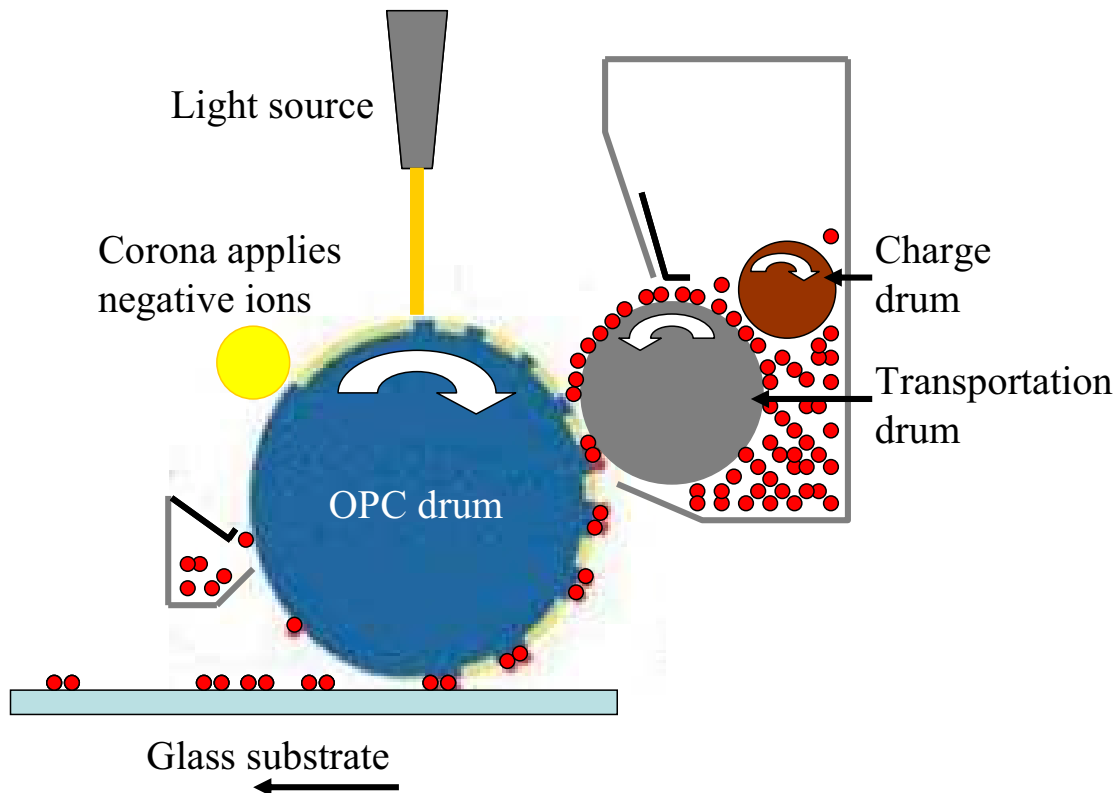


Figure 2.6: Particle deposition by laser printing techniques. The corona connects to a high voltage power source and applies negative ions onto the rotating OPC drum. The charged drum is selectively neutralized by light. The neutralized area takes the triboelectrically charged particles and prints them onto glass substrate with 4 kV/mm electrical field. [STA08-1]

Figure 2.7(a) shows laser printer with 20 different amino-acid units for the amino-acid particle printing. The 20 different types of particles are deposited onto glass slides in the long box. The printing process is controlled by computer. The glass substrate with printed amino-acid particles is shown in Figure 2.7(b).

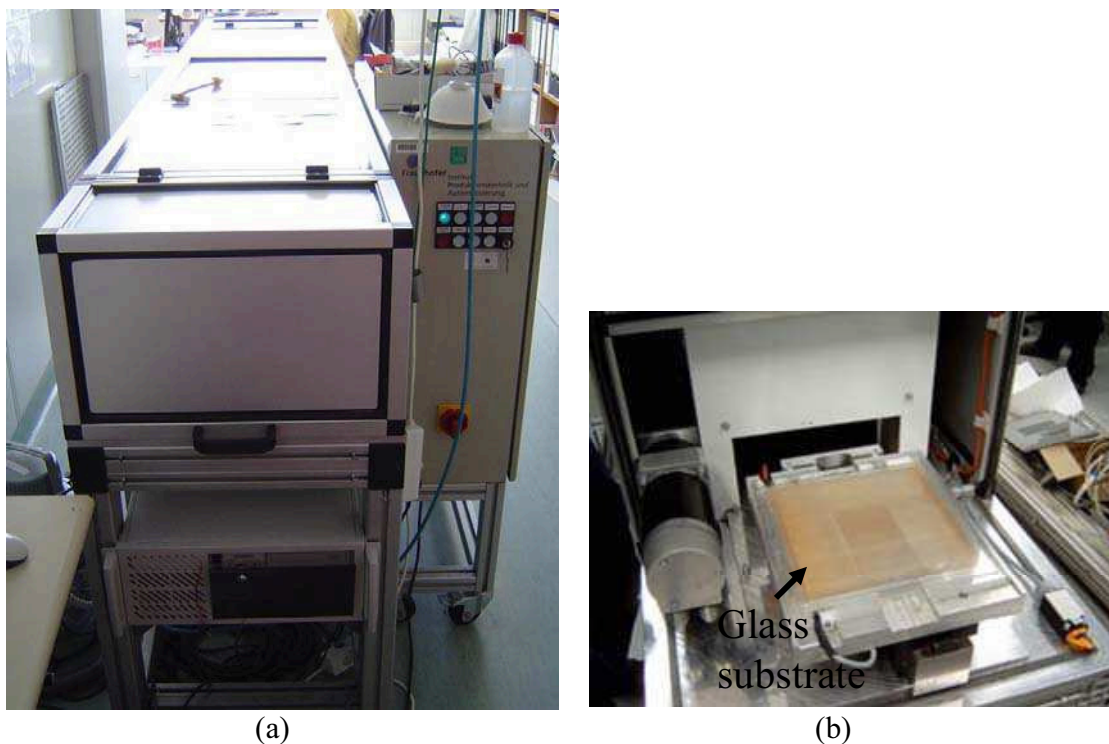


Figure 2.7 (a): The laser printer for printing 20 kinds of amino-acid particles onto glass substrate. It has 20 cartridges for 20 amino-acid toner particles, so it is much longer than the normal PC printer, which has only 4 toner cartridges. (b): The  $20 \times 20$  cm glass substrate with printed amino-acid particles. [PEPPE]

The corona in the laser printer rotates about 10,000 steps in 20 cm, which is the size of the glass substrate. This resolution is about  $10^8$  pixels in the  $20 \times 20$  cm<sup>2</sup> area (i.e.  $2.5 \times 10^5$  pixels / cm<sup>2</sup>). However, the pixel resolution does not represent spot density. The spot density based on laser printer technique is 400 spots / cm<sup>2</sup>. It is limited by the laser printer and its software, which is designed for human-eye resolution. The printer has 20 drums for 20 amino acids. During printing, the glass substrate is moved beneath the drums one by one and be loaded with different amino-acid particles. Therefore, aligning the printing of the 20 drums onto the glass substrate is difficult. In addition, the particles can not be fully loaded on each pixel, so some positions do not have enough particles on the pixels [STA08-1].

#### 2.2.4.3 Solid-particle Based Synthesis with CMOS-chip

Beside the laser printing method, CMOS chip is another method developed to address solid amino-acid particles onto the substrate [BEY07]. The spot density of CMOS-chip method is  $10^4$  spots / cm<sup>2</sup>, which is 25 times higher than the density of laser-printer

method. The CMOS chips developed for particle deposition have  $10^4 - 4 \times 10^4$  electrode pixels per  $\text{cm}^2$  and each pixel is programmable to be switched on or off. When a pixel is switched on, it has 100 Volt on its surface. The electrical field from pixels will address the negatively charged amino-acid particles onto the switched-on pixels [NES08] (Figure 2.8). Then the pixels are switched off and some other pixels are switched on to address another kind of amino-acid particles. After all the particles for a monolayer are addressed onto different pixels, the particles are melted to couple amino acids onto the substrate.

The negative charges of particles come from triboelectrical friction. Compressed air is injected into the particle reservoir and produces turbulent aerosol. The particles in aerosol turbulence rub against the walls of reservoir and tube, and charged the electrons from the plastic walls. The charge to mass ratio ( $q/m$  value) of the triboelectrically charged particles is about  $-4 \mu\text{C/g}$  [NES07-1, NES10-1].

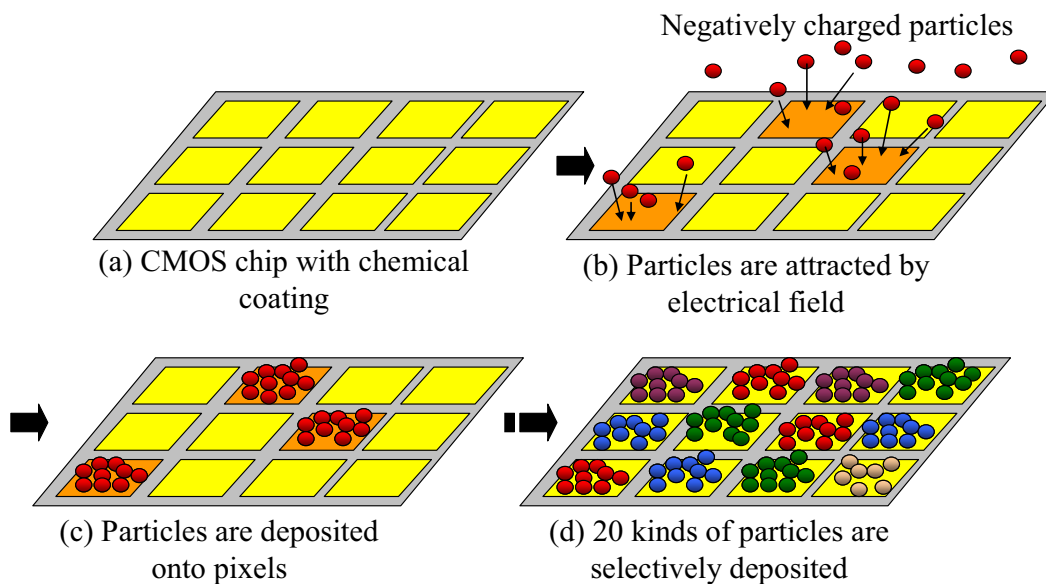


Figure 2.8 (a): The chemical coating on CMOS chip has  $\text{NH}_2$  groups for amino-acid coupling. (b): The 100 Volts on switched-on pixels induce electrical field to attract the triboelectrically charged amino-acid particles. (c): Particles deposit only on the switched on pixels. (d): Particle-deposited pixels are turned off. Some other pixels are switched on to attract another kind of amino-acid particles till 20 kinds of particles are deposited in desired pattern [BEY07].

The spot density of CMOS chip ( $10^4$  spots /  $\text{cm}^2$ ) is 25 times higher than the spot density of the laser printer ( $400$  spots /  $\text{cm}^2$ ), and it can be even higher [KÖN10]. However, there are still challenges for the CMOS chip methods: (1) The pixel area of the CMOS chip is only  $1.28 \times 1.28 \text{ cm}^2$ , so it can only produce only  $\sim 1.6 \times 10^4$  spots per chip. (2) The

CMOS chips are expensive (~ 400 Euro / piece). (3) The chip can be easily damaged by the chemicals in synthesis process or high voltage in printing process, even though the chip surface has protective coating. (4) The chip surface is uneven. Owing to the electronic circuits on the chip surface, the pixels and grids on the chip surface have different height. An uneven surface disadvantages the homogeneity of the synthesized array. These disadvantages can be solved if the combinatorial synthesis is conducted not on CMOS chip but on glass substrate, which is cheaper, more chemical robust, and more even than the CMOS chip.

In short, the advantages of CMOS-chip based solid-particle synthesis can be taken, and the chemical disadvantages of CMOS chip can be solved by transferring patterned particles from chip onto glass. This dissertation reports the realization of this concept and discusses the results.

## **2.3 On-slide Synthesis by Means of CMOS Chip**

As mentioned in section 2.2, the solid-particle based synthesis has higher spot density than the spot density of conventional SPOT synthesis, because the solid particles are smaller and more stable than droplets. The solid-particle based synthesis is also better than the photolithographic synthesis in terms of the number of coupling cycles. Furthermore, comparing the two solid-particle addressing methods, the CMOS-chip method has higher spot density than laser-printer methods, but has some chemical disadvantages. We can keep the advantages of CMOS-chip method and solve the chemical disadvantages by transferring the patterned particles from chip onto the glass substrate for synthesis.

In my Ph.D. work, a CMOS-chip based “printer” was built to print amino-acid particles from CMOS chip onto the glass substrate. Consequently, the array was synthesized on the glass substrate but no longer on the chip. With this chip printer, the CMOS chip is now reusable, and the array is synthesized on the glass substrate, which is cost-effective, robust to chemicals, and already well adapted for the biochemical application. In addition, the chip printer can print particles onto different area on the chip, so the spots synthesized on glass substrate can be 2-4 times more than the spots synthesized on chip. Accordingly, the density is  $10^4$  spots /  $\text{cm}^2$  so one substrate will have  $3.2 \times 10^4 \sim 6.4 \times 10^4$  spots per slide.

In this CMOS-chip based printing system, the amino-acid particles are first negatively charged and deposited onto the CMOS chip in the desired pattern. Afterwards, the particles on the CMOS chip are moved from particle outlets to the glass substrate, which is the microscope glass slide (75 mm ×26 mm) here. Then the particles are printed from the CMOS chip onto glass slide with 3 k Volt/mm electrical field. After the amino-acid particles are printed onto the glass slide, they are melted to release amino acids for combinatorial synthesis. This system should automatically deposit 20 kinds of amino-acid particles on the CMOS chip and then print the particles onto the glass slide for peptide synthesis.

The basic functions of this chip printer system include:

- Stir the amino-acid particles into turbulent aerosol and triboelectrically charge the particles.
- Address the amino-acid particles from the aerosol generator onto CMOS chip and then print the particles onto glass slide. The printing reproducibility should be smaller than 10  $\mu\text{m}$ , since the pixel size is 100  $\mu\text{m}$ .
- Parallelize the CMOS chip with glass slide. The tolerance should be less than 5  $\mu\text{rad}$ . The chip-to-slide distances should be unified throughout the pixel area, so the particles can be transferred onto glass slide uniformly and correctly.
- The CMOS chip, which is used as the printing head, should get the 20 different amino-acid particles from separate aerosol outlets and without contamination.
- Blow away the remaining particles on the chip after printing, and recycle the particles which are not deposited on the chip in aerosol.
- Provide the software and user interface.
- Monitor the particle deposition quality.

## 3. CMOS-chip Based Printing System

This chapter describes the design and construction of a CMOS-chip based printing system. With this printing system, the high spot-density advantage of chip-based synthesis can be kept and the chemical disadvantage of the chip can be solved. The printing system uses the CMOS chip as printing head to address the particles onto the electrode pixels and then print the particles onto the glass substrate. Besides, the CMOS chip has been designed and developed [KÖN10-2], and the prototype of aerosol generation system has also been constructed [LOF10]. Therefore, this printing system construction should also consider adapting the system for the chip and aerosol system.

### 3.1 Requirements and Limitations of the System

#### 3.1.1 CMOS Chip for Particle Deposition

Complementary metal-oxide-semiconductor (CMOS) is a technology to construct the integrated circuits. CMOS can be used to make both digital, such as microprocessor, and analog circuits, such as electronic amplifier. In our application, the CMOS composes high voltage pixels, which can provide 100 volt to address the amino-acid particles. CMOS consists of N-type metal oxide semiconductor (NMOS) and P-type metal oxide semiconductor (PMOS). Figure 3.1 shows the basic structure of NMOS. The n+ area is made by doping group 6 elements in silicon and it can provide extra conduction electrons. The p-type body is silicon doped with group 13 elements and provides conduction holes. When the voltage applied across gate and source ( $V_{gs}$ ) is 0, the NMOS is in “cut off” state. In cut off state, the current from drain to source ( $I_{ds}$ ) is 0. When the voltages applied across gate-source ( $V_{gs}$ ) and gate-drain ( $V_{ds}$ ) are both higher than the threshold voltage, a conduction electron channel will be induced beneath the dioxide insulator. In this “linear state”, the current from drain to source ( $I_{ds}$ ) is proportional to the voltage across drain to source ( $V_{ds}$ ), so the NMOS is “switched on.” When the  $V_{ds}$  is smaller than the threshold voltage and  $V_{gs}$  is bigger than threshold voltage, the area between gate and drain will still have no conduction electrons or holes. In this state, the current  $I_{ds}$  is independent to the voltage  $V_{ds}$  [SED04].



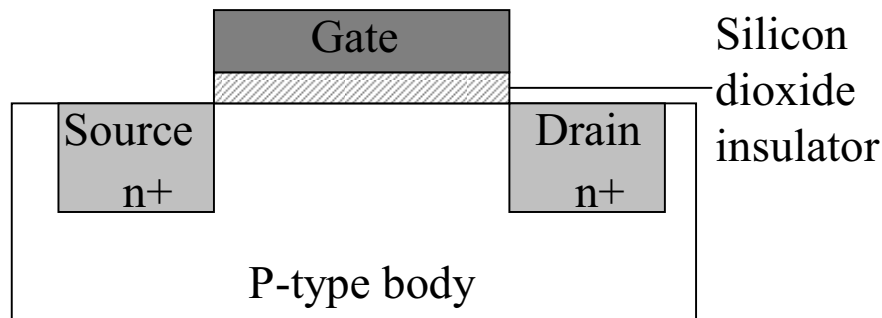


Figure 3.1: Structure of N-type metal oxide semiconductor (NMOS)

For safety reasons, the operating voltage should be reduced together with the miniaturization of the CMOS-chip feature size. To prevent electrical breakdown, the applied voltage should be scaled along with the reduced thickness of gate oxide layer. Another reason is that the power density increases together with the decreasing feature size. Therefore, the electronic microprocessors nowadays are operated with voltages lower than one volt. However, we need high voltage (around 80 volt) from the pixels to address particles correctly onto the chip pixels. Hence, the small pixel size (i.e. high spot density) and high voltage become trade off. Some semiconductor fabrication techniques have been introduced to prevent the chip from being damaged by high voltage [KÖN10-2].

To prevent the gate-oxide breakdown, the voltage across the gate oxide should be limited. In our case, the  $V_{ds}$  and  $V_{gd}$  could be up to 100 V and the  $V_{gs}$  should be only 7 V. To prevent avalanche effects when the transistor is in “on”, an established method is lightly doped drain (LDD). LDD decreases the field gradients at the pn-interface, so the voltage threshold of impact ionization is increased.

Some other measures to prevent breakdown include using conductive plates to shape the electrical fields, and limit the channel length of the devices.

Figure 3.2(a) shows the CMOS chip designed to address the monomer particles onto the chip pixels with electrical field [KÖN10-2]. The CMOS chip has 16,384 electrode pixels on the surface and the pixels are  $100 \times 100 \mu\text{m}^2$ . Every pixel is programmable and can be switched on or off. When the pixels are switched on, there will be 100 volt on the pixels to attract the particles. On the contrary, the switched-off pixels have no voltages and cannot attract particles.

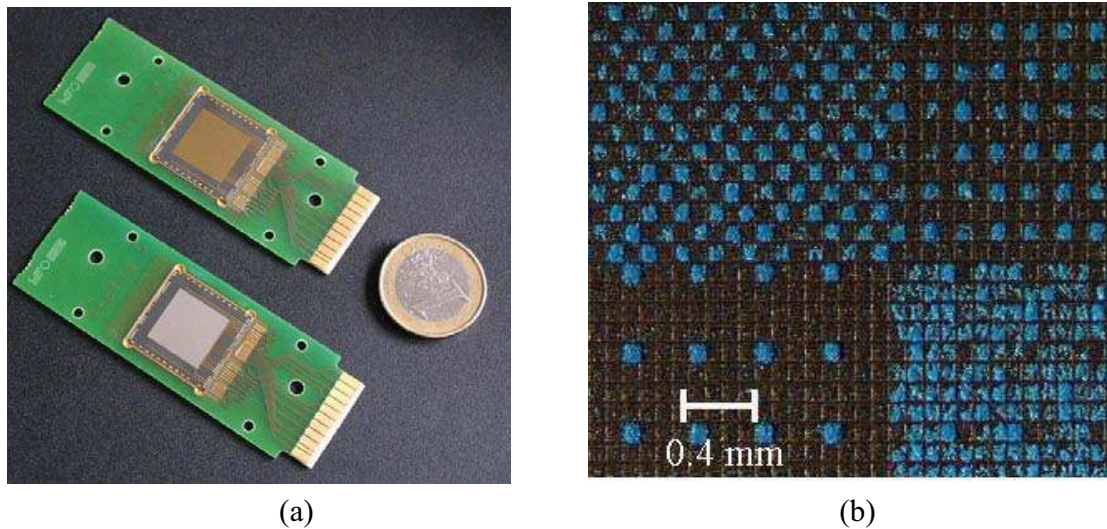


Figure 3.2(a): The CMOS chip on the support, printed circuit board (PCB). The areas of the pixels are the large golden or silver area in the center of each chip, surrounded by the dark seal area. The bond wires and bond contacts are on the right side of each chip. They are wired to the PCB connector on the right edge of the PCB. [KÖN10-2] (b): The chip pixels with deposited toner particles. The blue toner particles deposit only on the switched-on pixels and no particles deposit on the switched-off pixels.

### 3.1.2 Aerosol Generation System

The amino-acid particles are deposited onto the CMOS chip in the desired pattern, and then printed onto the glass slide. To address the particles onto chip, the chip is placed in particle aerosol so that the particles can be attracted by the electrical field from the chip pixels [BEY07, LOF10]. An aerosol generation system has been developed for generating the aerosol for particle deposition. The experiments also show that the system should be able to generate dense and homogeneous particle aerosol, which is important for thick and homogeneous particle deposition on the CMOS chip.

The concept of the aerosol generation system is shown in Fig. 3.3. The transport air goes into the particle reservoir and induces turbulence. In the turbulence in reservoir, the particle powder is stirred and transformed into aerosol. The aerosol is pumped out from the reservoir with transport airflow and the density is controlled with the dosage airflow. The particles have friction against the walls of reservoir and tube, so they are triboelectrically charged ( $q/m$  is around  $-4 \mu\text{C/g}$ ). Then, the generated aerosol goes through a sieve on the aerosol outlet.  $-1 \text{ kV}$  is applied to the sieve to accelerate the particles and prevent the negatively charged particles from aggregation. Afterwards, the particle aerosol goes perpendicularly to the CMOS chip and the particles are addressed onto the pixels [LOF10].

The aerosol is generated and jetted out when transport airflow comes in. The dosage air controls the density of the aerosol. Besides, another compressed airflow vibrates the tube to prevent particle aggregation. All the airflows can be switched by electrical valves, which are controlled by the Twincat Beckhoff system.

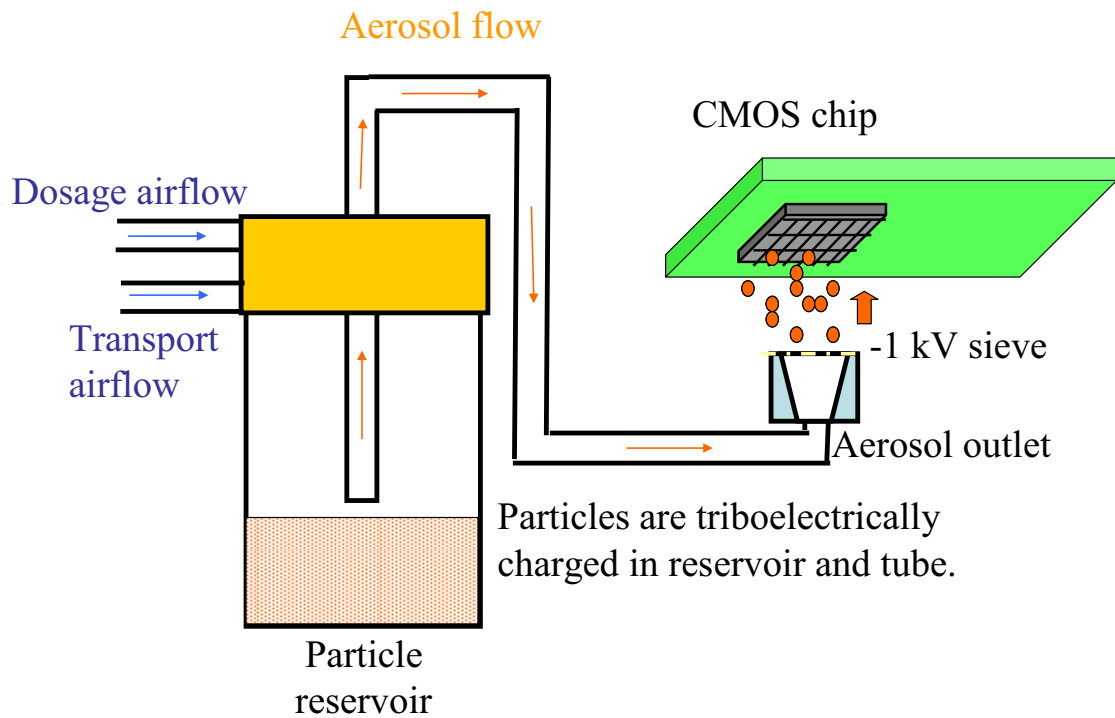


Figure 3.3: The aerosol generation system. The particles in the reservoir are stirred and pumped out from the reservoir by the compressed air. The transport airflow pumps out the aerosol and the dosage air controls the aerosol density. The particles are then triboelectrically charged by the friction against the wall of reservoir and tube. At last, the particles go out from the aerosol outlet and deposit onto the CMOS chip [LOF10].

### 3.1.3 Requirements of the Printing System

Given the CMOS chip and aerosol generation system, the basic functions of the printing system are getting the particles from the aerosol system with the CMOS chip and printing the particles onto the glass slide (Figure 3.4). The printing reproducibility and homogeneity are important issues of the printing system, since they directly influence the correctness of the synthesis result. Therefore, the solutions for printing reproducibility and homogeneity were discussed first. Then, the other system components for quality control of particle deposition, particle recycling, and user interface were developed. At last, the whole printing process was automated on this system.

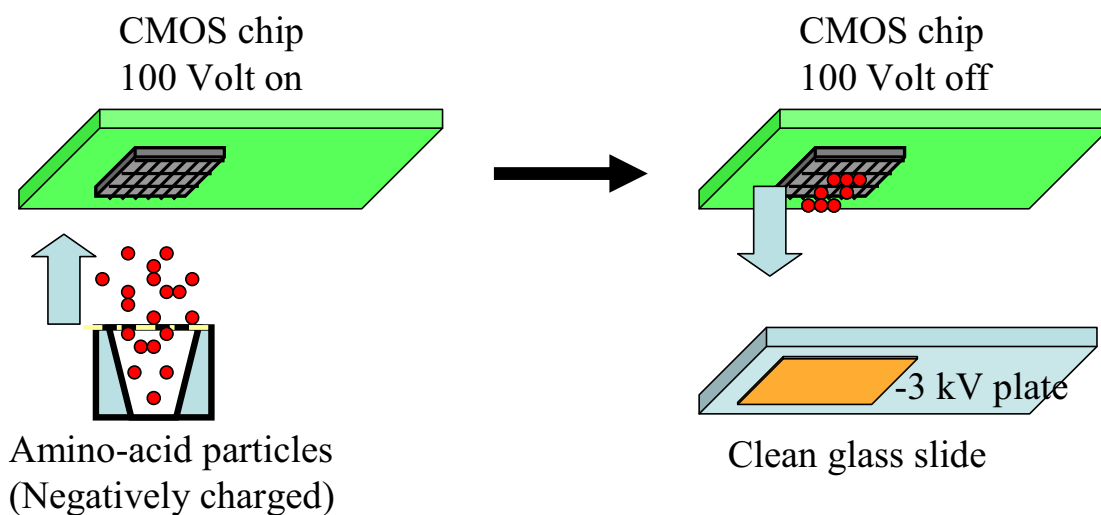


Figure 3.4: The basic functions of the printing system. The CMOS-chip should be moved to the aerosol outlet to get the generated amino-acid particles. The particles are addressed onto the switched-on pixels with electrical field. Then the chip, together with the addressed particles, is moved to the slide and “printed” on to the glass slide with high voltage (-3 kV). For ideal printing, the chip should be parallel to the slide and should print onto the same position reproducibly.

## **3.2 Homogeneity and Reproducibility of Particle Printing**

The printing homogeneity and reproducibility are two fundamental issues of system construction because they directly influence the synthesis results. Therefore, the system design should consider the solutions for these two issues first. To find the most feasible solutions, the mechanical, elastic material and sensor methods are discussed.

### **3.2.1 Methods for the Homogeneity of Particle Printing**

The yield and quantity of synthetic peptides on pixels should be homogeneous, so the binding efficiency between peptides and targets can be correctly analyzed. To synthesize peptides on the surface homogeneously, the amount of amino-acid particles printed on each spot should be unified throughout the substrate, so the amount of amino acids joining the coupling reaction can be homogeneous. Most amino-acid particles are transferred from chip onto substrate by means of  $-3$  kV/mm electrical field, and some particles are transferred by adhesion force. That is, to print particles homogeneously, both the electrical field and contact pressure between pixel area and substrate should be homogeneous. Therefore, the chip-printing system should parallelize the chip and substrate. Since the particle diameters are about  $3-5$   $\mu\text{m}$ , the parallel tolerance through out the CMOS chip surface should be less than  $10$   $\mu\text{m}$ .

The possible methods for homogeneous particle deposition are discussed and listed in Table 3.1. The methods include mechanical design (Figure 3.5), elastic material (Figure 3.6) or sensors (Figure 3.7). As shown in Figure 3.5(a), the printing CMOS chip is fixed by spring on one side, and tilted by the screw on the other side. The screw pushes the chip, till the chip is parallel to the glass substrate. This mechanical method is simple, but the parallelity is evaluated only by eye. In Figure 3.5(b), the chip is mounted onto a metal plate, whose tilt is adjusted by three screws. The screws are turned till the chip is parallel to the substrate. The tiltness of metal plate and glass substrate is measured by a distance meter. Assuming the thickness of the metal plate is uniform, the chip will be parallel to the substrate when the metal plate is parallel to the substrate. In Figure 3.5(c), the glass substrate is fixed on a rolling shaft. When the chip presses the glass substrate, the rolling shaft rolls till the pressure is homogeneous. Then the glass substrate is parallel to the chip surface.

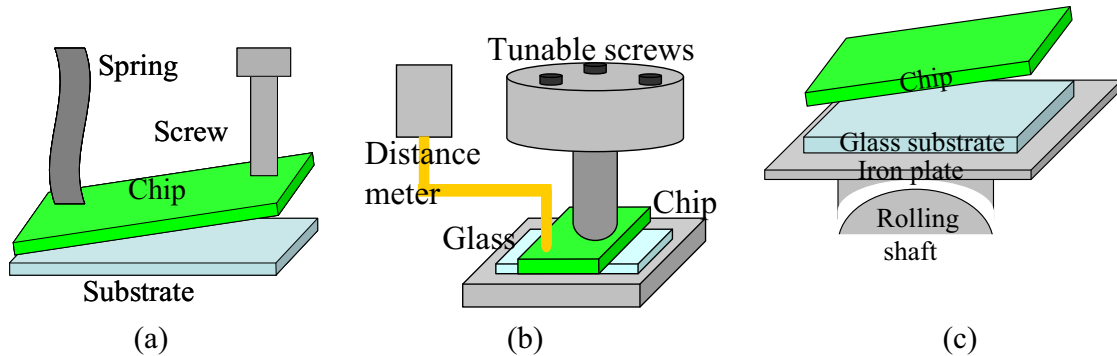


Figure 3.5(a): The chip is fixed with spring on one side and adjusted with a screw on the other side. (b): The parallelity of chip is adjusted with three tunable screws. (c): The slide is mounted on a rolling shaft so it can be parallelized to the chip by pressure.

The methods with elastic materials are also considered (Figure 3.6). An elastic material such as rubber will be padded under the glass substrate, so that the substrate can tilt a bit to match the chip (Figure 3.6(a)). Simply using an elastic substrate to replace the stiff glass substrate is also an alternative. The elastic substrate can be deformed so the pressure between substrate and chip can also be homogeneous (Figure 3.6(b)).

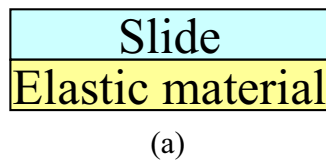


Figure 3.6(a): Padding an elastic material beneath the slide so the slide can be tilted according to the chip pressure. (b): An elastic membrane. The pressure between membrane surface and chip is always homogeneous.

In addition, laser reflection and contact sensor are considered to parallelize the chip with glass substrate (Figure 3.7). In Figure 3.7(a), a laser is mounted beneath the chip board, and shines through a chink on chip board. Then the laser beam is reflected by a mirror on the substrate and received by a CCD camera. The relative tiltiness between chip and substrate will be amplified by laser reflection and calculated by software. Then the chip will be tilted by two tilt stages according to the calculation results. The electrical contact sensor is also considered for parallelity (Figure 3.7(b)). On the CMOS chip, there are three contact sensors and these sensors, which can be used for parallelizing the chip and substrate. When the sensor contacts metal surface, an electric short will be formed. This electric short can be easily detected by a simple LED circuit. Therefore, a holder is built to reproducibly fix the upper surface of the glass substrate in a “zero” position, i.e. in a defined distance to the chip surface. Afterward, a metal wafer will be mounted in the holder and the chip will be parallelized with the metal wafer by means of the electrical

contact sensors. Then the wafer will be replaced with glass substrate, and the chip is now parallel with the glass substrate.

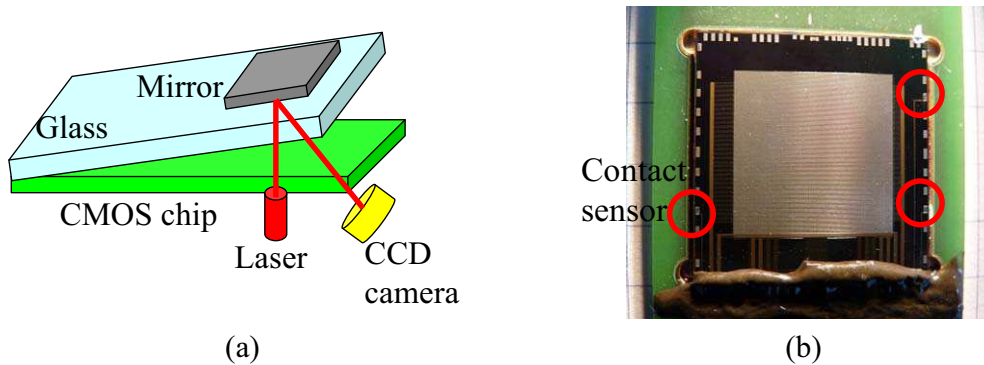


Figure 3.7(a): Laser reflection method. The laser is mounted beside the chip, and the laser beam is reflected by a mirror on the glass substrate. The reflected laser beam is detected by CCD camera and is analyzed for tilting the chip. (b): Three contact sensors on the chip surface. With LED circuits, the electrical contact between sensor and metal surface can be detected.

After comparing the methods, the contact sensor method is adopted. The problem for mechanical methods (Figure 3.5) is that eye evaluation is not precise, and the tolerance can not even be estimated. The problem for rolling shaft and elastic material (Figure 3.6) is poor reproducibility. When the rubber is deformed or the shaft tilts for homogeneity, the substrate position can also be moved. The CMOS chip should print particles onto the glass substrate repetitively, and even a small deformation or shift from the rubber or rolling shaft can result in tolerance of particle deposition. In addition, the mechanical methods in Figure 3.5(a) and 3.5(c) can not adjust the distance between chip and glass substrate, while finding a proper distance for particle transfer is important for ideal printing. The laser reflection method in Figure 3.7(a) has several problems as well. It is difficult to align the laser and CMOS chip surface and make them exactly perpendicular. Besides, the CMOS chips are manually stuck on to the chip board with glue, so the tiltiness of each CMOS chip on board is a bit different. Therefore, parallelizing chip board with substrate does not represent parallelizing the chip with substrate. In addition, this laser method is too complicated and may result in systemic tolerance.

At last, the contact-sensor method (Figure 3.7(b)) is most suitable for parallelizing chip and glass substrate, because it is simple and harmless to printing reproducibility. In addition, this method allows controlling the printing distance between chip and slide. The LED switches on as soon as the electrical short between contact sensor and metal wafer is induced. Therefore, the chip position of “distance 0” is found with the LED and the

distance between chip and substrate can be controlled with high-precision motor. With high-precision motors, good reproducibility also becomes possible with the substrate holder. Besides, the three contact sensors are fabricated on the CMOS chip already, so there is no additional cost.

### **3.2.2 Methods for the Reproducibility of Particle Printing**

The peptides of a functional peptide array have 8-20 (or even more) amino acids, so 20 amino-acid monolayers have to be coupled for a peptide array. For coupling 20 monolayers, the chip-printing system should deposit amino-acid particles 20 times onto the glass substrate. The printing reproducibility is very important, since the wrongly deposited particles result in wrong amino-acid sequences. In addition, the glass substrate will be removed from chip-printing system for chemical coupling processes, and then be remounted into the system for next printing. Hence, the reproducibility of substrate positioning is also important. The combined tolerance of substrate position and chip printing is expected to be less than 10  $\mu\text{m}$ , since the spot size of the chip is 100  $\mu\text{m} \times 100 \mu\text{m}$ . To achieve this reproducibility, several methods are considered and listed in Table 3.2 and Figure 3.8 – 3.10. These methods include mechanical, optical, and magnetic methods.

Fixing the relative position between chip and substrate mechanically was considered first (Figure 3.8). Figure 3.8(a) shows wedge method and Figure 3.8(b) shows holder method. In Figure 3.8(a), the substrate is fixed on a plate with four guiding holes, and the chip is fixed on a plate with corresponding guiding wedges. When the chip moves downward to the substrate, the guiding wedges should fit the holes. Accordingly, the relative position between chip and substrate is fixed with the wedges in the holes. Figure 3.8(b) simply fixes the glass substrate into a holder with reference poles. This holder can also fit the needs of the holder made for contact sensor method (Figure 3.7(b)), because the contact sensor method needs a fixed substrate as well. That is, this holder solution can be used to solve both homogeneity and reproducibility problems. With springs, the glass substrate can be fixed in the holder. The substrates can be removed for chemical process and then remounted into the exact original position. For this method, the chip should be moved to exact same position as before, so the chip printing can be on the same position on the substrate.



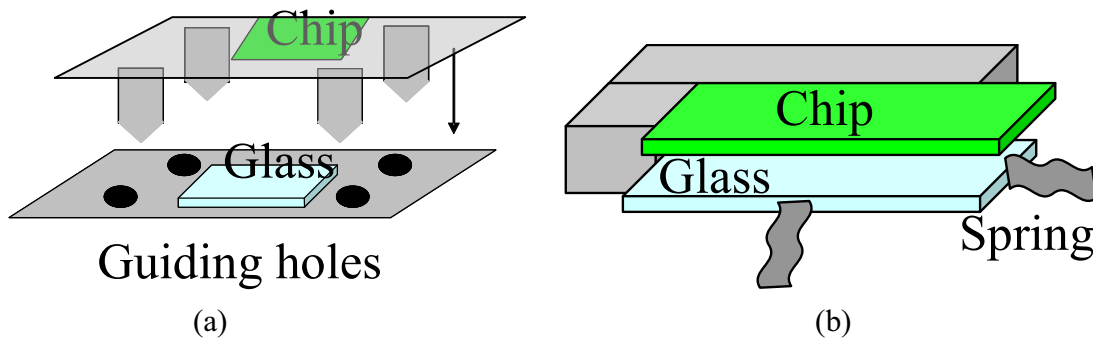


Figure 3.8(a): The wedge method. The relative position between chip and slide is fixed with guiding holes and wedges. (b): The holder method. The glass substrate is fixed in the holder with springs.

Optical methods are also considered to align the chip and glass substrate (Figure 3.9). In Figure 3.9(a), markers are used to align the chip and substrate. Two transparent glasses with markers will be mounted to the glass substrate and chip separately. The relative position of the two markers will be observed with microscope. When the markers overlap with each other, the chip is aligned with the substrate. In Figure 3.9(b), the marker is replaced with different aperture patterns. A mask with different aperture patterns is mounted on the chip and another mask with chink is mounted on the glass substrate. Beneath the chink mask, there is a laser light shining through the apertures. By observing the aperture patterns, the relative position between chip and glass substrate can be located. The chink can also be replaced by a scanner (Figure 3.9(c)).

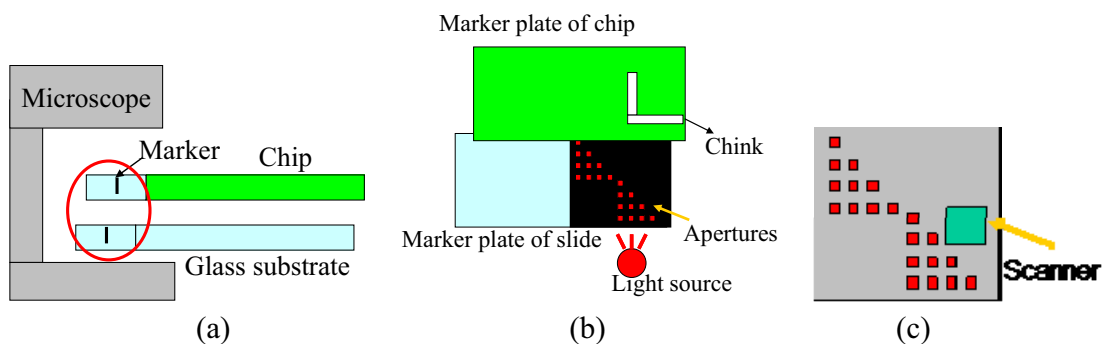


Figure 3.9(a): Marker method. Two glasses with markers will be mounted on the chip and substrate. With a microscope, the two markers can be aligned, so the chip and slide are also aligned. (b): Aperture pattern method. By observing the aperture patterns through the chink on slide, the chip can be located and moved to correct position. (c): Scanner method. The chink can be replaced with electrical scanner for automation.

Commercial position gauge is also considered (Figure 3.10). The gauges can be mounted on substrate and chip to measure the relative position between substrate and chip. The

electronic gauge can detect the motion of  $0.1\ \mu\text{m}$  (Figure 3.10(a)) and the optical gauge can detect  $0.5\ \mu\text{m}$  motion (Figure 3.10(b)).

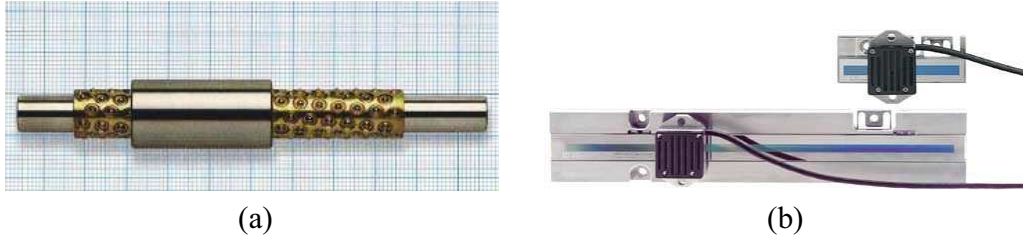


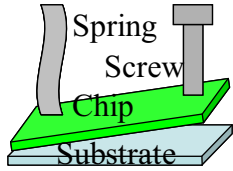
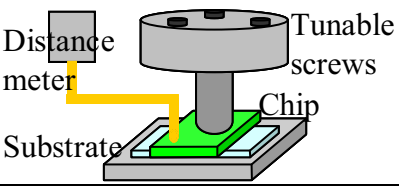
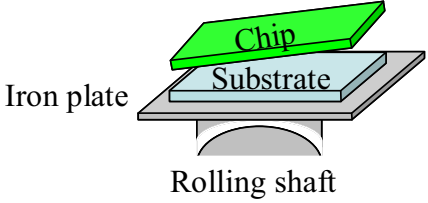
Figure 3.10(a): Electrical gauge. The detection resolution is  $0.1\ \mu\text{m}$ . (b): Optical gauge. The detection resolution is  $0.1\ \mu\text{m}$ .

Considering all the methods mentioned in Table 3.2 and Figure 3.8 – 3.10, the wedge method (Figure 3.8(a)) is quite difficult because of the friction between the holes and wedges. For high precision, the holes should fit the wedges, so the friction can be too strong to move the chip up and down. The optical methods (Figure 3.9) have three problems. First, the markers and apertures should be mounted to the chip and substrate, and the mounting may damage chip and substrate surface. Second, the alignment should be done manually and limits the automation of printing system. Third, mounting a microscope or scanner in the chip-printing system to observe the alignment also limits the geometry design of whole system, since they are both space consuming. For commercial gauges (Figure 3.10), no gauge can be mounted to glass substrate. Therefore, only the holder method (Figure 3.8(b)) fits the need of chip-printing system. Another advantage of the holder method is that the holder is also used in contact sensor method for printing homogeneity.

### 3.2.3 Design for Homogeneous and Reproducible Printing

#### 3.2.3.1 Design of the Devices

As discussed, the contact sensor method (Figure 3.7(b)) and the holder method (Figure 3.8(b)) fit the need and are most cost effective for homogeneous and reproducible printing. Therefore, a holder for reproducibly fixing the glass substrate is designed. With this holder, the substrate can be parallelized to the chip with contact sensors, and print reproducibly with high precision motors. The holder is designed to fix  $76 \times 26 \times 1\ \text{mm}^3$  rectangular stiff substrate, i.e. the microscope glass slide, which is most commonly used for peptide-array substrate.

Functions	Possible solutions		
Uniform distance or homogeneous pressure between chip and slide (Error $\leq 10 \mu\text{m}$ )	3.1.1 Adjust the tilt of chip with spring and screw. 	3.1.2 Adjust the tilt of chip with three screws. 	3.1.3 Rolling shaft. 
Advantages	1. Simple structure.	1. Can be tuned and fixed easily.	1. Simple structure.
Disadvantages	1. One dimension adjustment. 2. Manual adjustment, not precise. 3. Can not decide the distance between chip and slide. 4. The design of the chip motion system will be difficult.	1. The parallelizing adjustment is labor consuming. 2. The chip pasted on the chip board is not parallel to chip board.	1. Poor reproducibility. 2. Can not decide the distance between chip and slide.

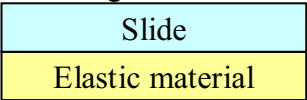

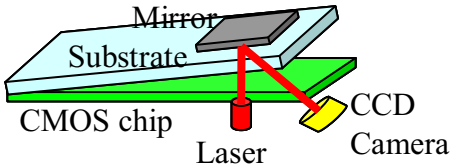
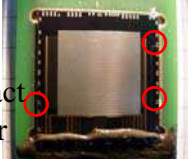
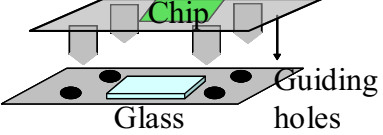
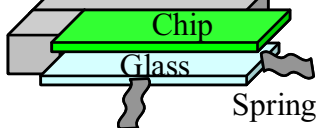
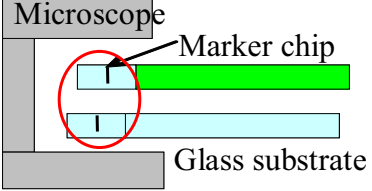
Possible solutions			
3.1.4 Putting an elastic material under the stiff glass substrate. 	3.1.5 Deposit particles onto membrane, and then pump air into the membrane. 	3.1.6 Laser reflection. 	3.1.7 <b>Contact sensors on CMOS chip.</b> 
1. Very simple and fast.	1. Very simple and fast. 2. Can control the stiffness by pumping air into it.	1. Can build a feedback loop for automation control.	1. Structure is simple and robust. 2. Needs to be tuned once for one chip.
1. Poor reproducibility. 2. Can not decide the distance between chip and slide.	1. Poor reproducibility. 2. Should find membrane with chemical robustness, and proper particle deposition quality.	1. Should align the laser with chip, and align mirror with glass. 2. Too complicated and will result in systemic tolerance.	1. The parallelizing adjustment is labor consuming.

Table 3.1: Solutions for the printing homogeneity. The solution with yellow background (3.1.7) is the chosen solution.

Functions	Possible solutions		
3.2 Reproducibility of particle deposition (Error $\leq 10 \mu\text{m}$ )	3.2.1 Guiding weges and holes. 	3.2.2 Fix the output substrate in holder with spring and then move the chip with high precision motor. 	3.2.3 Marker on glass 
Advantages	1. Simple structure.	1. Simple structure.	
Disadvantages	1. The friction may be too strong if $10 \mu\text{m}$ tolerance is required.	1. Needs good mounting skills for good reproducibility.	1. May damage the slide and chip. 2. The positioning can not be automated. 3. The microscope limits the geometry design of whole system.

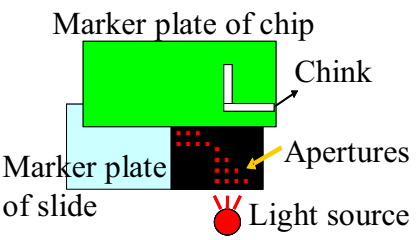
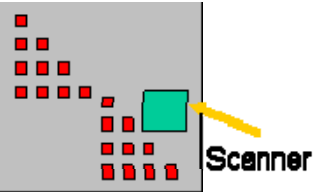

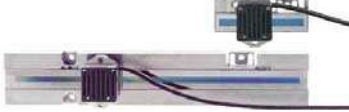
Possible solutions			
3.2.4 Laser barcode 	3.2.5 	3.2.6 Magnetic gauge 	3.2.7 Electrical gauge Heidenhein company  1D, precision: $0.5 \mu\text{m}$ . 2D, precision: $2 \mu\text{m}$ .
		1. High precision.	1. High precision.
1. May damage the slide and chip. 2. The positioning can not be automated.	1. May damage the slide and chip. 2. Could be automated with scanner.	1. The gauge can not be mounted to slide. 2. The gauge can not survive chemical process.	1. The gauge can not be mounted to slide. 2. The gauge can not survive chemical process

Table 3.2: Solutions for printing reproducibility. The solution with yellow background (3.2.2) is the chosen solution.

Figure 3.11 shows the holder for the glass substrate (slide). For reproducible printing, the holder has three poles as reference points of the slide. The holder has a screw beneath to screw upward and fix the glass slide. In between the screw and glass slide are a plastic plate, a rubber pad, an Al foil and an isolation tape, from bottom to top. The Al foil will be attached beneath the slide. The plastic plate can distribute the pressure; the rubber pad protects the slide from being damaged; the Al foil provides a  $-3 \text{ kV} / \text{mm}$  voltage for particle printing. The printing head (CMOS chip) is moved to the immobilized slide by high-precision motor with  $0.5\text{-}\mu\text{m}$  minimal incremental motion. Therefore, the relative position between slide and printing chip can be precisely controlled with the holder and motor. For homogeneous printing, the holder has two metal pillars, which can reproducibly fix the upper surface of the glass slide in a “zero” position, i.e. in a defined distance to the chip surface. From top to down, the slide is immobilized by a rubber, a plastic plate, and a screw. Thereby, the glass slide can be removed for chemical process and afterward repositioned at the same distance from the “chip printing head.”

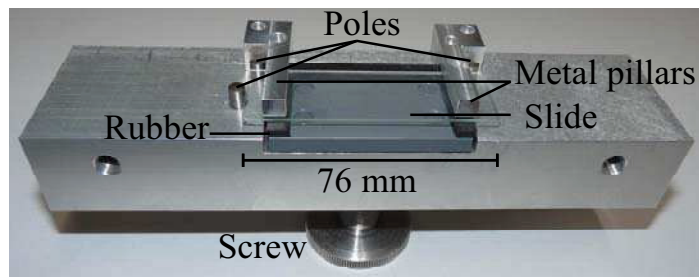


Figure 3.11: Slide holder. With three metal pillars and the poles, the slide holder can fix the glass substrate in the same position.

To parallelize the chip and the slide, a conductive (gold-coated) wafer is first mounted in slide holder to contact the electrical contact sensors on the chip surface (Figure 3.12). On contact, the sensor and gold-coated slide form an electric contact and induced electrical short in a LED circuit. When the LED switches on, the corresponding contact sensor just touches the surface. The chip will be tilted by the machine, until all three sensors just contact the upper surface of the gold-coated wafer. The thickness tolerance of the  $76 \text{ mm}$  long slide is  $10 \mu\text{m}$ , so for the  $12.8 \times 12.8 \text{ mm}^2$  printing area the tolerance is about  $1.68 \mu\text{m}$ . The measured experimental tolerance of this parallelization is  $\sim 5 \mu\text{m}$ .

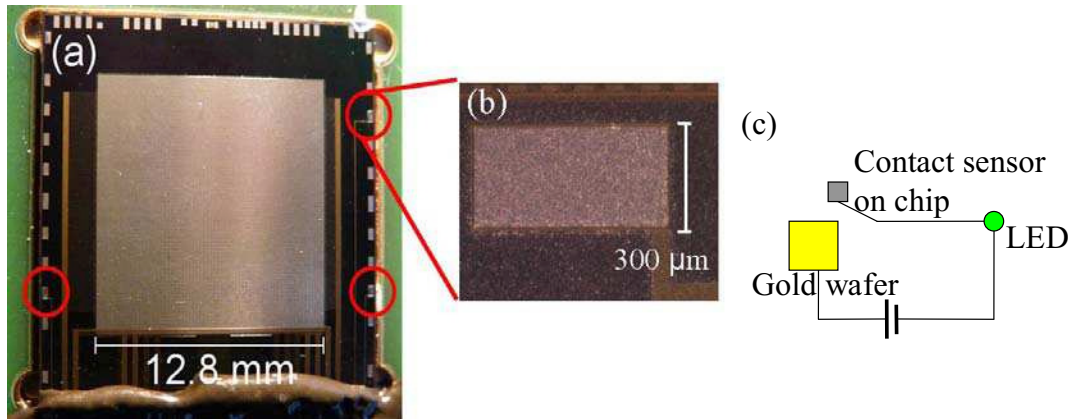


Figure 3.12(a): CMOS Chip with three sensors. (b): The contact sensor is a  $300 \times 600 \mu\text{m}^2$  aluminum plate fabricated on the chip surface. (c): The circuit involves LED light, metal plate in holder, and the contact sensor on chip. When the contact sensor touches the gold wafer, the LED switches on. Therefore, the electrical contact is detected.

### 3.2.3.2 Contact Sensor

The contact sensors are aluminum plates on the CMOS-chip surface (Figure 3.12). The height difference between chip and sensor should be predictable, so the parallel between chip and slide can be adjusted precisely. Besides, the surface of the aluminum plate is about  $0.4 \mu\text{m}$  lower than the chip surface, so it should be padded to be higher than the chip surface.  $\text{Cu}^{2+}$  plating and  $25\text{-}\mu\text{m}$  bonding wire are used to add a predictable height on sensor surface.

Figure 3.13(a) shows the contact sensor without  $\text{Cu}^{2+}$  plating. The  $\text{Cu}^{2+}$  plating electrodeposits the  $\text{Cu}^{2+}$  ion onto the cathode-connected aluminum plate, and the resulted height was profiled by Dektak 6M stylus surface profilometer. To plate on the contact-sensor surface, the 1 nm oxidized-aluminum ( $\text{Al}_2\text{O}_3$ ) layer on the surface was etched away with 7% HCl solution for 20 seconds. Otherwise, the  $\text{Al}_2\text{O}_3$  layer will isolate electrons and made electrodeposition of  $\text{Cu}^{2+}$  ion difficult. Then the surface was plated in 2.5%  $\text{Cu}^{2+}$  solution for 5 minutes with  $\sim 4\text{V}$  voltage. The plating results of  $2 \mu\text{A}$  and  $1 \mu\text{A}$  current are shown in Figure 3.13(b) and (c), respectively. The height difference between chip surface and the Cu layer was measured by Dektak 6M stylus surface profilometer.

Figure 3.13(b) is the plating on surface, and the current was  $2 \mu\text{A}$ . The surface is rough because the Cu deposition is too fast. Hence, the current was reduced to  $1 \mu\text{A}$  (Figure 3.13(c)), and the resulting Cu coverage rate is good for electrical contact. The surface is much more even than the other two plating results. The height of the Cu layer is  $30\text{-}40 \mu\text{m}$  in the middle and  $\sim 50 \mu\text{m}$  on the edge, because the electrons can go out easier from

the junction than from the surface. Besides, Figure 3.13(d) shows the plating on contact sensor without etching away the  $\text{Al}_2\text{O}_3$  layer. The black area is the Cu deposition, and the Cu electrodeposition is few and uneven. The electrons can only leak from the scratch on the surface (i.e. scratch on the  $\text{Al}_2\text{O}_3$  layer), so the electrodeposition is very inhomogeneous. Therefore, the  $\text{Al}_2\text{O}_3$  layer on surface should be etched away in advance to make sure the whole surface is conductive for electrodeposition.

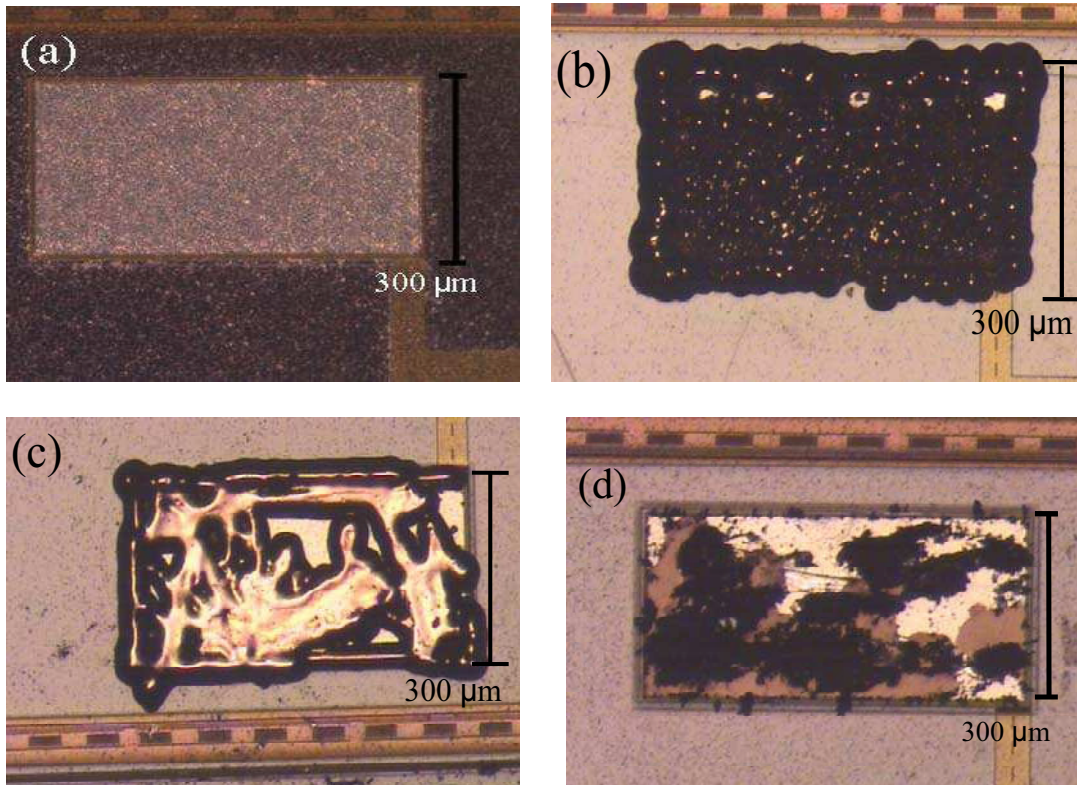


Figure 3.13(a): Contact sensor surface without  $\text{Cu}^{2+}$  plating. (b):  $\text{Cu}$  plating on sensor,  $2\mu\text{A}$ , 5 minutes. The surface is rough because the ion deposition is too fast. (c):  $\text{Cu}^{2+}$  plating on sensor,  $1\mu\text{A}$ , 5 minutes. The surface is smooth with low plating current. (d):  $\text{Cu}^{2+}$  plating on surface with  $\text{Al}_2\text{O}_3$  layer. After plating, the surface is washed with HCl solution for 20 seconds. The black area is Cu plated onto the surface; gold area is aluminum surface; brown area is etched surface.

In addition to the Cu plating, the bonding wire method is another method considered to increase the height of contact-sensor surface. Three  $25\text{-}\mu\text{m}$  bonding wires were soldered onto the sensor surface (Fig. 3.14 (a)) and then were coated with conductive glue to prevent scratching (Fig. 3.14 (b).) The height of bonding wires is  $25\text{ }\mu\text{m}$ , so the height of the sensor surface is  $25\text{ }\mu\text{m}$  plus the thickness of thin glue layer.

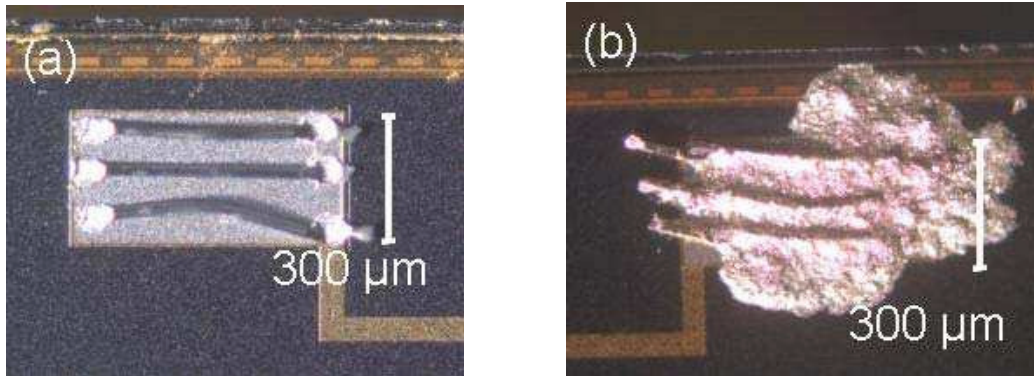


Figure 3.14(a): Contact sensor with three bonding wires. The bonding wire is 25  $\mu\text{m}$  thick. (b): Contact sensor with bonding wires and conductive glue. The conductive glue can protect the bonding wires.

Comparing the bonding-wire method with the  $\text{Cu}^{2+}$ -plating method, the bonding-wire method is simpler than  $\text{Cu}^{2+}$ -plating method, and needs no chemical process, which may damage the printing chip. The disadvantage of bonding wires is that the surface is uneven, but this problem can be solved by using three bonding wires to increase the electrical-contact area. The height precisions of both methods are similar. The diameter of bonding wire is 25  $\mu\text{m}$  with thin glue layer, and the height of  $\text{Cu}^{2+}$ -plated sensor can be measured by Dektak 6M stylus surface profilometer, whose resolution can be 200 angstroms. The height of  $\text{Cu}^{2+}$ -plating sensor is about 30-40  $\mu\text{m}$  and varies with plating time. However, the bonding-wire method needs less preparation process than the  $\text{Cu}^{2+}$ -plating method, and has similar height precision to  $\text{Cu}^{2+}$ -plating method. Therefore, the bonding-wire method was adopted to enhance the height of contact sensor.

### 3.3 Construction of the Chip-printing System

The methods for homogeneous and reproducible printing were discussed and described in section 3.2. These methods should be adopted and involved into the construction of the chip-printing system. The basic function of this system is repetitively getting the amino-acid particles from particle outlets with the CMOS chip, moving the chip to the glass slide, and then printing particles onto the slide. Besides, this system also generates the particle aerosol, observes the particle deposition on chip, prevents the unused particles from spreading, and recycles the unused particles. The software for system control and graphic user interface was also developed.



### 3.3.1 Frame Design

The possible structures for getting particles from particle outlet and printing particles onto glass slide are listed in Figure 3.15. The system can either move 20 particle outlets to chip (Figure 3.15(a), (c)) or move the chip to 20 particle outlets (Table Figure 3.15(b), (d)). Linear motion or rotation are both considered. The linear motion was chosen, since it is easy for the geometry design and motion control. For CMOS-chip motion, the up-down motion of the chip should be very precise ( $< 1 \mu\text{m}$ ), so the travel range should be as short as possible. Aligning the glass slide with aerosol outlets can make the up-down travel range short, so moving the chip between the glass slide and aligned particle outputs (Figure 3.15(b)) was chosen. For printing reproducibility, a high precision motor was used to move the chip between substrate and aerosol outlet. At last, the system has 20 aerosol outlets and each is  $40 \times 40 \times 40 \text{ mm}^3$ , so the total length of outlets is 800 mm. Therefore, the particle outlets were arranged into two rows, so the travel range for moving different particle outlets to chip is 400 mm. Moving particle outlets to the chip does not need high reproducibility, so a high precision motor is unnecessary. The motions of chip and particle outlets were designed to be perpendicular.

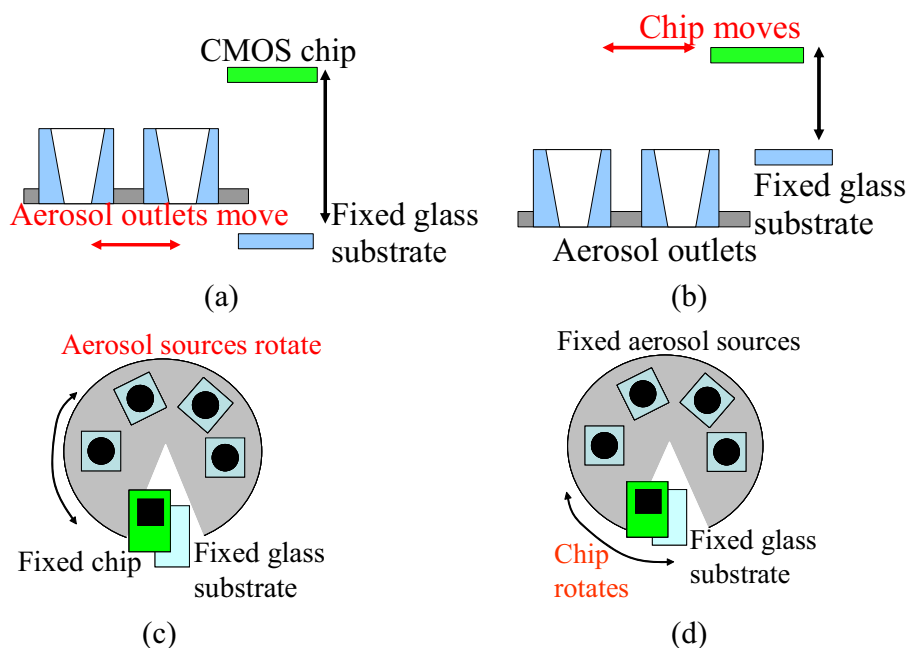


Figure 3.15(a): The aerosol outlets are linearly moved to the chip. The chip only moves up and down. (b): The chip can be linearly moved to the aerosol outlets and glass substrate. (c): The aerosol outlets are rotated to the chip. (d) The chip is rotated to the aerosol outlets.

Figure 3.16 is the 3D frame of the system drawn by the software, UniGraphics. The X motor (motor for moving chip along x axis) moves the “CMOS-chip printing head” between the particle outlets and glass slide with high precision. The printing head includes the chip, two tilt stages and motor for Z motion. The Z motor moves the chip up and down and the tilt stage parallelize the chip with the glass slide. The glass slide is fixed in the holder, so the slide can be in the same position after remounting. This holder together with slide can be moved by a Y motor, so that the chip can print particles on two different locations on the slide, doubling the spot number on the slide. For good reproducibility, these Y motor, Z motor, and tilt stages are all high-precision motors. Only the particle outlets are moved to the chip by a normal step motor. In this design, the X motor for chip motion has some free travel range to move the chip for other purpose, e.g. monitoring particles on glass slide and blowing off the remaining particles on chip.

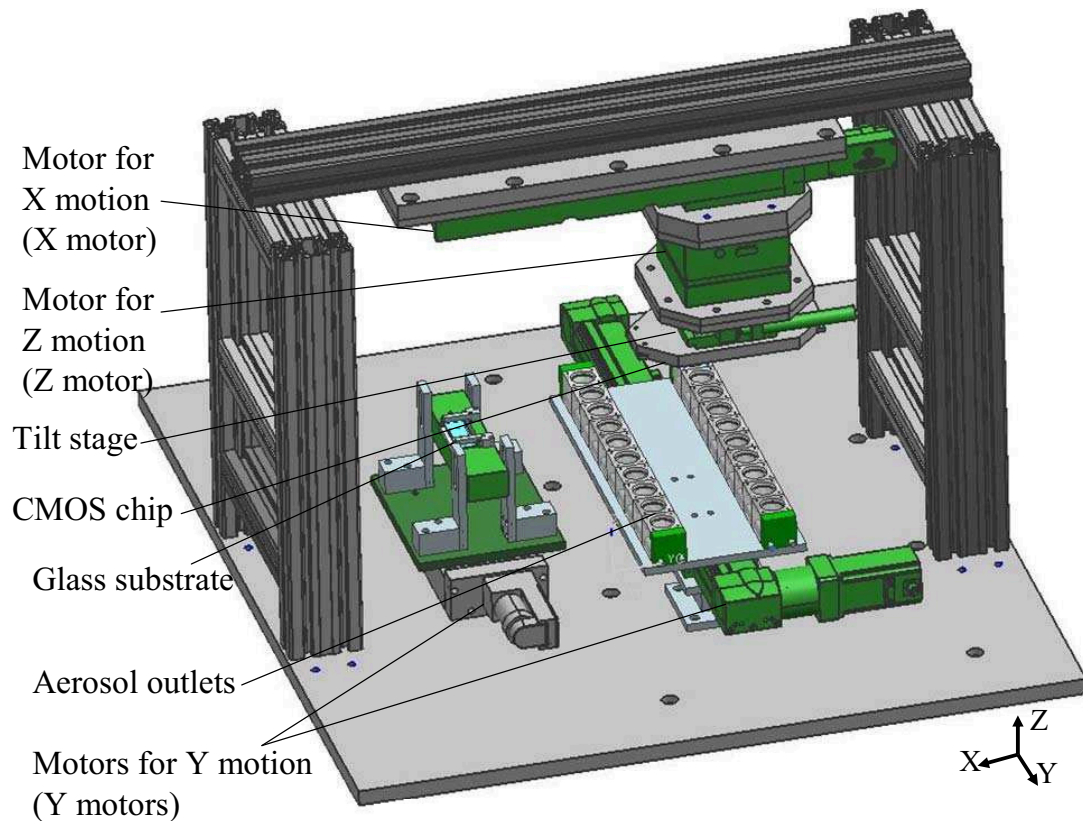


Figure 3.16: The machine frame, drawn by the UniGraphics software. The CMOS chip is mounted on the high-precision X motor, Z motor and two tilt stages, so the position of the chip can be reproducible. The glass holder is also mounted on high-precision motor. The particle sources are mounted on a normal motor with long travel range.

For the printing reproducibility, the printing head and glass slide are moved by high-precision motors, and the minimal incremental motions of these motors are all

smaller than  $0.5 \mu\text{m}$ . The specifications of all the motors in the chip-printing system are listed in Table 3.4. For the printing reproducibility in X axis, the slide is fixed in X direction. The incremental motion of motor X, which moves the chip between slide and particle outlet, is  $0.5 \mu\text{m}$ . For the printing reproducibility in Y axis, the chip is fixed in Y direction. The slide is moved in Y direction by a motor with minimal incremental motion of  $0.5 \mu\text{m}$ . Therefore, the relative printing tolerance between chip and slide will be less than  $0.5 \mu\text{m}$  both in X and Y direction. For the tolerance of parallel between chip and glass slide, the chip is moved by a tilt stage with minimal incremental motion of  $5 \mu\text{rad}$ . That is, the angular tolerance is smaller than  $5 \mu\text{rad}$ . The CMOS chip is about  $20 \text{ mm}$ , so the tolerance will be less than  $20 \text{ mm} \times 5 \mu\text{rad} = 0.1 \mu\text{m}$ . To sum up, the theoretical tolerances from the machine are no bigger than  $0.5 \mu\text{m}$  in any axis, and  $0.5 \mu\text{m}$  is less than the tolerance needed, which is  $10 \mu\text{m}$ , for the  $100 \times 100 \mu\text{m}$  pixels.

	Minimal incremental motion	Travel range	Company and type
X motor	$0.5 \mu\text{m}$	300 mm	Physik Instrumente M 414.3PD
Z motor	$0.1 \mu\text{m}$	12.5 mm	Physik Instrumente M 501.1DG
Tilt stage	$5 \mu\text{rad}$	$\pm 1.4 \text{ mrad}$	Physik Instrumente M 227.10
Y motor for glass slide	$0.5 \mu\text{m}$	100 mm	Physik Instrumente M 414.1PD
Y motor for aerosol outlets	1.8 deg	450 mm	Festo

Table 3.4: The high precision motors of the machine. The X motor moves the printing head, including the CMOS chip, between aerosol outlets and slide. The Z motor moves the CMOS chip up and down toward the glass slide and the aerosol outlets. The two tilt stages tilt the chip so that the chip surface can parallel to the slide surface. The Y motor for glass slide moves the slide holder so the CMOS chip can print onto different area on the slide surface. The Y motor for the aerosol outlets moves different aerosol outlets to the CMOS chip. These motors are controlled by LabVIEW program through PCI (peripheral component interconnect) cards and a control box (see Appendix 4).

### 3.3.2 Particle Confining and Recycling System

During the printing process, only few aerosol particles are deposited onto the CMOS chip for printing, and most of the particles diffuse into the air. These amino-acid particles can be harmful if they enter human body through respiration. Therefore, a fume hood covers the whole printing system to prevent particles from dispersing, and a particle suction system is built to suck away the unused particle aerosol. In addition, the amino-acid

particles are very expensive (20-50 Euro / g, depending on the side chain protecting group) so the sucked-away particles are collected and recycled by filters, which are mounted into the suction system. One filter was mounted for each aerosol outlet so the different particles will not contaminate each other. Besides, a cleaner will blow away the particles remaining on chip after printing, so the chip is clean for next printing.

### 3.3.2.1 Fume Hood

The fume hood is built to prevent particles from diffusing into the room during the printing process (Figure 3.17). The frame of this fume hood is made of aluminum profile (Bosch Rexroth) and the wall is made of plexiglas (Evonik). It can be opened at front and left side for system calibration and experiments. The air comes in from the gap at down front side and is sucked away through the tube on the top. This tube connects the fume hood and the in-house suction system. The positions of air inlet (the gap) and outlet (tube) form an up-going air flow. This up-going air flow can bring the diffusing particles into the in-house suction system, and prevent the particles from spreading into the room.

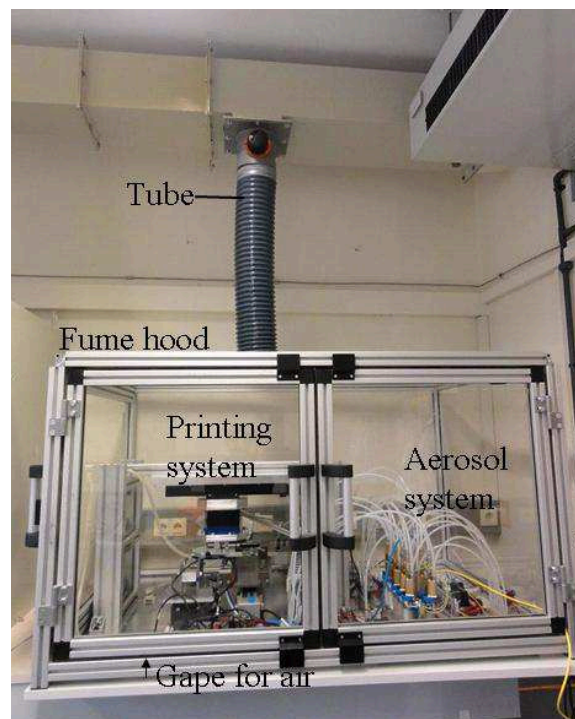


Fig. 3.17: The fume hood connects to the in-house suction system and sucks the air and unused particles away. The fume hood can be opened from the front side or left side for experiment operation.

### 3.3.2.2 Particle Suction and Recycling System

Most amino-acid particles diffuse into the air during the particle deposition process. Since the particles are expensive, the unused particles should be recycled. After depositing particles onto the chip, the particle aerosol goes out, and then the two suction cups suck the particles away (Figure 3.18). Then aerosol goes through the filter. The membrane in the filter filters out the particles in aerosol, and the air is sucked into the vacuum generator. The suction cup setup, filter, and the vacuum generator is shown in Figure 3.19. The CMOS chip is unmounted from the printing head in Figure 3.19, so the relative position between chip and suction cups can be clearly shown. The filter connected to the suction cup is (Millipore XX4304700) and the other side of this filter is connected to a vacuum generator (Nilfisk GM80). The maximum suction volume of Nilfisk GM80 is 2280 l / min, while the flow volume of the compressed is only about 200 l / min. The membrane in the filter for filtering the particles is Millipore FALP04700. The pore size of the membrane is 1.0  $\mu\text{m}$ , so most of the particles, which is about 4-5  $\mu\text{m}$ , can be filtered.

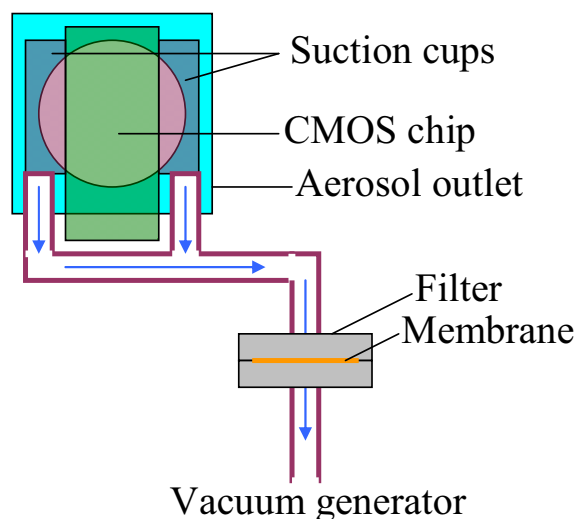


Fig. 3.18: The particle recycling system. After particle deposition onto CMOS chip, the unused aerosol is sucked by two suction cups at the side of the CMOS chip. Then aerosol goes through the filter and the particles are filtered out with the membrane. The rest air is sucked into the vacuum generator.

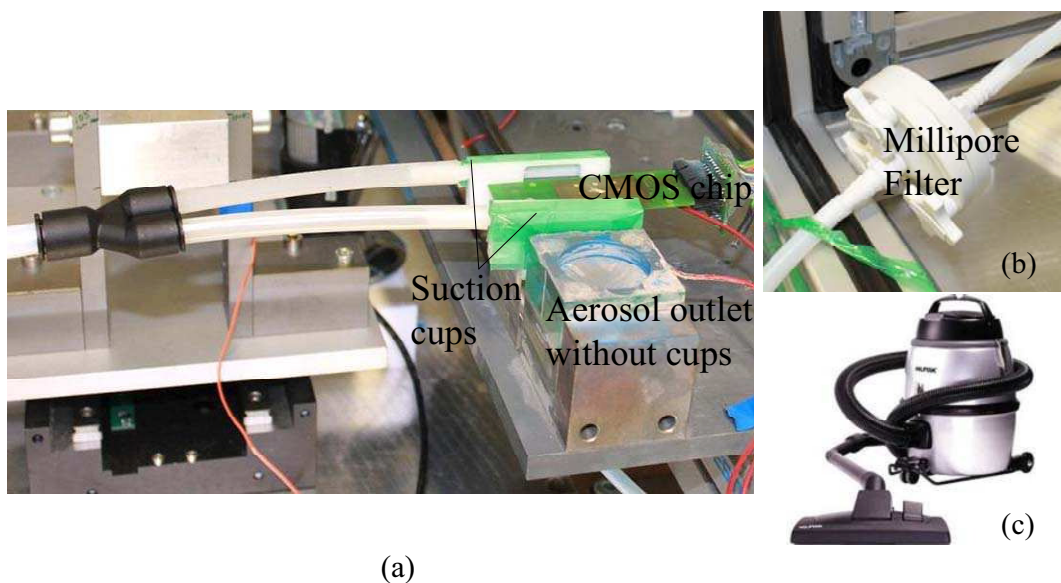


Fig. 3.19 (a): The suction cup is mounted on the aerosol outlet and connects to filter. The CMOS chip is unmounted from the tilt stage here so the chip and suction cups can be seen. (b): Millipore particle filter. The aerosol sucked by the suction cups goes through the filter to filter out the particles. The other side of the filter is connected to the Nilfisk vacuum generator (c).

The recycling efficiency of the recycling setting is tested with Xerox cyan particles, which is much cheaper than the amino-acid particles. The mean size of Xerox cyan particles is  $5.3 \mu\text{m}$ , and it is quite similar to the size of amino-acid particles ( $4\text{-}5 \mu\text{m}$ ). With pressure branch, the suction pressure applied on the filter outlet is  $0.2 \text{ bar}$  ( $6 \text{ inHg}$ ). In the test,  $0.897 \text{ g}$  particles are used and  $0.119 \text{ g}$  particles are recycled. The recycling rate is  $13.2 \%$ , which is not very high. The reasons for this recycling rate include:

1. Some unused aerosol is not sucked into the recycling system, and leak out from the space between suction cup and particle outlet.
2. Some particles remain on the suction cup, tube wall and particle outlet.
3. Many filtered particles adhere on the filter membrane, and can not be scratched down from the membrane.
4. The pores of the membrane are very small ( $1.0 \mu\text{m}$ ), so the pore can be blocked by the particles easily. Accordingly, the recycling filter should be cleaned several times and it complicates the recycling process.

### 3.3.2.3 Chip Cleaner

After the particles are deposited onto glass slide from CMOS chip, some particles still remain on the CMOS chip (Fig. 3.20(a)). These particles should be removed from the chip with compressed air so that the particles will not contaminate the slide in next

printing. The chip cleaning is done by the cleaner shown in Fig. 3.20(b). In the middle of the chip cleaner is a nozzle, which jets 4 bar compressed air to blow away the particles on chip. The blown-off particles are sucked into the cleaner, which is connected to a vacuum cleaner for fine particles. The vacuum cleaner, Nilfisk GM80, is specifically designed for collecting fine particles. Besides, the suction flow rate of this vacuum cleaner is about 2280 l / min, and it is much higher than the flow rate of the nozzle (200 l/min at 4 bar). Therefore, most of the blown-off particles will be sucked in to the vacuum cleaner but not spread into the air.

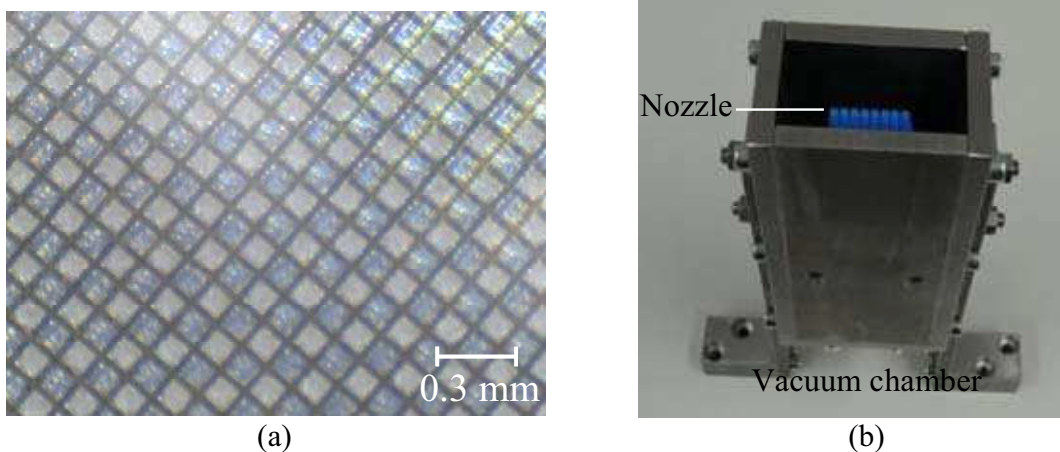


Fig. 3.20(a): Alanine particles remaining on the CMOS chip after printing. Still several particles remain on the chip pixels. (b): The chip cleaner. The compressed air from the nozzle blows the particles away from the chip surface. The blown-away particles will be sucked into the vacuum chamber, which is connected to the vacuum cleaner Nilfisk GM80.

### 3.3.3 High Voltage for Particle Transfer and Aerosol System

The printing process needs  $-3\text{ kV}$  DC voltage for particle transfer from chip,  $24\text{ V}$  DC voltage for aerosol generation system,  $220\text{ V}$  AC voltage for vacuum generation, and  $120\text{ V}$  DC voltage for CMOS chip. To switch these voltages, several relays are used to switch corresponding power supplies on and off (Fig. 3.21). By using an internet cable, the LabVIEW program in PC controls the Twincat system (Beckhoff), which provides  $24\text{ V}$  DC voltage. This  $24\text{ V}$  DC voltage switches on the  $220\text{ V}$  AC voltage with relay, and the  $220\text{ V}$  AC voltage switches the power supplies, which provide different DC voltages to the printing system. The  $-3\text{ kV}$  DC voltage is applied beneath the glass slide to attract the particles from the chip to slide; the  $100\text{ V}$  DC voltage is for pixels on the chip; the particle sources need  $1\text{ kV}$  to prevent particle aggregation.

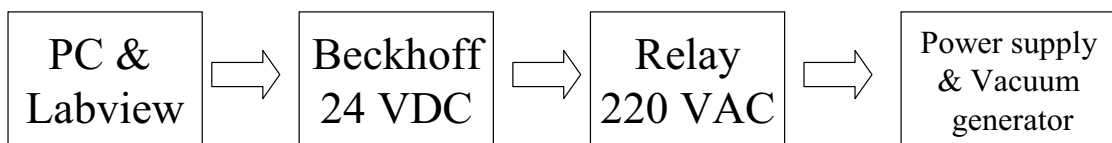


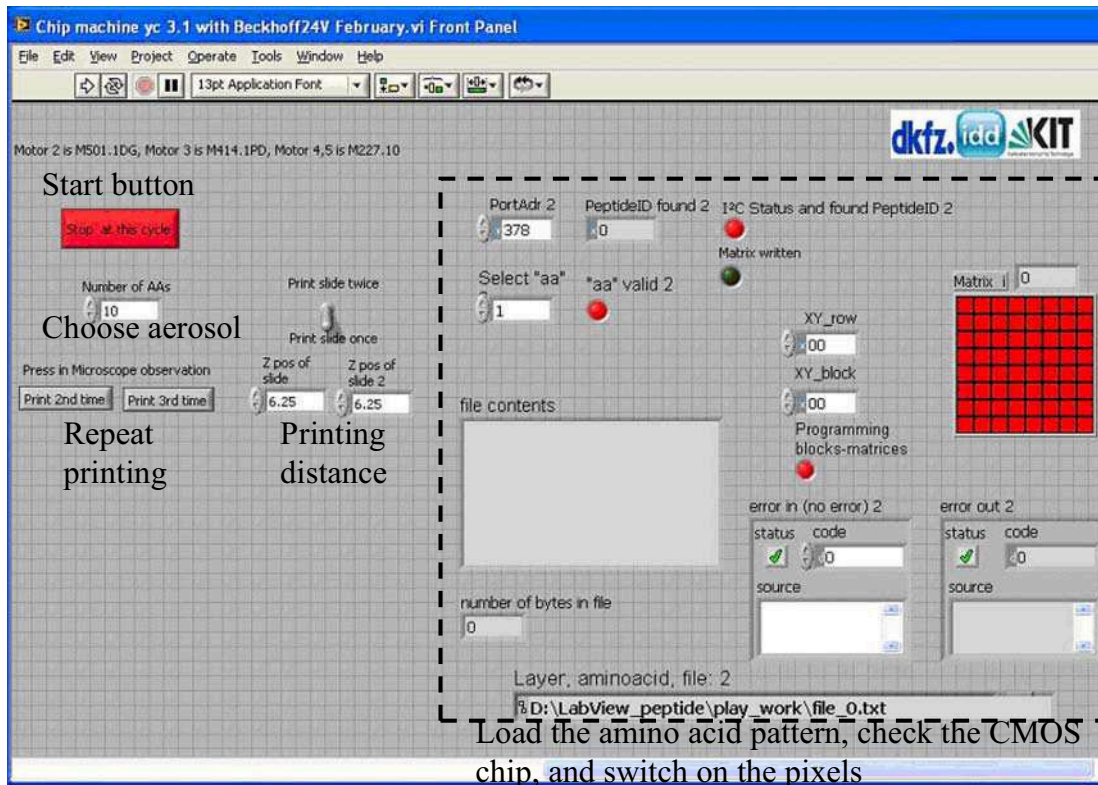
Figure 3.21: Voltage control: LabVIEW and personal computer → Twincat system switches 24V DC voltage → the relay amplifies the 24V-DC-voltage switch to 220V-AC-voltage switch → the 220V AC voltages switches corresponding power supplies for different voltages needed.

### 3.3.4 Control Software

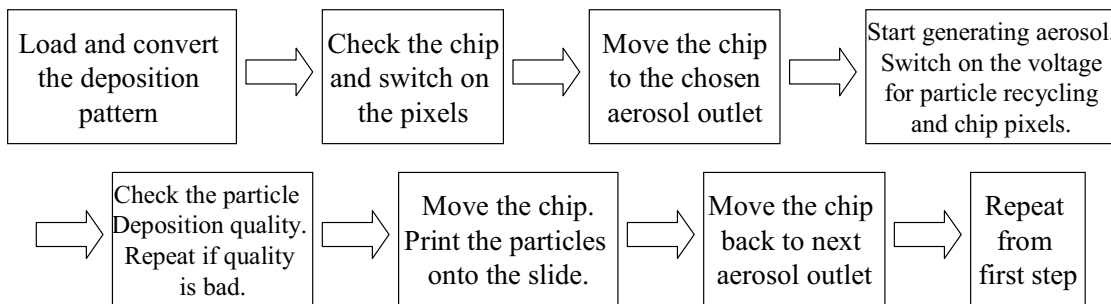
The software was developed to automate the whole system, and this software was programmed in LabVIEW 8.6 (see Appendix 2). This program controls every function of the automation printing process, including: read designed patterns, switch on the pixels on the chip, move all the motors in the chip printing system, switch on different power supplies, and generate particle aerosol, etc.

The control panel and control flowchart of the system is shown in Figure 3.22. In the control panel, the user can set the distance between the chip and slide in “Z pos of slide.” The user can also ask the system to deposit particles onto chip again, if the particles deposited on chip are not enough. The user can also choose to print once on the slide (for 16,000 peptide spots) or print on two different areas on the slide (for 32,000 peptide spots). The other commands include choosing the particle patterns, choosing the different amino-acid particles, and interrupting the whole printing system.





(a)



(b)

Figure 3.22 (a): The control panel of the LabVIEW program. On this control panel, the user can set the pattern of amino-acid deposition, the aerosol, the printing distance, and the times of printing. (b): The flowchart of the printing system.

An interface for converting the biologists' design into CMOS-chip command is written with LabVIEW. The flow chart is shown in Figure 3.23. A pattern of one monolayer has 20 numbers from 0-20, representing 21 amino acids and no amino acid. Each kind of amino acid has its own binary pattern. The number "1" means switch on for the amino-acid particles and 0 means switch off for no particles. Then every 8 digits in a row is separated to two 4 digits, and converted into two hexadecimal digits, separately. The

two hexadecimal digits then are reversed and prefixed with “#,” which is used as a marker.

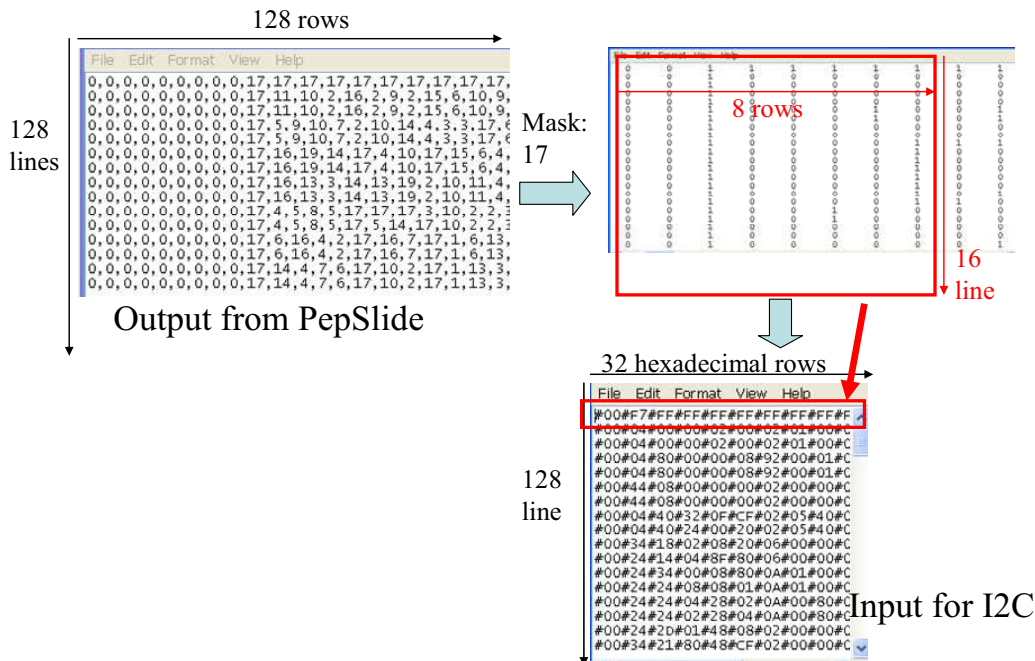


Figure 3.23: The converting flow realized by LabVIEW program. The top left matrix is a monolayer pattern from a program PepSlide, which is used to design peptides by biologists. Each amino acid has a number, from 1 to 20, and 0 means no monomer. The up right figure is the pattern for amino acid number 17. The down right matrix is hexadecimal table for CMOS chip controlling program, I2C.

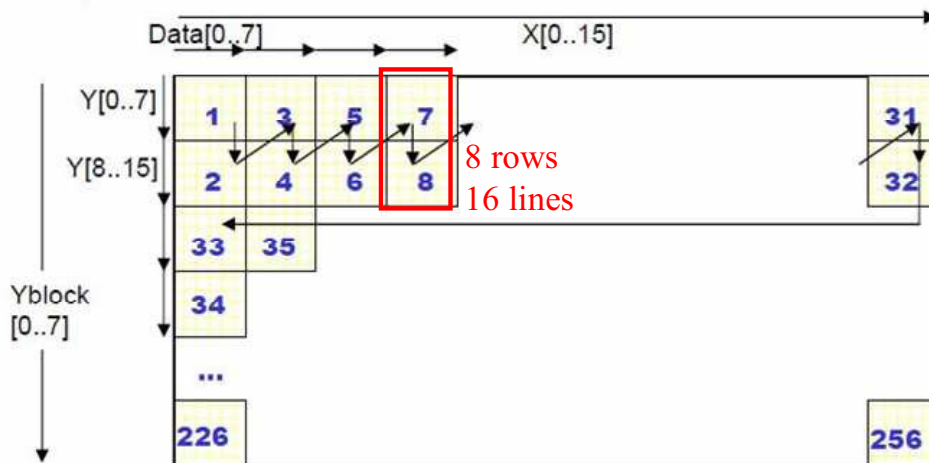


Fig. 3.24: Write order of the matrices of pixels on the CMOS chip. It starts at Yblock = 0, Xblock = 0. Each block has 8 × 8 binary digits, which will be converted into 32 hexadecimal digits. The hexadecimal digits are arranged following the arrows. [KÖN10-2]

The detail of converting order is shown in Figure 3.24. The converting starts from Block Y[0]X[0]. Each block has  $8 \times 8$  binary digits so it will be converted into  $2 \times 8$  hexadecimal digits. The converting order is indicated by the arrows, and the converted hexadecimal digits are linked into one line.

### 3.3.5 Quality Control of Particle Deposition

For the synthesis yield, the amino-acid particles printed from chip onto the spots should be enough on each pixel and be homogeneous throughout the glass slide. To ensure the printing quality, the particle-deposition quality on chip should be checked before printing. Several methods, including commercial microscope, laser attenuation, stylus profiler, and digital microscope, are considered (Figure 3.25).

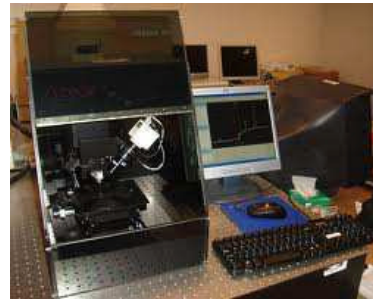
The particle quantity on chip pixels can be evaluated by high resolution microscope, such as Keyence microscope VHX 2000 (3.25 (a)) [KEY]. With built-in software, this microscope can calculate the volume of the particle pile on the pixels. However, the commercial Keyence microscope has three problems. First, the volume can be evaluated only one pixel by one pixel, but there are about 16,000 pixels on the chip. The size of the microscope lenses is another problem, since the lenses are all longer than 155 mm, which is the space preserved for the observation lenses. In addition, the microscope is very expensive, so the cost-performance ratio of this method is low.

The stylus profiler (Dektak 6M stylus surface profilometer) is also considered (3.25 (b)) [VEC]. The stylus profiler has a stylus to scan across a layer for the height profile. With equation 3.1, the height of particle layer can be calculated by the power consumption of the stylus. The symbol  $T$  is the layer thickness, 200 is the maximum power of the pin, and  $a$ ,  $b$  are constants. This stylus profiler measurement does not work because the stylus pressure is too strong. The stylus divides the particle layer but not scan across the layer. Besides, the stylus profiler is very big (508 mm  $\times$  305 mm  $\times$  438 mm) and can not be mounted into the chip-printing system either.

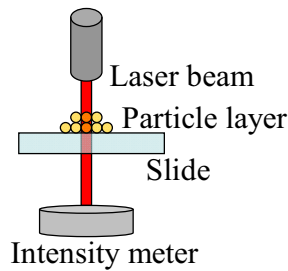
$$Power (mW) = 200 \times a \times e^{-bT(\mu m)} \quad (\text{Eq. 3.1})$$



(a)



(b)



(c)



(d)

Figure 3.25 (a): Keyence microscope. (b): Dektak 6M stylus surface profilometer. (c) Laser attenuation based on The Beer-Lambert law. (d): Digital USB microscope.

The Beer-Lambert law (Eq. 3.2) is also considered to evaluate the layer thickness with laser attenuation rate.  $A$  is the light transmissivity;  $I_0$  and  $I_t$  are the intensity of the incident light and the transmitted light, respectively;  $K$  is the molar absorption coefficient;  $l$  is the path length and  $c$  is the molar concentration. Since the  $K$  and  $c$  are same, the  $\log_{10}(I_0 / I_t)$  is directly proportional to  $l$ . A red-light laser beam goes through the particle layer and slide (Figure 3.25 (c)). The transmitted laser intensity  $I_t$  is measured to calculate the thickness of particle layer  $l$ . This method is very simple and cheap. However, the problem of this method is that the glass slide should be mounted in the opaque slide holder, so the laser light cannot go through the slide. Another problem is that the laser beam is too thick ( $\sim 1\text{mm}$  in diameter), while the pixels are  $100 \times 100 \mu\text{m}^2$ . Therefore, this laser-attenuation method can only evaluate the thickness distribution on the slide surface, but not the layer thickness on single pixel.

$$A = \log_{10}(I_0 / I_t) = K \times l \times c \quad (\text{Eq. 3.2})$$

Using digital USB microscope (Figure 3.25 (d)) [YOU] to observe the particle distribution on the chip is also an alternative. A microscope can be mounted between slide holder and aerosol outlets. After particle deposition, the chip will be moved to the

microscope to take the image on chip surface. A C++ program was developed to analyze the particle coverage rate on pixels [WAG10]. When the deposition parameters are higher than a desired value for all the pixels, the program will send an “OK” to the control program of chip-printing system. However, the problem of this method lies on the limitation of image analysis. The analysis program cannot estimate 3D volume from 2D image. However, good synthesis yield needs not only good coverage rate but also thick particle layer. The program can only analyze the coverage rate but can not estimate the thickness of the layers. Therefore, the image on chip surface can only be checked by eye, which is disadvantageous to system automation.

Comparing these four methods, the Keyence microscope and stylus profiler can not be involved in the printing system to evaluate the deposition quality. These two systems are both very large and expensive, so they can not be mounted into the printing system. Measuring the transmitted light intensity and calculating the layer thickness with Beer-Lambert law is cheap, but the slide holder is not transparent. Therefore, only the digital USB microscope method is feasible. The digital microscope is much smaller (about 15 cm) and cheaper than the Keyence microscope and stylus profiler. However, the image analysis program can still not evaluate the particle amount on pixels, so the quality of particle deposition can only be estimated by eye now.

## **3.4 Discussion**

### **3.4.1 System Automation**

The eventual goal of the chip-printing system is automation of printing process: mount a clean glass slide into the holder, press “start,” and then get a reproducible particle print on the slide. The system can and repeatedly generate the aerosol, deposit particles onto the chip, move to the microscope, print the particles onto slides in holder, and then move the chip to another aerosol outlet. However, the system is still semi-automated now, and some problems make full automation challenging. These problems include the reproducible printing does not have a feedback control and needs very careful manipulation, deposition quality cannot be automatically monitored, and chip can be burnt accidentally by the high voltage.

The printing reproducibility is now realized by high-precision motors and a slide holder. The theoretical reproducibility can be less than 0.5  $\mu\text{m}$ , if the slide is mounted carefully and the chip-printing system is not vibrated. However, the whole manipulation should be

done repeatedly and carefully, and it limits the automation and yield stability. A feedback control for chip-slide alignment should be developed for the automation.

For good particle deposition quality, the aerosol generation system should generate dense aerosol repeatedly. However, the density of generated aerosol is very unstable, and sometimes even no aerosol is generated. For generating dense aerosol, the injected compressed air should be fine tuned depending on the particle size, particle quantity,  $q/m$  value and humidity. In addition, the particles can easily block the tubes, sieves, and outlets in the aerosol generation system. Because of the unstable aerosol and the particle blocking, the automation of aerosol generation becomes very difficult, and hence the chip-printing system automation is also restricted.

The monitoring of particle-deposition quality on chip is also a problem. The quality monitor can only be done by eye now, and it limits the automaton as well. Besides, the CMOS chip can be easily burnt accidentally, which is also disadvantageous for system automation.

### **3.4.2 Theoretical Reproducibility and Homogeneity of Printing**

As discussed in section 3.3.1, the reproducibility of the printing can be less than  $0.5\ \mu\text{m}$  in chip-printing system. The slide together with the slide holder is fixed in X direction, and the minimal incremental motion in Y direction is  $0.5\ \mu\text{m}$ . On the other hand, the CMOS chip printinghead is fixed in Y direction and the minimal incremental motion in X direction is  $0.5\ \mu\text{m}$ . Therefore, the total printing tolerance should be less than  $0.5\ \mu\text{m}$  in both X and Y direction. The homogeneity tolerance will be less than  $20\ \text{mm} \times 5\ \mu\text{rad} = 0.01\ \mu\text{m}$ . The experiment results will be described and discussed in chapter 4.

### **3.4.3 Geometry Design and Particle Recycling**

Two geometry problems came up, when the chip-printing system is built. One is the motion of several aerosol tubes, and the other is the space for recycling system.

As mentioned in section 3.3.2, the 20 aerosol outlets and aerosol reservoirs are connected by 20 tubes. Besides, since each particle outlet needs two suction cups, the recycling system needs 40 tubes to connect these 40 suction cups. To sum up, 60 PVC tubes are needed for the aerosol and recycling system. These 60 tubes should move 400 mm, together with the aerosol outlets, repeatedly during the whole printing process. This is

quite difficult since the tubes need a lot of space and motion of these stiff tubes needs big torque. Besides, the tubes for the aerosol outlet should not bend too much, or the aerosol flow can not go to the chip perpendicularly.

The space for particle-recycling system is another problem. The aerosol suction cups should be mounted on the aerosol outlets. However, the space beyond the aerosol outlets can only be 15 mm, which is the travel range of the high-precision motor. Therefore, many components, including the suction cups, chip, chip connector, and chip holder, should be arranged to fit into this 15 mm space. To solve this problem, the chip connector should be redesigned in the future.

The size of chip-printing system, including the cover, is 0.8 m × 1 m × 1.5 m (W × H × L) and the size of laser printer is 0.9 m × 1.2 m × 3.1 m (W × H × L). Therefore, the chip-printing system is less space consuming than the laser printer.

#### **3.4.4 Time Needed for Printing onto Glass Slide**

One printing cycle includes depositing the particles on chip, printing onto slide, and moving the chip to aerosol outlets, microscope, and slide sequentially. The whole cycle takes ~80 seconds. In addition, the cycle should be repeated if the deposition quality or printing quality is poor. To sum up, printing a whole particle layer with 20 kinds of amino acid particles takes at least  $80 \text{ (seconds)} \times 20 = 1,600 \text{ (seconds)}$ .

## 4. CMOS-chip Based Particle Printing

After the whole chip-printing system is constructed, the system will be used to print the amino-acid particles from chip onto the glass slide. This chapter discusses how to get good particle printing quality on the slide. In section 4.2, the particle characteristics for ideal particle deposition on the chip will be discussed, since the deposition quality directly relates to the particle printing quality. The deposition quality on the chip depends on the number of particles deposited, particle contamination, and homogeneity. The number of particles deposited on the pixels should be enough for synthesis, so the coverage rate of melted particles can approach 100 %. Besides, the particles should not contaminate the adjacent spots to avoid wrong amino-acid sequences. The particle size and the environment humidity influences are discussed because they are very critical factors for deposition. Section 4.3 will compare the printing reproducibility and homogeneity of the system with the theoretical estimation in Chapter 3. The printing voltage, printing distance and particle cross contamination will also be discussed.

### 4.1 Particle Composition and Manufacture

The amino acids are encapsulated and protected in the solid particles, and then the amino-acid particles are addressed onto the glass slide for synthesis. For array synthesis, two requirements of these amino-acid particles should be met. In physics aspect, the particles should be precisely and reproducibly deposited onto slide by means of an electrical field. Therefore, the physics characteristics such as particle size and charge-to-mass ratio ( $q/m$  values) should be considered. In chemistry aspect, the particle components should be compatible to the synthesis process. That is, the components should not interfere with the amino-acid coupling and should be removable by the washing process. The viscosity of melted particles should also be considered, so the melted particles can merge together to cover the gap between particles. Accordingly, the coverage rate of the deposited amino acids can be increased. On the other hand, the melted particles should not spread to the nearby pixels and contaminate the pixels. At last, the melting point of 90 °C degree is chosen. At 90 °C temperature, the amino acids can couple efficiently, but still remain stable [BRE11].

The components of the particles include resin, “solid solvent,” protected amino acids, and charge control agent (Figure 2.4) [BRE11, KÖN10-2].



About 60 % of the particle mass is resin. The resin makes the particle thermally and mechanically stable. The resin used in the particles is SLEC PLT 7547 from Sekisui.

The solid solvent is at 25 % of the particle mass. It replaces the liquid solvent, such as DMF, used in the conventional liquid-based solid phase peptide synthesis. DMF is colorless liquid and is miscible with water and majority of organic liquids. With low evaporation rate, DMF is usually used as solvent. DPF and DPSO, which have melting points around 70 °C, are used here as solid solvent (Figure 4.1).

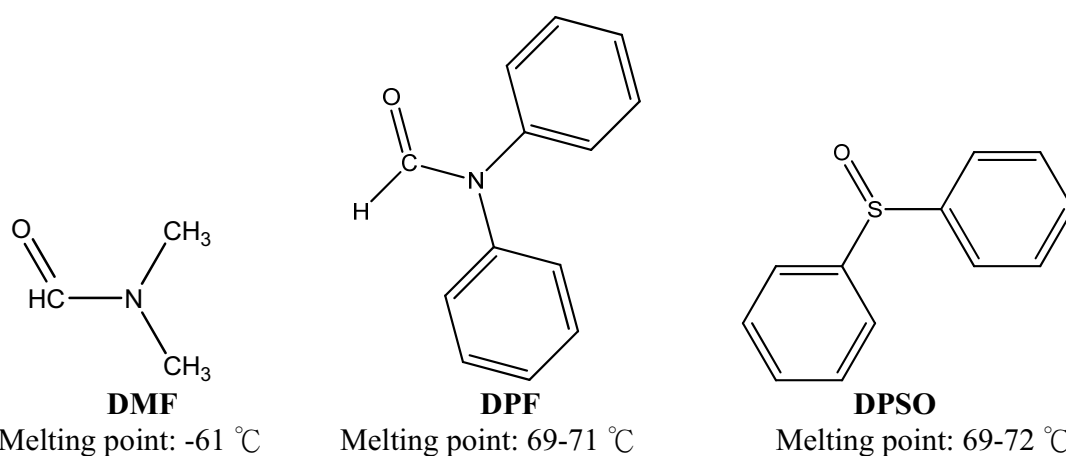


Figure 4.1: Chemical structures and melting points of solvents for conventional liquid-based solid phase peptide synthesis and solid-particle peptide synthesis [BEY05]. The DMF melts at -61 °C, and is used in solid phase peptide synthesis. The DPF and DPSO melt at around 70 °C, so they are used in solid-particle peptide synthesis.

The amino acids in the solid particles are in protected and activated form, as Fmoc-aminoacid-OPfp (see section 2.1.2). Typically, the amino-acid compounds contribute 10 % of the particle mass. Since different amino acids exhibit different molecular weight, the molar contents of different amino acids in the typical particles differ. For same mass, the lowest molar amino acid content (Fmoc-His(Trt)-OPfp, 785.77 g/mol) is about 59 % of the highest molar amino acid content (Fmoc-Glu-OPfp, 463.36 g/mol). This molar content difference should be considered when printing particles on to the slide, because the number of all amino acids joining the coupling reaction should be excessive.

Particles charge control agents are added to stabilize the particle charge, so the discharge in air of these particles will be slowed down. The charge control agents contribute 5 % of the particle mass. 4 % particle mass is pyrazolone orange and 1 % is sodium-di(aqua)-di(2-hydroxy-3-napthoic acid) ferrate(III).

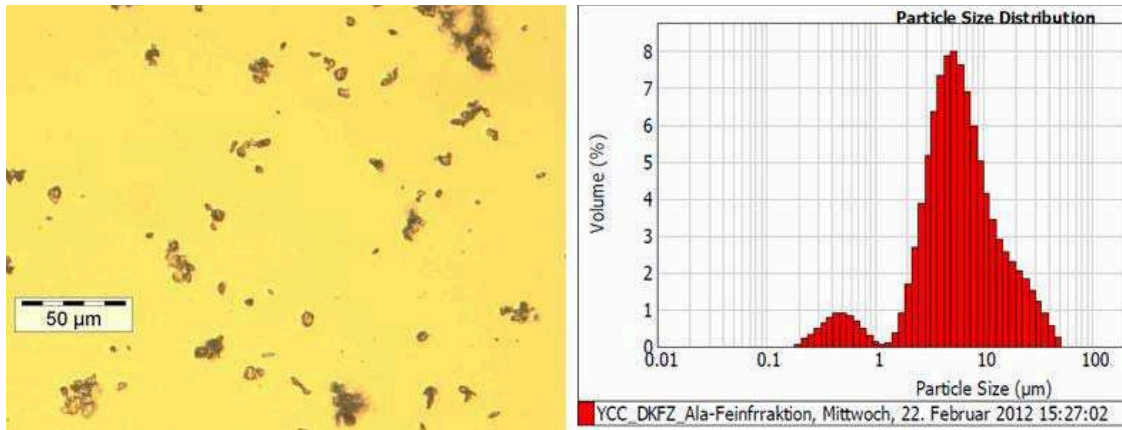
All the components were mixed and dissolved in acetone. Afterwards, the acetone was removed by various drying steps. Then the matrices were firstly roughly milled and then fine milled with air jet mill (Hosokawa Alpine 50AS). With analytical sieve (AS 200 digit, Retsch) and winnower (100 MZR, Hosokawa Alpine AG), the particles with desired size are sorted.

## 4.2 Particle Characteristics for Deposition

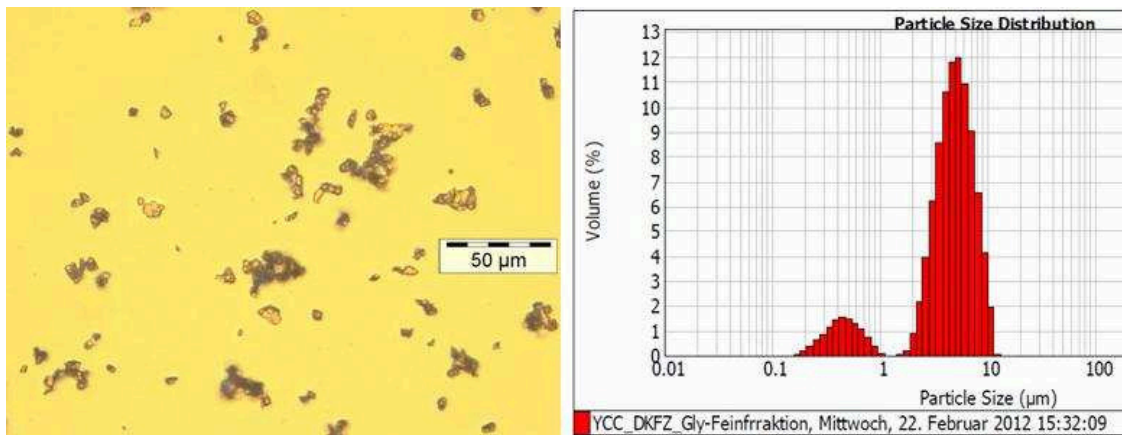
### 4.2.1 Particle Size

The particle deposition and printing quality is influenced by the particle size, shape, q/m value (charge to mass ratio), and environment humidity. Particles with uniform q/m values can be deposited more precisely onto assigned pixels and do not contaminate the adjacent pixels. The q/m values of particles were measured with a q/m meter (Trek, type 210HS-2) and the q/m value of the particles is around  $-4 \mu\text{C/g}$  [NES07-1]. Besides, round and small (2-6  $\mu\text{m}$ ) particles have better deposition quality than the other particles [LÖF11]. To classify the particles by size, the particles bigger than 32  $\mu\text{m}$  were removed by sieve. Then the distribution of particle size was measured by a Mastersizer (Malvern, type 2000).

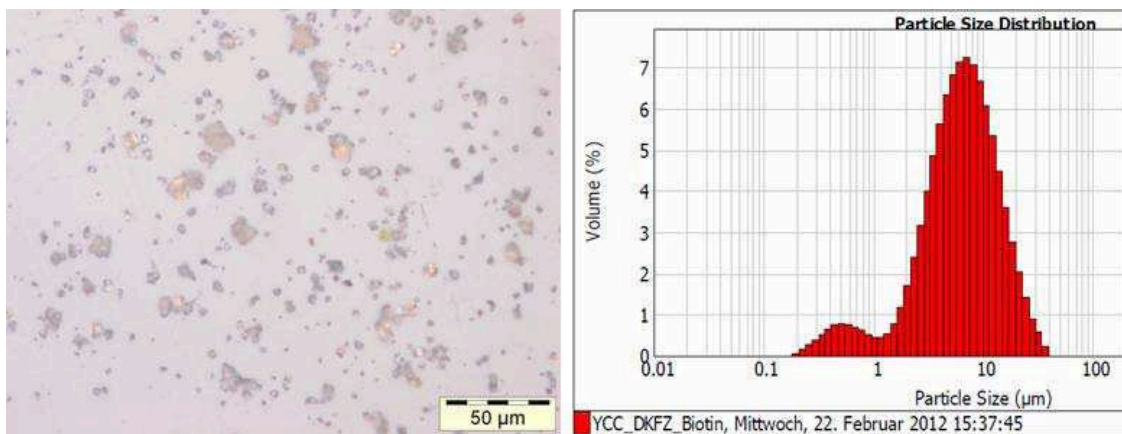
The size of alanine, glycine and biotin particles are shown in Figure 4.2. These three particles were printed onto a slide with the chip-printing system, and then were used for a combinatorial synthesis experiment. The diameters of most particles are between 1  $\mu\text{m}$  to 10  $\mu\text{m}$ . For alanine and biotin particles, 10-20 % of particles are bigger than 10  $\mu\text{m}$ . For glycine particles, almost all the particles are smaller than 10  $\mu\text{m}$ . The particles smaller than 1  $\mu\text{m}$  mainly come from the fine milling process. Another possible source might be the silica nanoparticles, which are added into the amino-acids particles after fine milling to prevent the particles from soaking water from air. The nanoparticles may be agglomerated and form bigger particles, which were detected by the Mastersizer. The different size distribution of particles comes from the milling procedure. Even the amino-acid matrices with exactly same composition have slightly different size distributions in terms of fine milled particles.



(a) Image and size distribution of alanine particles



(b) Image and size distribution of glycine particles



(c) Image and size distribution of biotin particles

Figure 4.2 The particle image taken with a microscope and particle size distribution measured with a Mastersizer (Malvern, type 2000). (a): Alanine particles (b): Glycine particles (c): Biotin particles. The glycine particles are smaller than 10 µm, while some alanine and biotin particles are bigger than 10 µm.

As shown in Figure 4.2, almost all of the glycine particles are smaller than 10  $\mu\text{m}$  while 10 % of biotin particles are bigger than 16  $\mu\text{m}$ . The glycine particles and biotin particles are deposited on chip pixels and then printed onto the slide to compare the influence of particle size (Figure 4.3). Most glycine particles are on the assigned spots and only a few particles contaminate the blank spots, i.e. are wrongly addressed. On the contrary, the printing result of biotin particles feature a lot of particle contaminations, and most of these contaminating particles are bigger than 10  $\mu\text{m}$ . The big particles can not be addressed onto the correct spot because they have higher mass and charge than small particles. After the electrical-potential acceleration between the aerosol sieve and the chip, the big particles have higher motion inertia, so the efficiency of selective electrical fields from the chip pixels decreases. Hence, the big particles can easily divert from the assigned pathway and be deposited on the wrong pixels [LEE09, LÖF11]. After printing, the particles addressed on the wrong pixels are also transferred by the electrical field and printed on the slide. In short, the printing results of glycine and biotin particles show that the particles smaller than 10  $\mu\text{m}$  can have better printing quality than particles bigger than 10  $\mu\text{m}$ .

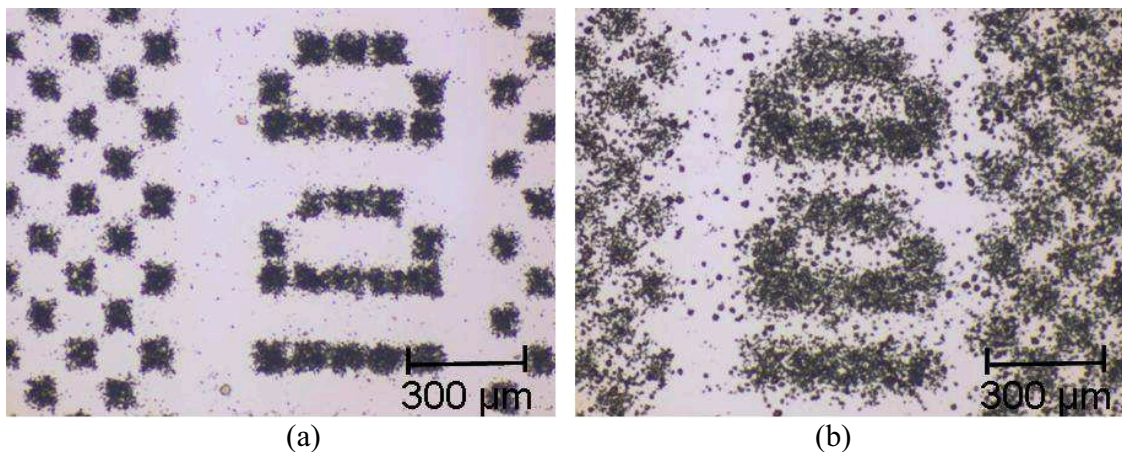


Figure 4.3: The particles printed onto the glass slide. (a): Glycine particles. (b): Biotin particles. The printing of biotin particles has a lot of contamination. Most of the wrongly deposited particles are the particles bigger than 10  $\mu\text{m}$ .

Since the particle size is an important factor of particle deposition and printing quality, the printer toners smaller than 10  $\mu\text{m}$  can also deposit with few contamination onto the chip. The commercially available printer toner particles are first used to test the deposition quality, e.g. the reproducibility, because the amino-acid particles are expensive (20-50 Euro / g). The printer toners cost almost nothing since 50-100 mL particles can be collected from a discarded cartridge. The size distribution of Xerox, Canon, OKI, and HP toner particles are measured by Mastersizer (Table 4.1). The Xerox

toner particles are chosen, because their size is smallest ( $\sim 6 \mu\text{m}$ ) and is close to the amino-acid particles ( $4\text{-}6 \mu\text{m}$ ). In addition, the Xerox toners are most round particles in these commercial particles and have a very good deposition quality on the CMOS chip (Figure 4.4).

	D(0.5), 50% of particles are under: ( $\mu\text{m}$ )	D(0.9), 90% of particles are under: ( $\mu\text{m}$ )	Span= $\{D(0.9)-D(0.1)\}/D(0.5)$
Alanine particles	5.661	18.002	2.788
Glycine particles	4.704	7.965	1.540
Biotin particles	6.415	15.987	2.180
Xerox toner black	6.061	8.309	0.644
Xerox toner cyan	5.731	7.847	0.64
Xerox toner yellow	5.778	7.951	0.649
Canon toner cyan	9.268	12.197	0.551
Canon toner cyan	8.714	12.697	0.773
OKI toner black	9.991	14.836	0.816
HP toner black	11.662	17.259	0.807

Table 4.1: The size distribution of the particles.

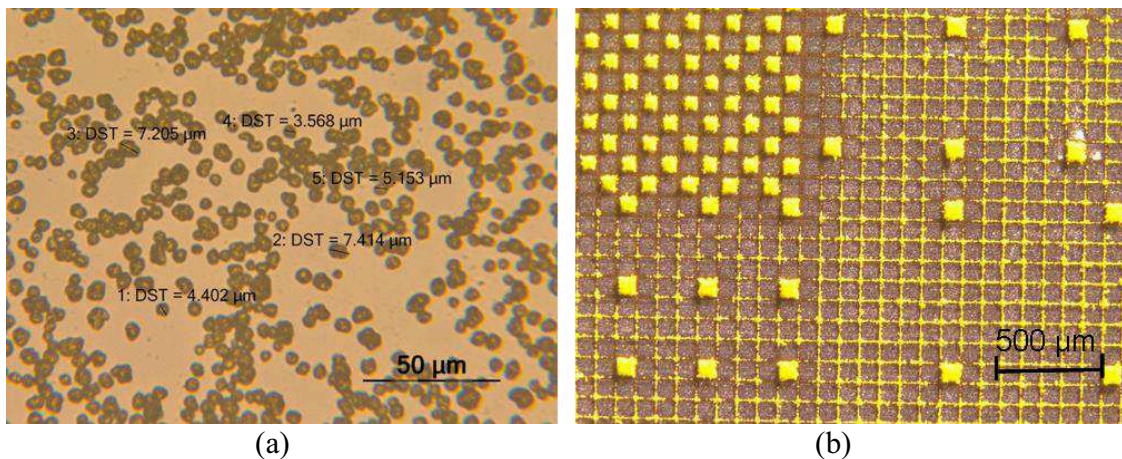
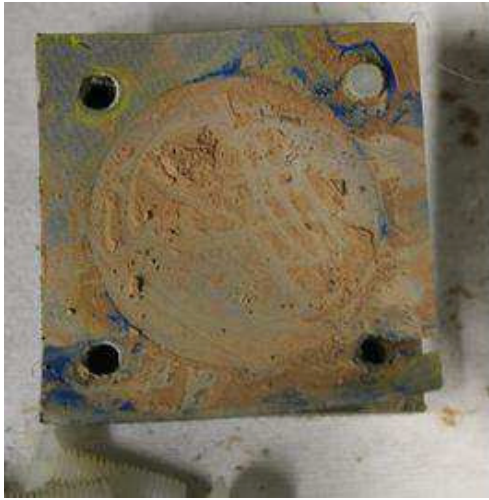


Figure 4.4 (a): The yellow Xerox toner particles. The particles are more round than the amino-acid particles. (b): The yellow Xerox toners deposited onto the CMOS-chip pixels. A large number of particles are addressed on the assigned pixels and few particles contaminate the blank pixels.

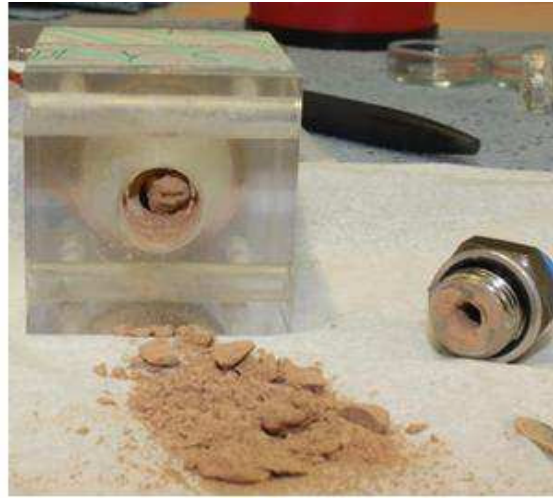
### 4.2.2 Humidity Influence on Particles

In addition to the particle size and shape, the water absorbed by the particles also influences the particle deposition and printing. Particles stored in a humid environment absorb water from the air and become moist. The humid particles will be agglomerated and are stickier than dry particles. These agglomerated and sticky particles can easily block the sieve at the aerosol outlet, and prevent the aerosol from going out (Figure 4.5(a)). The particles will therefore remain in the aerosol outlet and form even bigger bulks. The particle bulks make the air flow more difficult and the whole aerosol system is blocked with agglomerated particles eventually. Figure 4.5(b) shows the particle bulks cleaned out from the outlet. These agglomerated particles are one important reason of unstable aerosol generation. With unstable aerosol, the quality of particle deposition on chip can be hardly controlled. Even though some humid particles can be deposited on the chip pixels, the humid particles will adhere on the chip pixels. Hence, only a few humid particles can be transferred from chip onto slide with 2.6 kV/mm electrical field (Figure 4.6(a)), and most particles remain on the chip.

To solve the humidity problem, the particles should be stored in an air-conditioned room with relative humidity below 30 %. Otherwise, the particles should be mixed with more silica nanoparticles and dried with a desiccator. Hydrophilic fumed silica nanoparticles (Aerosil, 0.05 % of particle mass) were added into the particles. These nanoparticles attach themselves to the particle surface and prevent the particles from soaking water. Besides, the particles were dried overnight with vacuum desiccator at room temperature. In vacuum environment, the water in the particles evaporates and is absorbed by the drying beads in the desiccator. A dehumidifier was also used to control the humidity in the chip-printing system. Figure 4.6 shows the printing result of humid and dried particles. The printing quality of dried particles is much better than that of particles without drying processes.

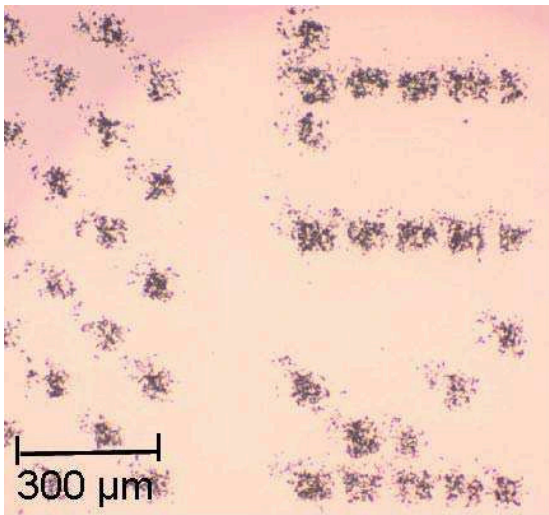


(a)

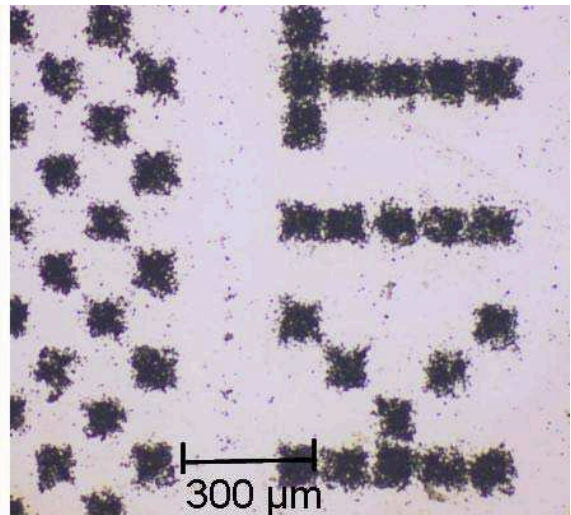


(b)

Figure 4.5 (a): Biotin particles block the sieve (10- $\mu\text{m}$  meshes), so the aerosol can hardly go out from the outlet. (b): Particle bulks in the aerosol outlet. The whole outlet chamber is filled with particle bulks.



(a)



(b)

Figure 4.6: Glycine particles printed onto the glass slide (a): The humid particles. Only a few particles can be printed onto the slide. (b): The particles are mixed with silica nanoparticles and are dried in a desiccator. Most of the dried particles can be printed with the electrical field.

## 4.3 Particle Printing from CMOS Chip onto Glass Slide

As discussed in Chapter 3, the expected tolerances of the printing reproducibility are smaller than  $0.5\ \mu\text{m}$  in both X and Y directions and the expected tolerance of the printing parallelity is smaller than  $5\ \mu\text{rad}$  (or  $0.1\ \mu\text{m}$ ). The reproducibility is checked with Xerox toners, and the parallelity is estimated with the three contact sensors on the CMOS chip. The printing distance, printing voltage, and particle cross contamination are also discussed.

### 4.3.1 Reproducibility of Printing

The printing system should be able to print particles precisely (tolerance  $< 10\ \mu\text{m}$ ) on the same position repetitively, so the particles will not be printed on the adjacent pixels by mistake. For the printing reproducibility, a slide holder was made to fix the slide and high-precision motors were used to move the chip. Hence, the reproducibility of the particle printing can be considered in two aspects separately. One is the positioning reproducibility of the CMOS-chip printing head and the other is the positioning reproducibility of the remounted glass slide. If both the chip and slide can be precisely and repetitively located, then the relative position between chip and slide is reproducible. That is, the printing precision is reproducible. The positioning reproducibility of the chip printing head is checked by printing particles onto a fixed glass slide repetitively. Subsequently, the positioning reproducibility of slide mounting is tested.

To test the printing-head reproducibility, a clean glass slide is fixed in the slide holder, and the yellow Xerox toner particles on the CMOS-chip are printed onto the slide. Afterwards, the CMOS-chip printing head moves back to the aerosol outlet to deposit the cyan Xerox toner particles, and then the printing head moves to the fixed slide again to print the cyan toner particles. The printing result is shown in Figure 4.7. On the left side are the toner particles printed from the switched-on chip pixels. The grids on the right side are the toner particles from switched-off pixels, since the unused toner particles are collected by the electrical field from chip grid. The overlap of toner particle grids shows that the tolerance of cyan toner-particle printing and the yellow toner-particle printing is very small (smaller than  $5\ \mu\text{m}$ ). That is, the positioning reproducibility of the printing head is very good. The printing test of fixed slide and repositioned printing head has been done more than 10 times, and the tolerance can be always smaller than 10 or even  $5\ \mu\text{m}$  under two conditions. One condition is that the chip should be fully fixed on the printing head, so the chip will not be shifted by any external force. The other is every part of the



system, including the slide holder, chip, and printing head, should not be vibrated during the printing process.

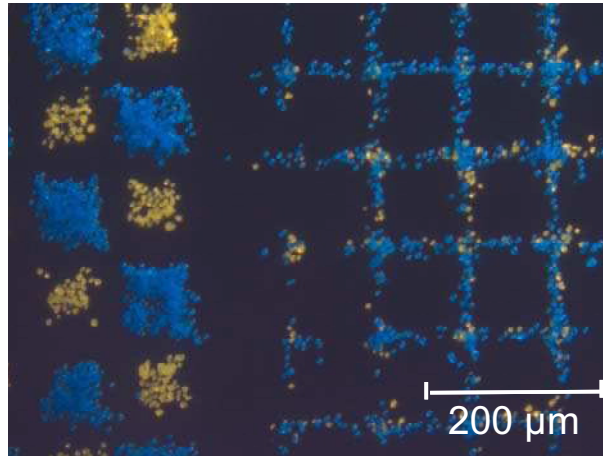


Figure 4.7: Xerox cyan and yellow toner particles are printed onto a slide to test the reproducibility of printing head positioning. The slide is fixed, and the chip printing head has been repositioned in between the yellow toner-particle printing and cyan toner particle printing. The spots on the left side are toner particles printed from the switched-on pixels. The grids on the right side are the toner particles, which are printed from the grid. The grid voltage (40 V) collects the particles nearby the switched-off pixels, so the particles will not contaminate the switched-off pixels.

After the test of printing-head reproducibility, the reproducibility of slide mounting in the holder was tested. The slide was remounted in the holder in between the printing of cyan toner particle and yellow toner particle. Since the printing head has very small repositioning tolerance ( $< 5 \mu\text{m}$ ), the printing head was also repositioned to get new particles in between the two printing steps. Hence, the tolerance of the printing result is the summation tolerance of printing head repositioning and slide remounting. The printing result is shown in Figure 4.8. The spots are toner particles printed from the switched-on chip pixels and the grids are toner particles from switched-off chip pixels. Figure 4.8(a) shows a good printing reproducibility (tolerance  $< 10 \mu\text{m}$ ) and Figure 4.8(b) shows a bad printing reproducibility (tolerance  $> 20 \mu\text{m}$ ). The tolerance mainly comes from the slide remounting, since the printing-head repositioning has small tolerance. If the slide is remounted into the holder carefully, the tolerance can be small (Figure 4.8(a)). However, the tolerance can be 20-30  $\mu\text{m}$ , if the slide is not fixed in the exactly same position (Figure 4.8(b)). This tolerance of slide positioning can come from several possible reasons. One main reason is that the slide is mounted in the holder manually, and a small mistake can move the slide. To solve this problem, the mounted slide was tenderly knocked on the edge with a hammer, so the slide edge was fixed by the fixing

poles in holder. Another reason is that beneath the slide, a line for particle-printing voltage is attached. If this line is moved, the slide will also be moved. Therefore, this line was fixed with tape.

To sum up, the tolerance of printing reproducibility can be smaller than  $5\ \mu\text{m}$ , if some rules are followed in the printing process:

- The whole system should not be vibrated during the printing process.
- The chip should be fully fixed on the printing head. The chip cable should also be fixed, or the chip may be moved by the cable.
- The slide should be fixed in the holder tightly, so the slide will not be moved by a small vibrate.
- The particle-printing voltage line connected to the holder should be fixed. Therefore, the line will not have influence on the slide when it moves.
- After mounting the slide into the holder, a hammer should be used to knock the slide edges tenderly to make sure the slide edge contacts the poles tightly.

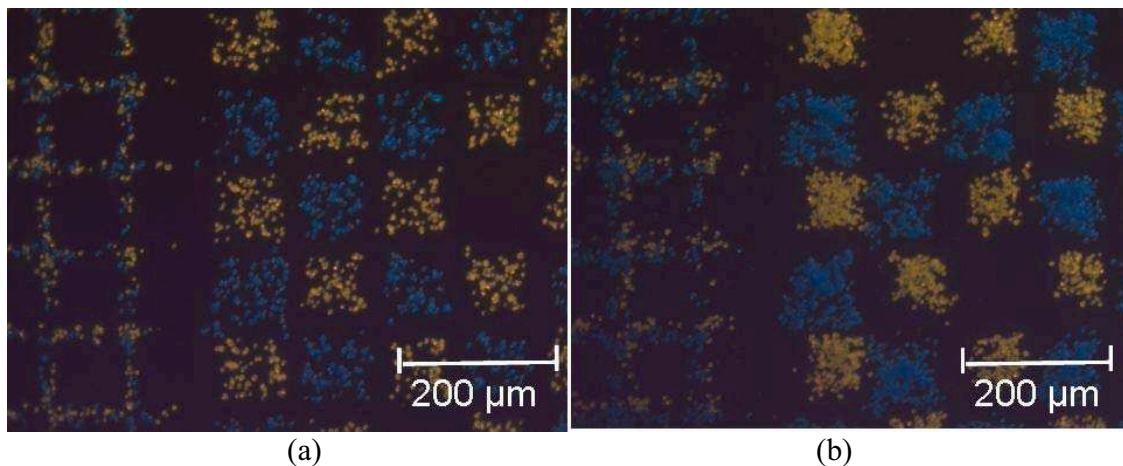


Figure 4.8: Xerox toner cyan and yellow particles printed on slide to test the reproducibility of slide mounting. The slide was remounted once between the printing of cyan and yellow toner particles. (a): Good printing reproducibility. (b): Poor printing reproducibility (tolerance  $\sim 30\ \mu\text{m}$ ).

To make sure that the particles are printed on the same position repetitively, a reference marker for the particle printing position is necessary. The previously printed particles can not be used as this reference since the particle residues will be washed away after coupling, so nothing on the slide can be seen after washing process. Hence, some markers were made on the glass slide as references. Figure 4.9 (a), (b), and (c) shows the marker made by laser, small rolling saw, and glass scribe (Glascribe<sup>®</sup> F44150), respectively. Both the markers made by the laser and rolling saw are thicker than  $300\ \mu\text{m}$  while the

marker made by diamond scribe is about 20  $\mu\text{m}$ . Therefore, the marker made with glass scribe was used as the position reference. Three markers were scribed on the slide as position references. After every printing, the images of the particle pattern together with the marker were taken, so the reproducibility of printing can be checked by comparing the markers and the printed particles.

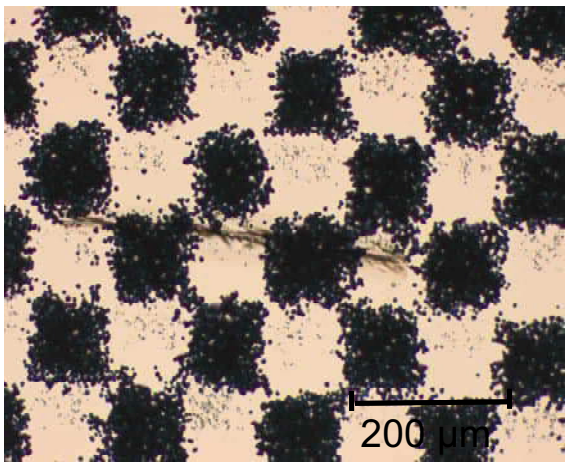
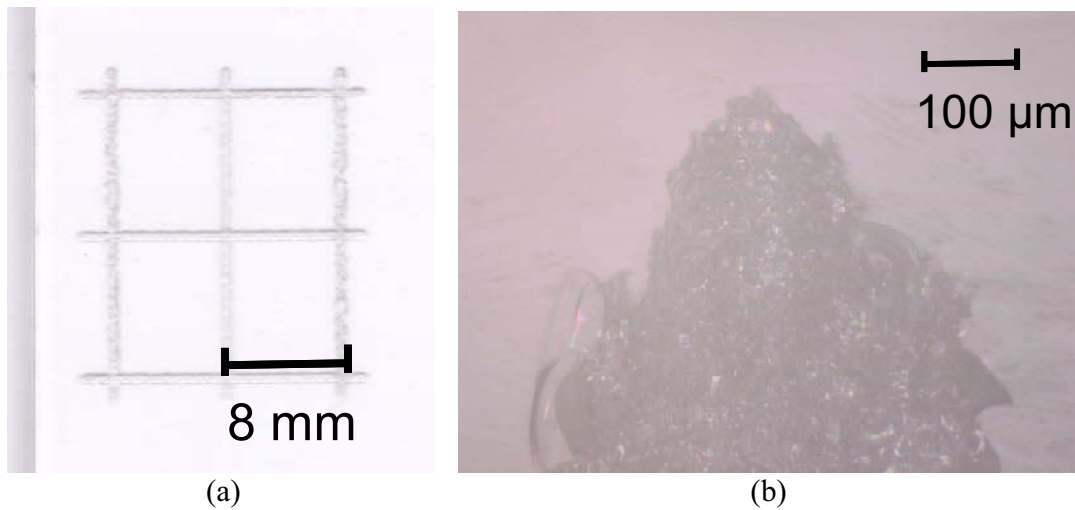


Figure 4.9: Reference markers on glass slide. (a): Marker made by laser, the line thickness is  $\sim 600 \mu\text{m}$ . (b): Marker made by rolling saw. (c): Marker made by glass scribe and printed particles.

To sum up, the printing tolerance of the printing system can be small ( $< 5 \mu\text{m}$ ) if the printing process is done carefully. Generally, the tolerance of the printing head reproducibility is smaller than 5  $\mu\text{m}$ . With correct and careful slide mounting, the reproducibility of the slide mounting can also be acceptable. Three markers are made on

the slide as position references. Therefore, the reproducibility of particle printing can be evaluated even if the previous particle residues are washed away.

### **4.3.2 Homogeneity of Printing**

To make the number of peptides synthesized on different spots similar, the amino-acid particles should be homogeneously transferred onto the glass slide. Two issues were considered for printing particles homogeneously on slide. One is the chip should be parallel to the glass slide surface during printing. The other is the particles should be deposited onto the chip homogeneously. As discussed in Chapter 3, the theoretical parallel tolerance results from the tilt stage is smaller than 5  $\mu\text{rad}$  (or 0.01  $\mu\text{m}$ ). The experiment tolerance was estimated with three contact sensors and the high-precision motors.

As mentioned in section 3.2.3, there are three contact sensors on three corners of the CMOS chip, and the sensor is 25  $\mu\text{m}$  higher than the chip surface. When the contact sensor touches the conductive surface (such as gold wafer), the LED light in corresponding sensor circuit switches on. During the chip adjustment, the chip is tilted and moved till the three LED just switch on, and then the chip is parallel to the surface. After the adjustment, the chip traveling range for switching all the LED lights from on to off can be 10-20  $\mu\text{m}$ . That is, the tolerance of parallelity is 10-20  $\mu\text{m}$ . The difference of printing electrical field caused by this tolerance is small, since the slide thickness is 1 mm and insulating. The electrical field tolerance caused by this tolerance is only about 2 % (voltage divided by 1 mm and by 1.02 mm). However, parallelizing the chip to slide is still important since the size of big particles is about 10  $\mu\text{m}$ . If the chip tilts too much, the particles between chip and slide will scratch the chip surface.

The homogeneity of particle deposition on the CMOS chip was also considered for homogeneous printing. Figure 4.10 shows the particles printed on the glass slide. The figures from left to right correspond to the parallel area on the slide from left to right, respectively. The particles printed onto both sides are more than the particles printed onto the middle area. It indicates that the inhomogeneous printing does not result from the unparallelity between slide and chip. In addition, the particle contamination on the right side is more than the contamination on the left side. The reason for this inhomogeneity may be the inhomogeneity of particle deposition on CMOS chip. Since the particles are deposited on the CMOS chip in aerosol, the aerosol turbulence results in some “particle dunes” on the chip surface (Figure 4.11). Hence, the particles deposition on the chip surface is not homogeneous, so the particles printed on the slide is inhomogeneous either.

A solution for this problem is depositing and printing particles twice, since the particle distribution is random because of the turbulence. Hence, the spots with only few deposited particles can get enough particles for synthesis.



Figure 4.10: Glycine particles printed on the glass slide. The three figures are parallel on the slide. Left, middle, and right figures correspond to the left, middle, and right slide area, respectively. The particles on both sides are more than the particles in the middle.

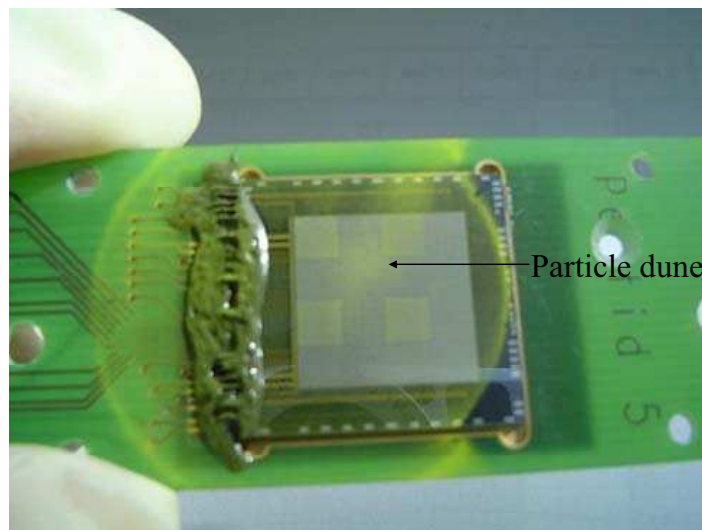


Figure 4.11: Xerox toner particles deposited on the CMOS chip. Some areas have more particle deposition and have the “particle dune.” The circle around the chip comes from the round aerosol outlet.

To sum up, the tolerance of parallelity between chip and slide can be 10-20  $\mu\text{m}$  after adjustment. The main problem of homogeneous printing is not the parallelity between chip and slide but the homogeneity of particle deposition on the chip. A solution for this problem is to deposit and print the particles twice.

### 4.3.3 Voltage and Space between Chip and Slide

During the particle printing, the space between chip and slide is also an important factor for deposition quality. If the space is small ( $< 30 \mu\text{m}$ ), the chip surface will be scratched

or pressed by the particles. Accordingly, short circuits are induced from distorted chip and damage the chip during the high-voltage printing. If the space is too big ( $> 100 \mu\text{m}$ ), the particles spread during the transfer and contaminate adjacent pixels. Besides, the maximum printing voltage was discussed to prevent the electrical breakdown.

Figure 4.12 shows damaged pixels on a CMOS chip and burn mark on a slide. The space between chip surface and slide was  $20\text{-}30 \mu\text{m}$  during printing. In Figure 4.12(a), the pixels and grid were burnt and melted, and the blue spots on pixels are the melted toner particles. If the chip surface is close to the slide ( $< 30 \mu\text{m}$ ), the particle piles press the chip surface. Hence, the thin ( $3 \mu\text{m}$ ) metal layer fabricated in the chip will be deformed. In high-voltage particle printing, the deformed metal layer can easily cause short circuits and the circuit will be burnt. The particles will be melted by the high temperature at the same time. When the circuit is burnt, the high temperature also caused a burn mark on the glass slide (Figure 4.12(b)). To prevent the short circuit from burning the chip, the printing distance should be bigger than  $40 \mu\text{m}$ . Besides, the  $100 \text{ V}$  pixel voltage and  $30 \text{ V}$  grid voltage applied on chip should be switched off, so the pixels and grid can be grounded. Grounding the pixels and grid can bring away excessive electrons and protect the circuit during the high-voltage printing.

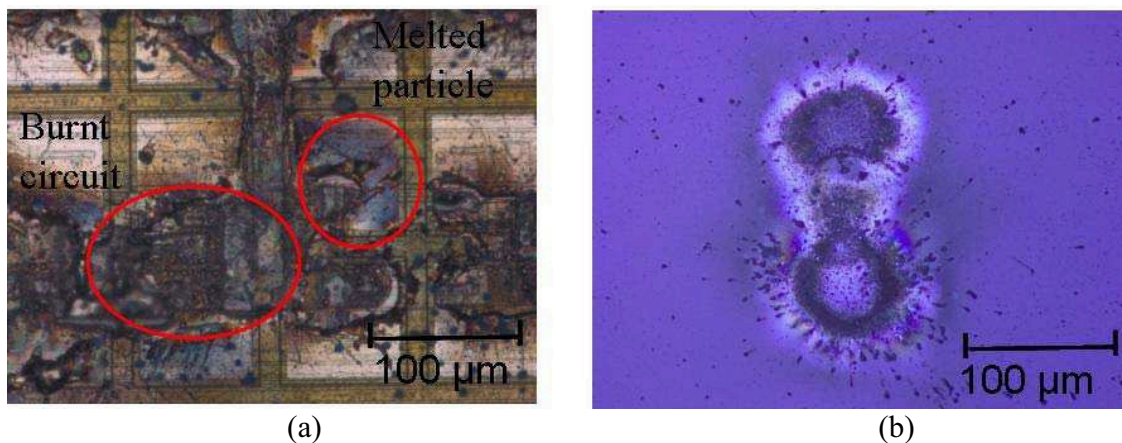


Figure 4.12 (a): The burnt CMOS-chip pixels grid. The blue spots are the melted toner particles. The breakdown cascade and the pixels are burnt in a row. (b): The burn mark on the surface of glass slide. The toner particles are melted and adhere onto the slide.

The chip surface cannot be too close to the slide, but can not be too far away from the slide either. If the distance between chip and slide is too big, the particles will spread during the long transfer distance. Accordingly, the particles will contaminate the adjacent pixels (Figure 4.13(a)). If the space is only  $40\text{-}50 \mu\text{m}$ , the particles will not spread in this transfer distance, as shown in Figure 4.13(b).

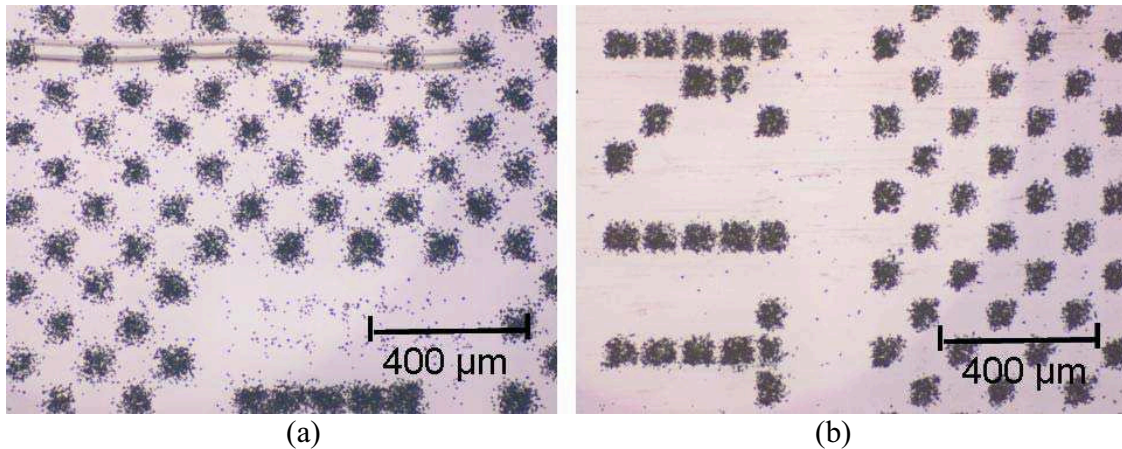


Figure 4.13: Alanine particles printed onto the glass slides with different chip-to-slide distances. (a): 150-160  $\mu\text{m}$ . The particles spread and contaminate the adjacent blank pixels. (b): 40-50  $\mu\text{m}$ . Few particles spread and contaminate the blank pixels.

The electrical breakdown caused by high electrical field is also considered. The threshold of electrical breakdown in air ( $E_{kp}$ ) is 33k V / cm, and the electrical field applied to the particle printing is 3 kV / 0.1 cm = 30 kV/cm. The glass slide used for printing has higher electrical-field threshold than the threshold in air. Therefore, the electrical breakdown will not appear if the voltage is smaller than 3 kV. 2.5-2.6 kV is chosen for the printing process to prevent the electrical breakdown.

To sum up, to prevent the chip from being burnt, the space between chip and slide during high-voltage printing process should be big enough ( $> 30 \mu\text{m}$ ), so that the particles will not press the chip. The space should not be too big either, or the particles will spread to adjacent pixels. Therefore, the optimal space for particle printing is 40-50  $\mu\text{m}$ . In addition, the pixel and grid voltage should be switched off to protect the circuit. The printing voltage should be 2.5-2.6 kV.

#### 4.3.4 Cross Contamination of Printing Result

After the printing parameters are optimized, the cross contamination of different particles was discussed. As mentioned in section 4.2, particles with proper size, shape and  $q / m$  value can correctly deposit on switched-on pixels, and do not contaminate the switched-off pixels. However, the particles near the area with only switched-off pixels cannot be collected by the electrical field and may deposit on the switched-off pixels. To prevent this contamination, a grid was fabricated on chip and connected to 30 V. The electrical field from the grid can collect the unused particles to prevent the particles from depositing onto the switched-off pixels [KÖN10-2].

To check the cross contamination of particle deposition, toner particles but not amino-acid particles were used, because different amino-acid particles still have similar color and appearance. Two kinds of Xerox toners, which are quite small ( $\sim 6 \mu\text{m}$ ) and round, were deposited on the CMOS chip and then were printed onto a glass substrate. The printing result is shown in Figure 4.14. The grid beside the switched-off pixels collected the excessive particles, so the particles will not contaminate these pixels. The switched-on pixels can collect toner particles and no toner particles are addressed onto wrong pixels. Based on this result, one can say that there should be few contamination on blank pixels if the particles are round, small and with proper  $q/m$  value.

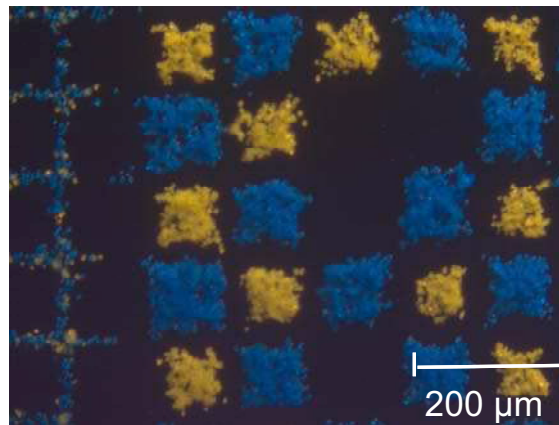


Figure 4.14: Cyan and yellow Xerox toners printed onto the glass slide. The spots are particles printed from switched-on pixels and the grids are particles form switched-off pixel area. Few particles contaminate the blank or adjacent spots.

## 4.4 Discussion

In this chapter, the particle characteristics, printing distance and printing voltage were discussed to optimize the particle printing quality. The reproducibility, homogeneity and cross contamination of the printing result were also discussed. For ideal particle deposition quality on the chip, the particles should be round and small ( $2\text{-}6 \mu\text{m}$ ). Big particles ( $> 10 \mu\text{m}$ ) have big inertia and can not always be correctly addressed onto the pixels by the electrical field. The  $q/m$  value of particles should be around  $-4 \mu\text{C/g}$ . In addition, the particles should be dry for printing. Otherwise, the moist particles will adhere on the chip and the agglomerated particles will block the aerosol system. The best method for getting dry particles is storing the particles and chip-printing system in an air-conditioned room with humidity below 30 %. Another possibility is adding some silica nanoparticles to the particles and, every time before use, the particles should be dried in a desiccator.



The printing reproducibility of the chip-printing system can be good (tolerance  $< 5 \mu\text{m}$ ) if the printing system has not been vibrated and the slide is mounted in the holder correctly. The tolerance of printing head repositioning is smaller than  $5 \mu\text{m}$ , and the main printing tolerance comes from the slide mounting and slide holder. However, the slides can still be precisely repositioned with tender knock and correct mounting. With high-precision motors and contact sensors on the chip, the chip surface can also be parallelized to the slide with tolerance less than  $20 \mu\text{m}$ . However, the homogeneity of the particle printed onto the slide is influenced not only by the chip parallelity but also by the particle layer homogeneity on chip. Unfortunately, the homogeneity of particle deposition on chip is still difficult to control, because the particles are deposited on chip by aerosol. To solve the homogeneity problem of particle deposition, the particles are deposited on chip and printed on slide twice, so the spots with too few particles can be covered with enough particles for synthesis. However, if a spot is deposited with too many particles, the particles will also spread and contaminate the adjacent spots.

During printing, the optimal distance between chip and slide is  $50\text{-}60 \mu\text{m}$ . With this distance, the chip surface will not be pressed by particles and the short circuit will not be induced. The distance is also not too big such that the particles will not spread and thereby contaminate the adjacent spots. The toner experiments also shows that the particles will not cross contaminate the nearby spots if the particles are round and small.

On the other hand, the chip-printing system can still be improved in several aspects. For the system automation and printing reproducibility, a position sensor for detecting the relative position between chip and slide is necessary. With the position sensor, a feedback control of the chip positioning can be setup so a good printing reproducibility can be achieved more easily. A photo sensor might be considered for the position detection. Mounting a USB camera beneath the slide holder to observe the chip position is another alternative. For the aerosol generation system, stable aerosol generation and homogeneous particle deposition on chip are both important issues. The aerosol generation system should be improved or another solution for depositing particles onto the CMOS chip homogeneously should be developed.

## 5. Combinatorial Synthesis with Chip-printing System

After the chip-printing system was calibrated, the particles can be printed onto slide with good reproducibility, high coverage rate and few contaminations. Then the printed particles were melted to release monomers for synthesis. The synthesis result was stained and scanned to see whether the chip-printed particles work for peptide synthesis. For the synthesis experiment, two different sequences with biotin, alanine, and glycine were designed. The two sequences were stained with different protein separately for cross control. This chapter describes the chip-printing based chemical synthesis process, and discusses the synthesis results.

### 5.1 Synthesis with Amino Acids and Biotin

Two kinds of sequences were designed and synthesized with the chip-printed particles, and then the sequences were stained with two different labeled proteins. The two sequences are glycine-glycine and alanine-biotin (Figure 5.1). The glycine and the alanine were chosen since these two amino acids have no functional group. Therefore, the side group protection and deprotection did not have to be considered during the synthesis process. The glycine-glycine sequence was coupled with a hemagglutinin (HA), which can be stained with anti-HA antibody. The biotin was stained with streptavidin (STP). The anti-HA antibody was labeled with Cy5 (wavelength 647 nm) and the streptavidin was labeled with Cy3 (wavelength 546 nm). At last, scanner detected the emission of 647 nm from the glycine pattern and the emission of 546 nm from biotin pattern, and then the quality of chip-based particle printing and synthesis process was evaluated by the pattern.

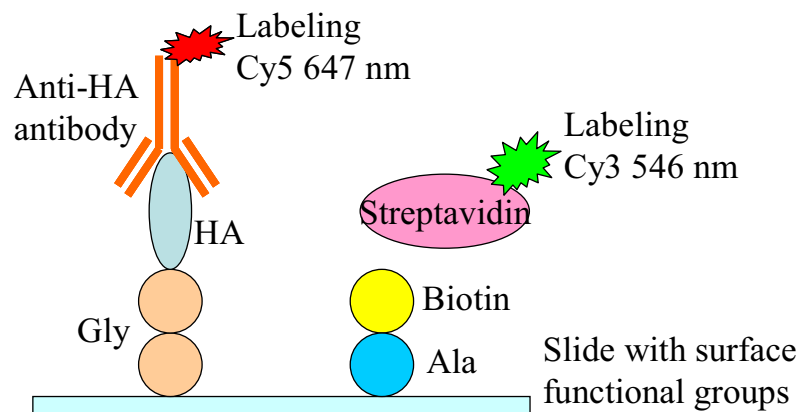


Figure 5.1: Two sequences were synthesized with the particles printed by the system. The last glycine was coupled with HA epitope, which was stained with Cy5 labeled anti-HA antibody. The biotin was stained with streptavidin (STP), which was labeled with Cy3 fluorescent dye.

Figure 5.2 shows the chemical structure of biotin. Biotin has extraordinarily high and specific binding affinity for streptavidin. The dissociation constant of biotin and streptavidin is on the order of  $10^{-14}$  mol / L [HOL05]. The HA epitope consists of nine amino acids (YPYDVPDYA). It can be stained with anti-HA antibody.

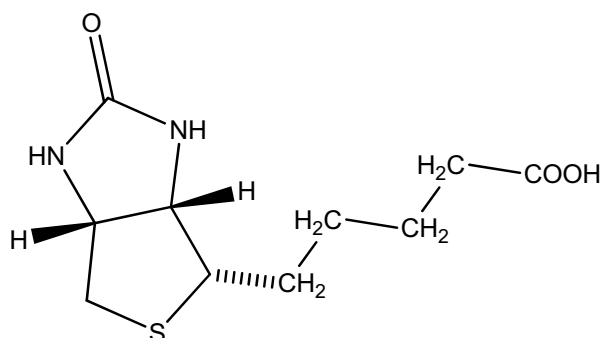


Figure 5.2: The chemical structure of biotin.

## 5.2 Chemical Synthesis and Staining

Most steps of the particle-based synthesis are the same as in the conventional solid phase peptide synthesis, except the coupling step. The printed particles are melted to release amino acid for coupling [STA08-1]. After coupling, the coupled monomers are deprotected and particle residues are washed away (Figure 5.3). Then the next particle layer is printed, so the next monolayer can be coupled. This coupling-deprotecting cycle continues till the whole sequences are synthesized. Afterwards, the side groups on the sequence will be deprotected for staining.

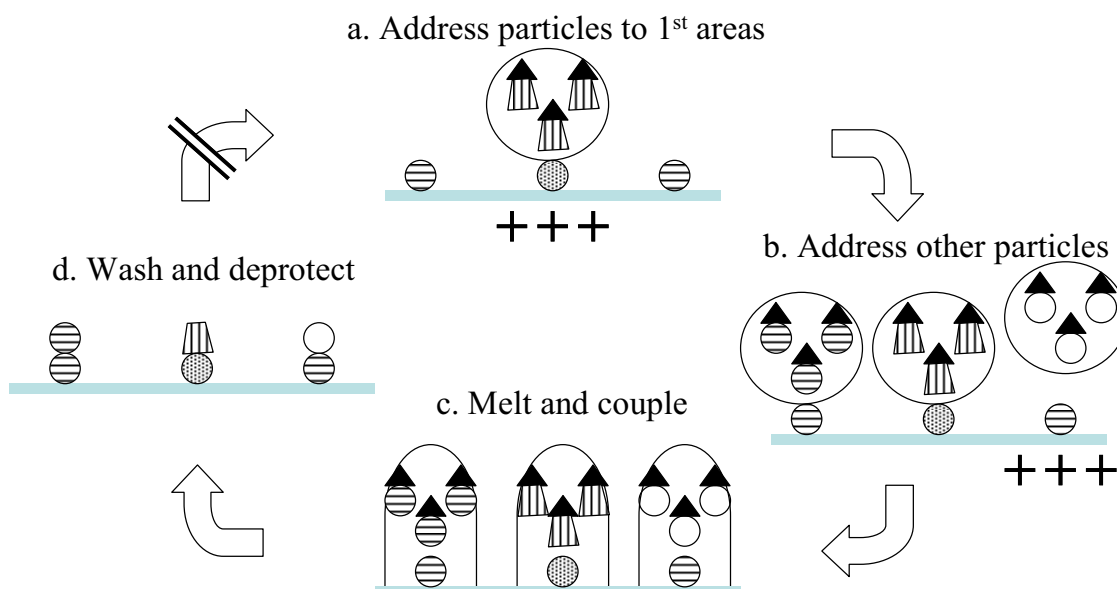


Figure 5.3: Scheme for particle-based combinatorial synthesis. (a): On the CMOS chip, individual pixels are switched to voltage and generate a pattern of electrical fields. The particles are addressed onto the switched-on pixels by electrical field. (b): Different patterns of the pixels are switched to voltage to address all 20 different amino-acid particles onto the chip surface. (c): The whole layer of addressed particles is melted to induce the coupling reaction at the same time. (d): Excessive monomers and the particle residues are washed away. The Fmoc protecting group is deprotected. The coupling cycle repeats till the peptide array is generated.

### 5.2.1 Materials

Dichloromethane (anhydrous, analytical grade), Ethanol (analytical grade), and Methanol (analytical grade) were purchased from AppliChem (Darmstadt, Germany).

Poly(ethylenglycol)methylmethacrylat (PEGMA, mol. wt., ~360 g/mol), N,N-Dimethylformamid (DMF, anhydrous, dried over 0.4-nm molecular sieve.), Acetic anhydride (analytical grade), Bovine serum albumin (BSA, 98 %, MW66000 Da) and N,N-Diisopropylethylamine (DIPEA, analytical grade) are purchased from Sigma-Aldrich (Munich, Germany).

Trifluoroacetic acid (TFA, 99 %) was purchased from Acros Organics, (Geel, Belgium).

Fmoc- $\beta$ -Alanin was purchased from Iris Biotechnology (California, USA).

Anti-HA antibody Cy5 (647 nm), Streptavidin Cy3 (546 nm, purified) were purchased from United States Biological (USA).

Slides with 2D-amino and 3D-amino coated slides were purchased from PolyAn (Berlin, Germany).

### **5.2.2 Printing and Melting of Biotin, Alanine, and Glycine Particles**

Before particle printing, the glass slides should be cleaned, coated and marked. The glass slides will be cleaned with KOH and acetone first. Then the slide should be coated so the slide surface will have amino groups for monomer coupling. On the coated slides, three markers are scribed with the glassscribe as position references.

After the slides are prepared, the particles will be printed onto the slide for synthesis. As shown in Figure 5.1, the first two monomers of the biotin-alanine and glycine-glycine sequences are alanine and glycine. The alanine and glycine particles are deposited on chip in desired patterns and then printed onto the glass slide (Figure 5.4 Left). The particles are deposited and printed twice, so the particles on the glass slide can be enough and homogeneous. Then the printed particles are melted and the released monomers are coupled to the surface (Figure 5.4 Right). The printed alanine particles are less than the glycine particles, since the glycine particles have much less contamination than alanine particles. The reason is that almost all the glycine particles are smaller than 10  $\mu\text{m}$ , and 10 % of the alanine particles are bigger than 18  $\mu\text{m}$  (see section 4.2.1). Hence, less alanine particles are printed to prevent alanine-particle contamination. The printed particles will be heated in an oven at 90  $^{\circ}\text{C}$  for 90 minutes to couple the monomers onto the slide surface. The melted glycine particles perfectly merged together and have very good coverage rate on the spots. On the contrary, the coverage rate of the melted alanine particles is not as high as that of glycine particles. One reason is the alanine particles printed on the spots are less than the glycine particles. The other reason is the particle size. A previous test shows that 13  $\mu\text{m}$  biotin particles should be put in 160  $^{\circ}\text{C}$  oven for 60 minutes to be fully melted. Therefore, the alanine particles bigger than 13  $\mu\text{m}$  can not be fully melted and spread on surface at 90  $^{\circ}\text{C}$ . These melted particles just shrink into small hemispheres (Figure 5.4 Downright). The alanine hemispheres makes the particles look unmelted, but the alanine in the hemispheres are coupled onto the surface actually. After melting and coupling, the particle residues were washed away and the coupled amino acids are deprotected for next coupling.

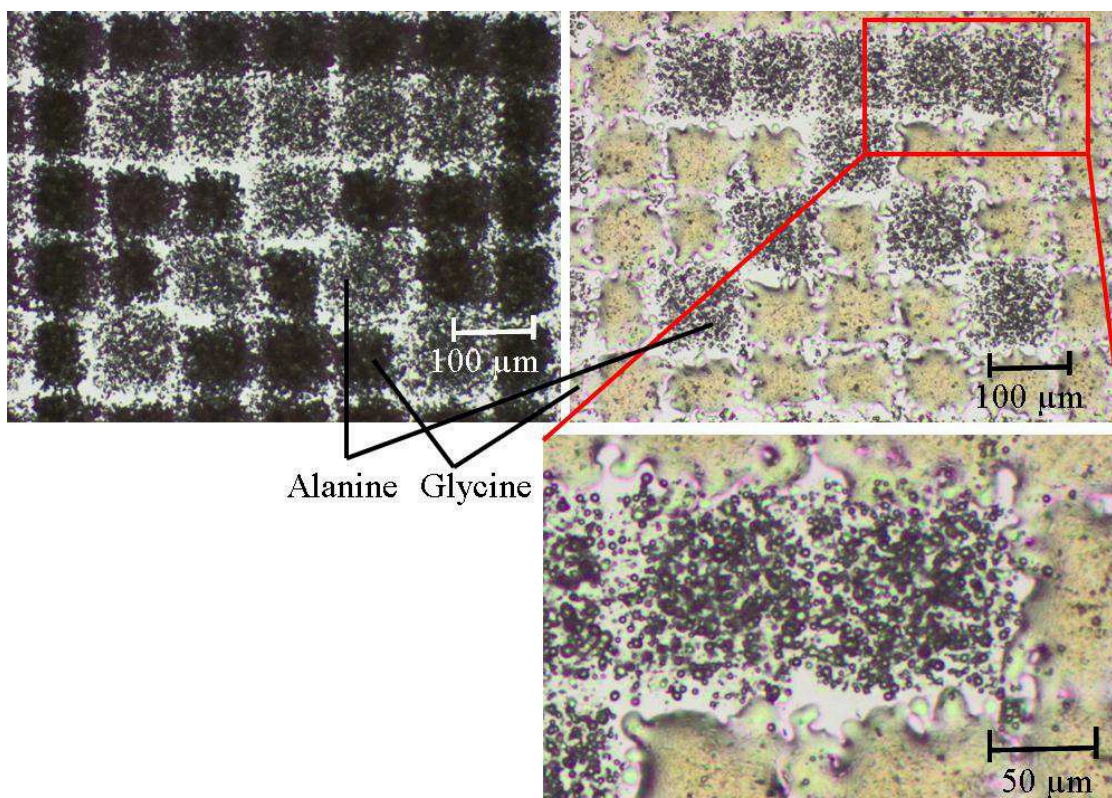


Figure 5.4: First layer of alanine and glycine particles on the glass slide. Left: unmelted particles. Right: particles melted and coupled onto the surface at 90 °C for 90 minutes. The glycine particle has better deposition quality than alanine particles because the glycine particles are smaller than alanine particles. Some melted alanine particles just shrink into hemispheres but not merged together so the alanine particles look unmelted.

The second monolayer of the alanine-biotin and glycine-glycine sequence includes glycine and biotin (Figure 5.5). 10 % of the biotin particles are bigger than 16 μm so the biotin-particle contamination is more than the glycine-particle contamination. The printing and melting protocol is changed a bit to overcome the contamination problem. The two particles are not printed and melted at the same time, but the glycine particles are printed and melted first (Figure 5.5(a)). Therefore, the deprotected pixels for glycine are coupled and blocked by glycine. Even though the biotin particles are deposited onto the surface which has melted glycine particles already, the biotin still can not couple to these glycine pixels. In Figure 5.5(b), some melted biotin particle can be seen on the melted glycine spots. In addition, Figure 5.5(b) also shows that the printing reproducibility is good enough for the synthesis. The slide with printed glycine particles was removed from the holder for melting, and then remounted for biotin-particle printing. The printing tolerance of biotin particles and glycine particles is very small and can be ignored.

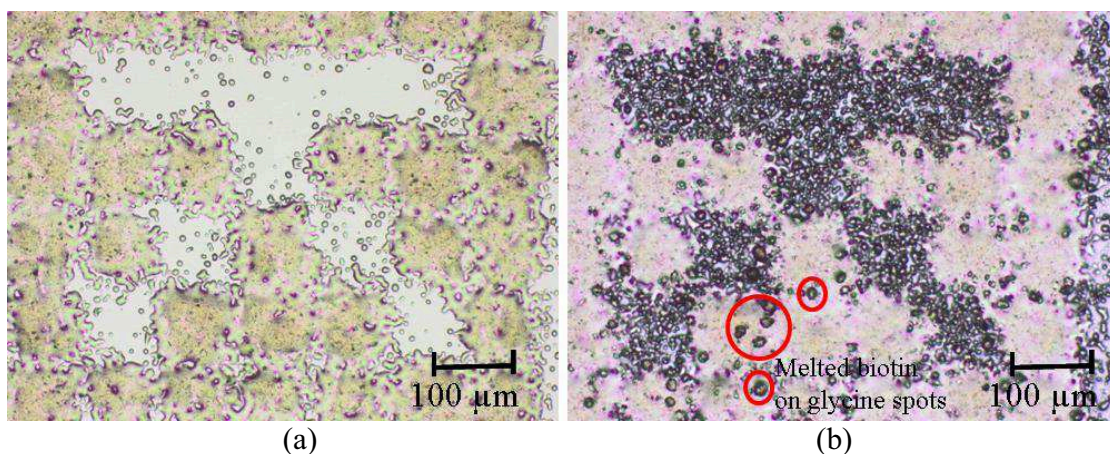


Figure 5.5: Second layer of glycine and biotin on the slide. Melted and coupled by 90 °C, 90 minutes. (a): The melted glycine particles. (b): The biotin particles are printed and melted afterward. Some biotin particles are melted on the glycine spots.

### 5.2.3 Protocols of Synthesis and Staining

When the particles are printed onto the slide surface, several chemical steps should be done to couple, block and deprotect the monomers. Besides, the unused chemicals should be washed away and the fluorescently labeled streptavidin and anti-HA antibody will be stained. The protocols of these steps are described as following.

#### 5.2.3.1 Coupling the Monomers

The particles printed on the slide should first be melted at 90 °C for 90 minutes. The monomers will be released from the particles. In the melted solid particles, the ester group (OPfp) in the Fmoc-amino acid-Opfp compound activates the carboxyl group (-COOH) of amino acids, so the amino acid can couple to the amino groups on the surface.

Protocol for Coupling:

- Put the slide in coupling chamber, and infuse N<sub>2</sub> into the chamber for 10 min.
- Put the coupling chamber into oven for 90 °C / 90 min incubation.
- Take the coupling chamber out and cool it down (10 min. ice cooling, 15 min. in cooling room, or put the coupling chamber in room temperature).
- Take the slides out.

### 5.2.3.2 Capping the Free Amino Groups and Washing the Residue

When the monomers are coupled on the surface, the uncoupled amino groups should be blocked with ESA (Acetic anhydride) to prevent synthesis of the false peptide sequence. In addition to ESA, the solution includes DIPEA (N,N-Diisopropylethylamine) and DMF (N,N-Dimethylformamid). The DIPEA is a base and is used to catalyze ESA to react with  $\text{NH}_2$  groups. The DMF is the solvent. When the amino groups are capped with ESA, the unused chemicals are washed away with acetone. In every first washing step, the slides will be lifted, so that the chemicals under the slides can be washed away as well.

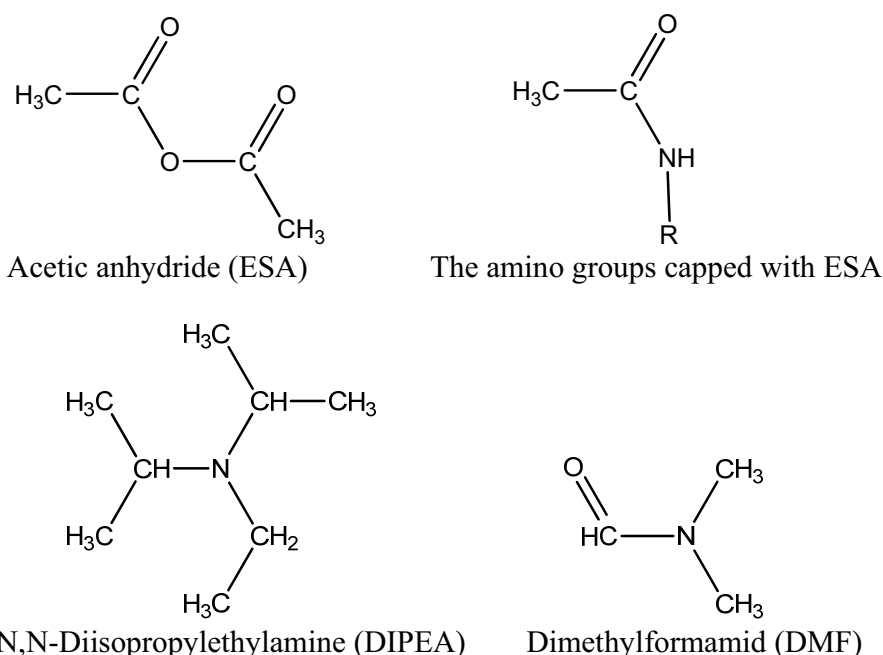


Figure 5.6: Chemicals used for blocking the residue. ESA is used to block the amino groups; DIPEA is base; DMF is the solvent.

#### Protocol for Capping/Blocking the Residue:

- Slide with **ESA/DIPEA/DMF** 10 %, 20 %, 70 % (volume concentration)
  - 1 x 5 min in **ESA/DIPEA/DMF** washing
  - 1 x 20 min in **ESA/DIPEA/DMF** washing
  - 2 x 5 min in **DMF** washing (lift slides to wash away the ESA/DIPEA)
- Wash (wash away the unused chemicals):
- 1 x 5 min in **Acetone** washing (lift slides)
  - Sonicate the slide for 20 sec in **Acetone**
  - 1 x 5 min in **Acetone** washing



### 5.2.3.3 Fmoc Deprotection

The amino groups of the amino acids are protected with Fmoc groups. After capping and washing, the amino groups should be deprotected, i.e. the Fmoc groups should be removed by piperidin. Therefore, the deprotected amino groups can couple to the next deposited monomers.

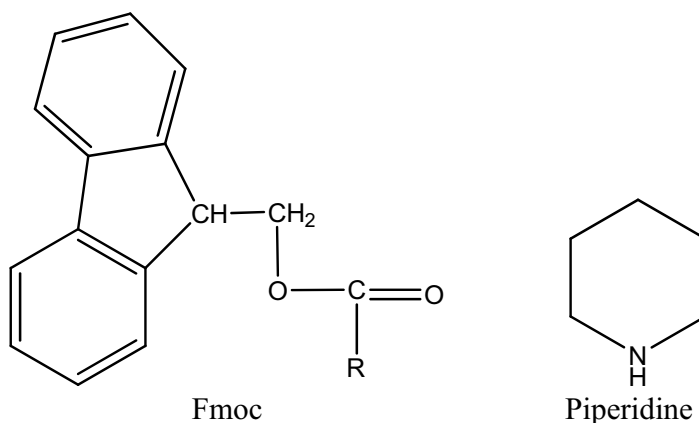


Figure 5.7: Fmoc is the protecting group of amino groups; piperidine is used to deprotect the monomers.

Protocol for Fmoc Deprotection:

- Put slide in **DMF** for 15 min (5 min. for the EG3 surface.)
- Shake 30 min with 20 %, 80 % (volume con.) **Piperidin/DMF** in shaker
- 3 x 5 min in **DMF** washing (lift slides).
- 2 x 3 min in **MeOH** washing; dry the slides with compressed air (lift slides).
- Store the slide in coupling chamber with N<sub>2</sub>, and in 4 °C for next step.

### 5.2.3.4 HA Coupling

The coupling-capping-deprotecting cycles repeat till the whole sequences are synthesized. Then, the HA epitopes are coupled to the glycine sequence for anti-HA antibody staining. The sequence used to couple to the glycine is Gly-Gly-Gly-Tyr-Pro-Tyr-Asp-Val-Pro-Asp-Tyr-Ala-Gly-Gly-Gly. Sequences of three glycines are coupled to both terminals to prolong the sequence. The HOBt/HBTU are used to activate the carboxyl group of HA epitope. After the HA epitope is coupled, the side-chain groups on HA sequence should be deprotected.

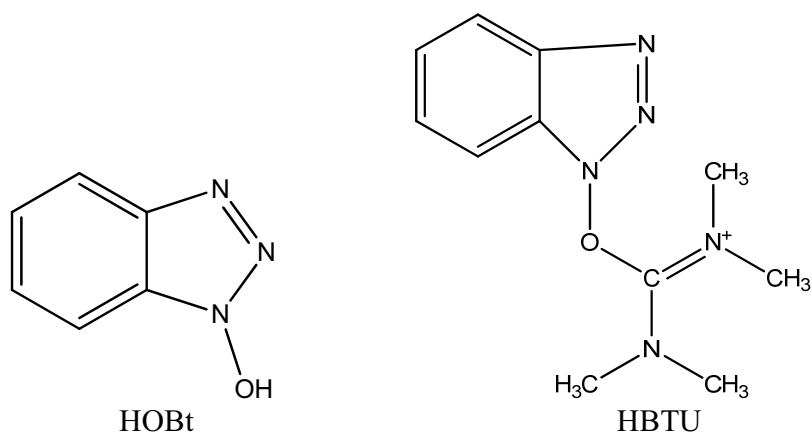


Figure 5.8 Chemical structures of HOBt and HBTU. HOBt and HBTU are both used to activate the HA sequence.

Protocol for HA Coupling:

- Prepare a 10 mM solution of the Fmoc-peptide in dry DMF (500  $\mu$ L for a microscopy slide).
- Add 500  $\mu$ L of a 12 mM solution of HOBt and HBTU in dry DMF. Stir/shake for 5 min.
- Add dry 20 mM DIPEA solution.
- Cover microscopy slide carefully with the prepared solution. Leave to react overnight in a desiccator in dry atmosphere.
- 3 x 5 min in **DMF** washing (lift slides).
- 2 x 3 min in **MeOH** washing; dry the slides with compressed air (lift slides).
- Store the slide in coupling chamber with  $N_2$ , and in 4  $^{\circ}C$  for next step.

### 5.2.3.5 Side-chain Deprotection

After the sequences are synthesized and coupled, the side chains in the sequences should be deprotected. The side chains are the groups in the monomers in addition to backbone. For example, the lysine and arginine have  $NH_2$  side chain and the cysteine has SH side chain. These side chains in the monomers can also couple to the chemicals or other monomers, so the side chains in the monomers should be protected during the synthesis process. Different side chains should be protected by different protecting groups.

In the Fmoc synthesis, the side chains can be deprotected with TFA (Trifluoroacetic acid) (Figure 5.9). The DCM (Dichloromethane) is used to preswell the synthesized sequences, so the sequences can fully react with the solution.

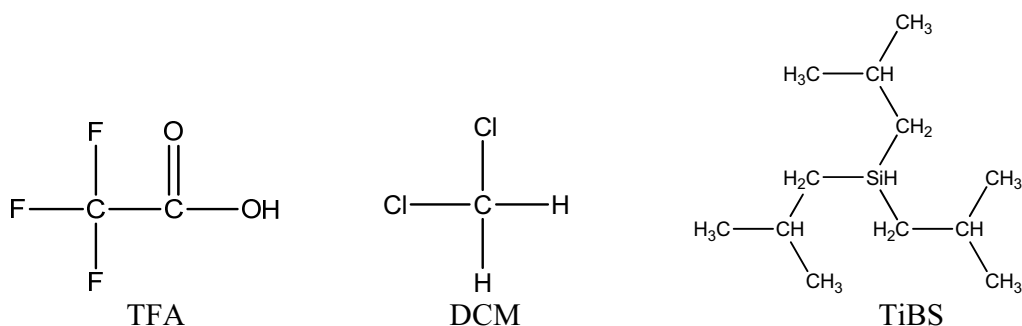


Figure 5.9: The chemical structure of TFA (Trifluoroacetic acid), DCM (Dichloromethane), and TiBS (Triisobutylsilane).

Protocol for Side-group Deprotection:

- Take the dry and cold slide.
- 1 x 30 min in **DCM** swelling
- Shaking for 3 x 30 min in (51 v% **TFA**, 3 v% **TiBS**, 44 v% **DCM**, 2 v% **H<sub>2</sub>O**)
- 2 x 5 min in **DCM** washing
- 1 x 5 min in **DMF** washing
- 1 x 30 min in **DMF/DIPEA 5%** washing
- 2 x 5 min in **DMF** washing
- 2 x 5 min in **MeOH** washing
- Dry with air and store in cold room with N<sub>2</sub>

### 5.2.3.6 Blocking the Surface with BSA

When HA epitopes are coupled to the synthesized glycine sequences, the slide surface should be blocked with BSA (bovine serum albumin). BSA is a serum albumin protein derived from cows. When the slide surface is blocked with BSA, the fluorescently labeled molecules (anti-HA antibody and Streptavidin here) can only couple to the target (HA and biotin here) but not to the blocked surface. Therefore, the labeled molecules will not contaminate the surface and produce false signal.

Protocol for Blocking the Surface with BSA:

- Prepare the TBS-T buffer. 45 mL distilled water, 3 TBS-T tablets, 23 μL Tween 20 (surfactant).
- Incubate the slide in TBS buffer for 30 min. to rehydrate the coating polymer film.
- Incubate the slide in the BSA solution (BSA: TBS-T buffer= 1:100), 1 hour, room temperature, on shaker. (For 45 mL TBS-T buffer, use 450 mg BSA.)
- 2 x 1 min in TBS-T washing with gentle shaking.

### 5.2.3.7 Staining with Anti-HA Antibody and Streptavidin

Finally, the sequences are stained with fluorescently labeled anti-HA antibody (labeled with Cy5, 647 nm) and streptavidin (labeled with Cy3, 546 nm). The dilution ratio of anti-HA antibody is 1:1000 and the dilution ratio of streptavidin is 1:5000.

Protocol for Staining with Fluorescence-labeled Molecules:

- If the slides are dried and stored in fridge, preswell the surface with TBS-T for 30 min.
- Incubate the slide in antibody solution (5 mL TBS-T buffer takes 5mg BSA, 5  $\mu$ L anti-HA antibody (1:1000), 1  $\mu$ L STP (1:5000)), 1 hour, room temperature, on shaker.
- 6 x 5 min in TBS-T washing with gentle shaking (Do not change the petridish, because the dish surface is also blocked by BSA.)
- Dry the slide with nitrogen stream and store in light-resistive container.
- The staining results are scanned with a fluorescence scanner. Two scanners are used here. One is the GenePix 4000b scanner (resolution: 5  $\mu$ m, scan wavelength 546 nm and 647 nm) and the other is Odyssey scanner (resolution: 21  $\mu$ m, scan wavelength 700~800 nm).

## 5.3 Coating on Slide

The synthesis slide should be functionalized with amino groups to enable the coupling of the first amino acid. Different coating materials have different influence on the coupling and staining. For example, the 100 % PEGMA coating will be detached from the slide surface by the TFA (trifluoroacetic acid) during the side-chain deprotection process [KÖN10-2]. The chemical structure of the coating materials is also important. The structure with few branches has little space for other molecules and result in steric indolence of coupling. Therefore, four different slide coatings were tested in the experiment to find the optimal surface for the synthesis and staining experiment. The coating materials included 10:90-PEGMA-co-PMMA polymer films (PMMA is polymethylmethacrylat; PEGMA is Poly(ethylenglycol)methylmethacrylat) and APTES (Aminopropyltriethoxysilane) [STA08-2, STA07]. Two other kinds of commercial slides from PolyAn (Berlin, Germany) were also used.

The chemical structure of the APTES is shown in Figure 5.10. The chemical structures of PEGMA/MMA and related chemicals are shown in Figure 5.11 - 5.13. The APTES is self-assembled monolayers (SAMs). The APTES layer is tens of angstroms thick. The silicon atoms in APTES couple to three oxygen atoms, which couple to the surface, and

the last bond of silicon couples to the carbon chain with amino groups. On the other hand, the PEGMA/MMA is nm-scale polymeric coating. The PEGMA/MMA coating is much thicker than APTES coating and provides a more 3D-like structure.

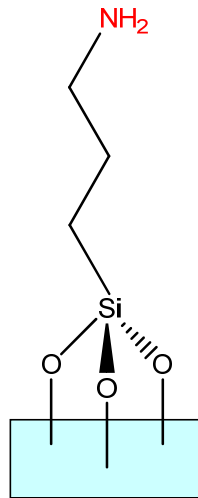


Figure 5.10: The chemical structure of APTES. The carbon chain binds to the surface with one silicon and three oxygen atoms. On the terminal of the carbon chain is an amino group for coupling.

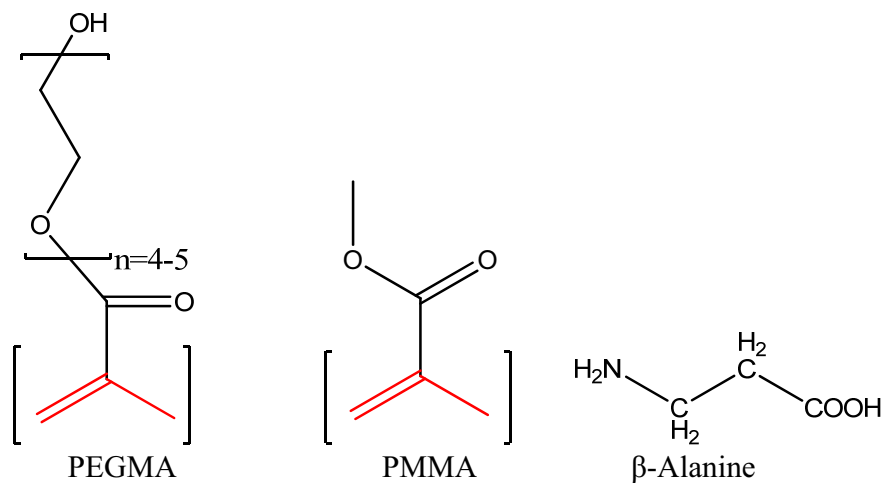


Figure 5.11: Chemical structure of PEGMA, PMMA and  $\beta$ -Alanine. The quoted parts of PEGMA and PMMA compose the backbone of the structure. The  $\beta$ -Alanine functionalizes the PEGMA/MMA structure with amino groups.

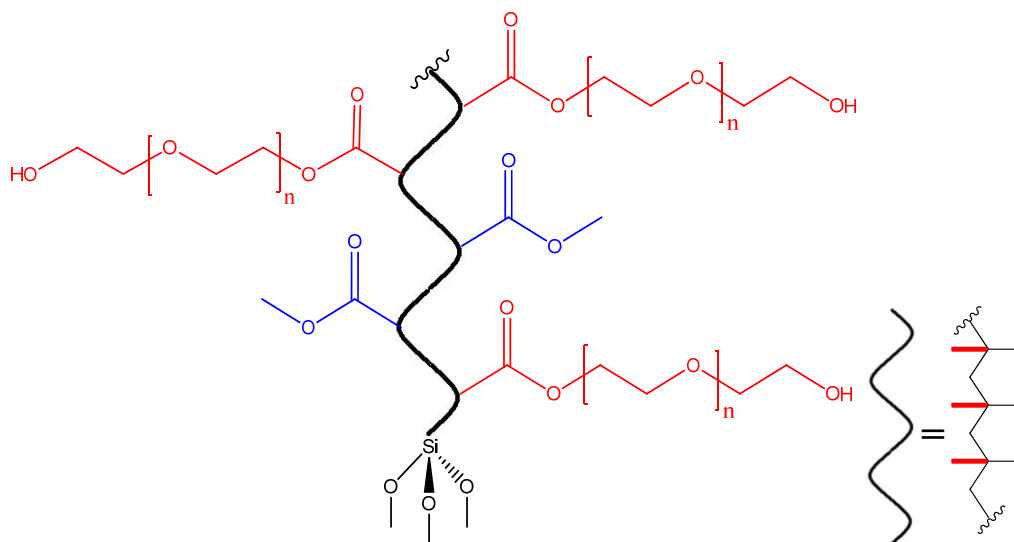


Figure 5.12: Chemical structure of PEGMA/MMA. The red branches come from PEGMA and the blue branches come from PMMA.

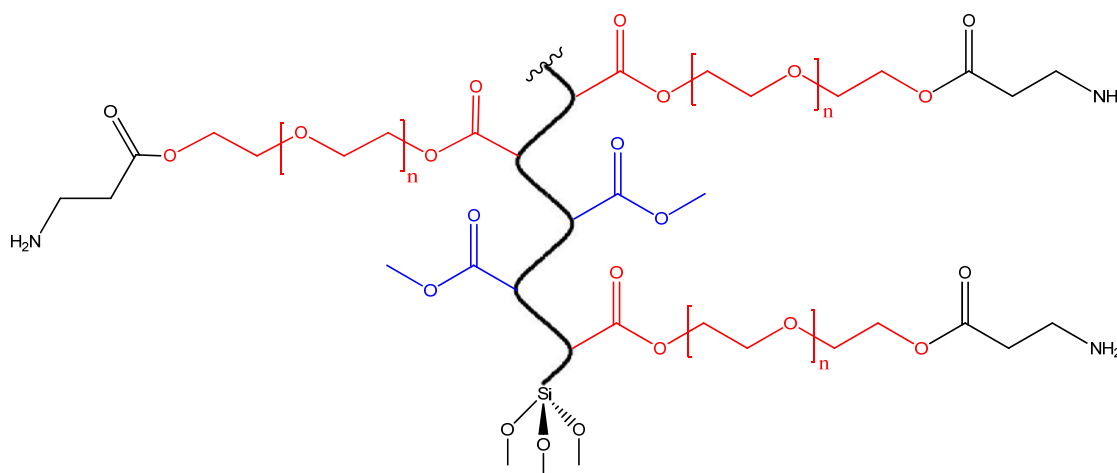


Figure 5.13: Chemical structure of PEGMA/MMA functionalized with  $\beta$ -Alanine. The  $\beta$ -Alanine binds to the PEGMA branch and provides amino groups.

In the PEGMA/MMA structure, the quoted carbon chains compose the backbone, and the rest parts become the branches of the structure. The terminals of the PEGMA branches were functionalized with  $\beta$ -Alanine and, hence, have amino groups. With the branches, the PEGMA/MMA structure is a tree-like structure so the amino groups have more space to couple with the other molecules.

Figure 5.14 and Figure 5.15 show the synthesis and staining result of 10:90 PEGMA-co-PMMA polymer coated slide and APTES coated slide, respectively. The green signal represents the Cy3 labeled streptavidin, which couples to the biotin. The red signal represents the Cy5 labeled anti-HA antibody, which couples to the HA epitope. In

the staining result of PEGMA/MMA coated slide, the streptavidin and anti-HA antibody stains the biotin and HA specifically. The two fluorescences can be clearly detected and the stained areas are distinct. In addition, the labeled streptavidin and anti-HA antibody do not have non-specific binding. The Cy3 and Cy5 signals around the chip come from the contamination particles. During particle deposition, the particles in the aerosol deposited not only on the pixel area but also on the area around. These contamination particles were transferred by electrical field and coupled onto the functionalized surface as well.

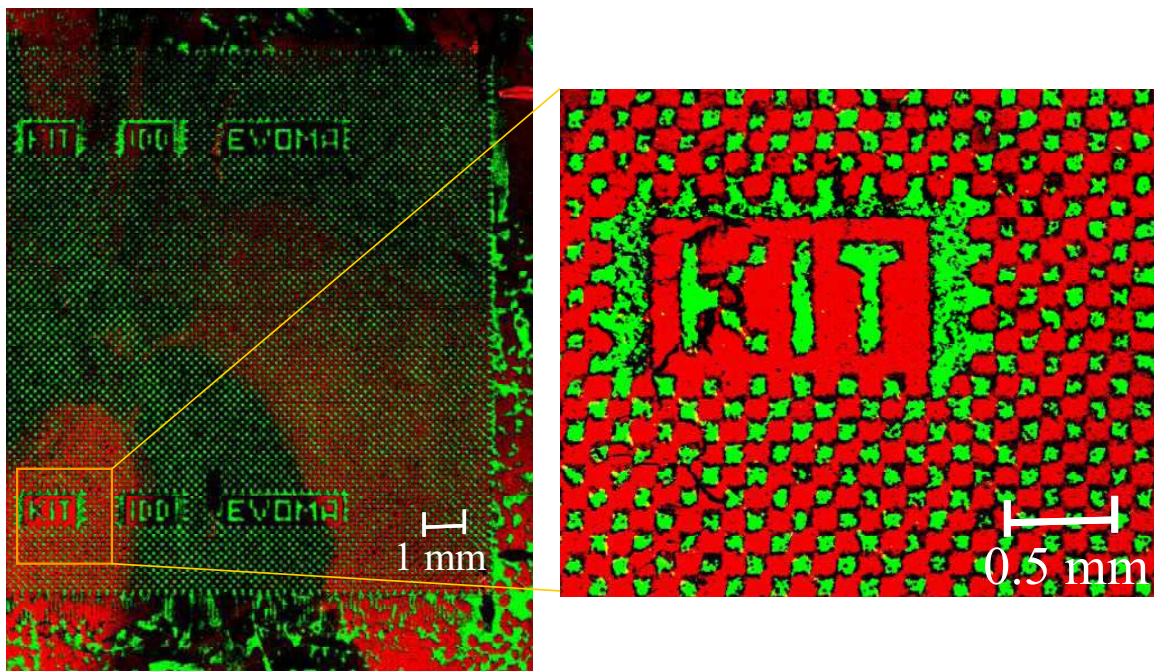


Figure 5.14: Staining result of 10:90 PEGMA-co-PMMA polymer coated slide. The green signals are Cy3 labeled streptavidin and red signals are Cy5 labeled anti-HA antibody. Scan resolution: 5  $\mu\text{m}$ .

The staining result of APTES coated slide is not as good as the result of PEGMA/MMA coated slide (Figure 5.15). More background was observed from the staining result of the APTES coated slide. The non-specific staining can be due to the different properties of different coatings.

In addition to the PEGMA/MMA and APTES slides, the commercial 2D and 3D slides from PolyAn are also used in the synthesis experiment. The staining result of the PolyAn 2D and 3D slides are shown in Figure 5.16. Although there are several non-specific staining in the staining result of PolyAn 3D slide, the pattern of Cy3 labeled streptavidin can still be seen. For the Poly 2D slide, no pattern can be seen in the scanning result. The

exact compositions of the commercial PolyAn 2D and 3D slides are unknown, so the reason for the contaminations can not be particularly discussed.

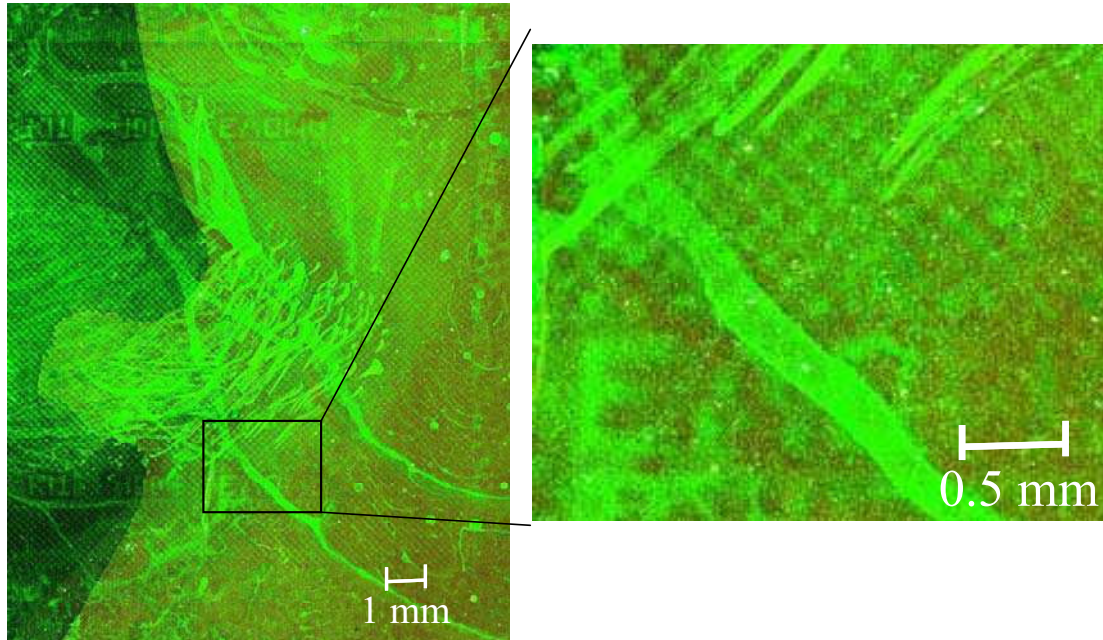


Figure 5.15: Staining result of APTES coated slide. The green signals are Cy3 labeled streptavidin and red signals are Cy5 labeled anti-HA antibody. Resolution: 5  $\mu\text{m}$ .

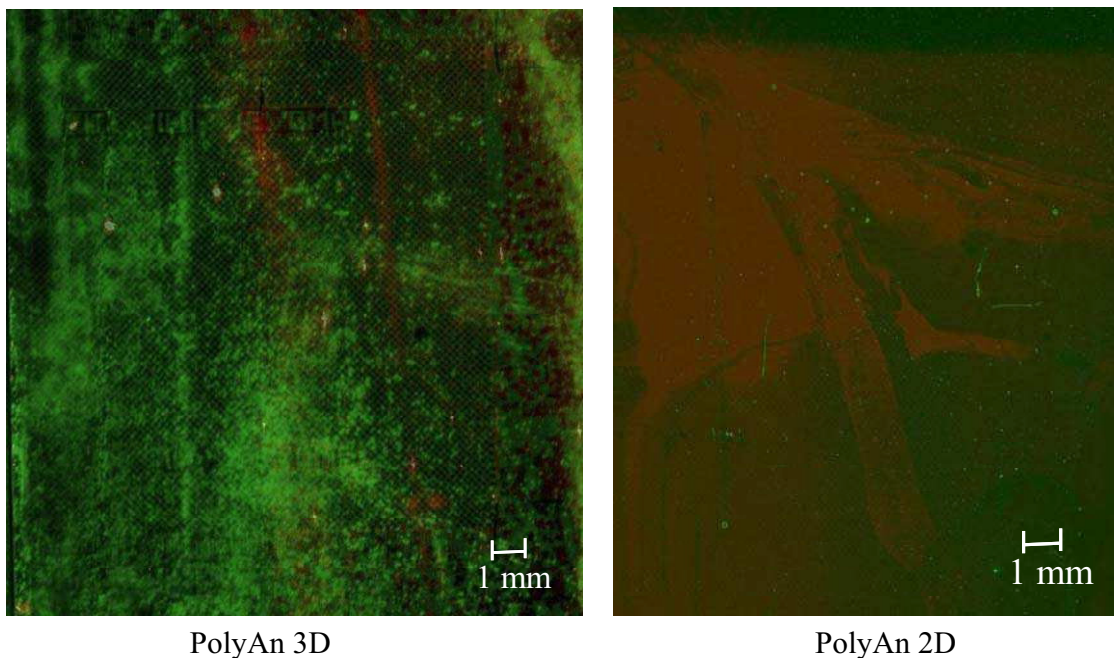


Figure 5.16: Staining result of PolyAn 3D and Poly 2D slide. The green signal is Cy3 labeled streptavidin and red signal is Cy5 labeled anti-HA antibody. Resolution of PolyAn 3D: 21  $\mu\text{m}$ . Resolution of PolyAn 2D: 5  $\mu\text{m}$ .



## 5.4 Discussion

In this chapter, the particle-based synthesis is performed with amino acids and biotin, and the array with spot density of 10,000 spots/cm<sup>2</sup> is successfully synthesized. This experiment shows that the surface can be functionalize with not only amino acids but also other monomers such as biotin. On the surface, the sequences can be synthesized with amino acids and other monomers, and can be used for several biochemistry applications such as further coupling and staining.

Comparing the staining result of different coated slides, including the 10:90 PEGMA-co-PMMA, APTES, PolyAn 3D and PolyAn 2D, the comparison indicates that the surface coating should be given preference. The 10:90-PEGMA-co-PMMA polymer shows better staining result than the other three kinds of coating. However, further investigation should be done to find the optimal coating, and the synthesis and staining should be discussed to find the reasons of the non-specific binding.

In the synthesis experiment, the particles are printed twice to solve the problem of inhomogeneous deposition, so that the particles printed onto the spots can be enough for synthesis.

# 6. Conclusion

## 6.1 Discussion of Results

This CMOS-chip based printing system enables us to synthesize 10,000 spots / cm<sup>2</sup> array on a substrate. Comparing with the synthesis-on-chip method [BEY07], the CMOS-based printing system makes the CMOS chip reusable, and now the array can be synthesized on glass substrate, which is cost-effective, robust to chemicals, even, and already well adapted for biochemistry use. Another advantage is that the particles can be printed onto different areas of the slide, doubling the number of total spots synthesized on a slide.

Comparing with the laser-printing system [STA08-1], the array synthesized with chip-printing system enables 25 times higher spot density (10,000 spots / cm<sup>2</sup> v.s. 400 spots / cm<sup>2</sup>) and better coverage rate of the printed particles.

Comparing with the SPOT method [FRA92, FRA02-1, FRA02-2] and photolithographic method [FOD91], the particle based synthesis enables much higher spot density than conventional SPOT synthesis (10,000 spots / cm<sup>2</sup> v.s. 25 spots / cm<sup>2</sup>). The time needed for synthesis is about 20 times shorter than the photolithographic method.

### 6.1.1 System Construction

The CMOS-chip based printing system is constructed to automate the particle printing process. The system reads particle printing patterns from the text file, generates particle aerosol, deposits particles onto CMOS chip in desired patterns, and prints the particles onto the glass slide. With proper manipulation, the reproducibility tolerance of particle printing can be smaller than 5 μm. The tolerance of parallelity between chip and slide is smaller than 20 μm after adjustment. The deposition quality on chip is monitored by a digital microscope. The time needed for printing one kind of particles is 80 seconds, so the printing time needed for 1 monolayer is 80 (seconds) × 20 (amino acids) = 1600 seconds (26.6 minutes). The time needed for printing 15 monolayers is 80 (seconds) × 20 × 15 = 400 minutes. Comparing with the time needed for synthesis, the chemistry reactions need more than 2 hours (see section 5.2.3), so the bottleneck of array fabrication time is still dominated by the chemistry-reaction time but not by the printing time.

However, the chip-printing system is not fully automated yet, and some problems still have to be solved for system automation. First problem is that several trivial requirements should be met for the printing reproducibility, since the system has no position sensor for feedback control of chip positioning. The problems for automation of particle deposition include the aerosol generation is not stable and the quality of particle deposition can not be evaluated automatically. The chip can be damaged easily also disadvantages the automation.

### **6.1.2 Quality of Particle Deposition**

The particle characteristics are important for depositing enough particles onto the chip and with few cross contamination. The particles should be small (2-6  $\mu\text{m}$ ) and have no particles bigger than 10  $\mu\text{m}$ . Besides, the particles should be round, and the q/m value should be about  $-4 \mu\text{C/g}$  [LÖF11]. In addition, the particles should be dry during printing so the particles will not block the aerosol system and stick on the chip surface. Therefore, the whole aerosol system should be stored in an air-conditioned room. Otherwise, the particles should be added more silica nanoparticles (Aerosil, 0.05 % of particle mass) and, every time before use, be dried in a desiccator.

For the printing homogeneity, although the chip surface can be parallelized to the slide with the printing system, the inhomogeneous particle deposition on the chip still makes the printing result inhomogeneous. Depositing and printing particles twice can make the particle layer more homogeneous and enable enough particles printed onto the spots.

The optimal printing distance between chip and slide is 50-60  $\mu\text{m}$ . With this distance, the chip will not be pressed by particles and not be burnt by the high voltage. On the other hand, the chip will not be too far away from slide so the particles will not spread on the slide surface.

### **6.1.3 Combinatorial Synthesis Result**

With the particles printed with the chip-printing system, we synthesized two different sequences, which consist of amino acids and biotin, on the slide surface. The deposition, printing and synthesis process is proven to be work with the staining results.

Comparing the scanning results of different coated slides, the 10-90-PEGMA-co-MMA polymer coated slide shows better staining result than the other three coatings. However,

further investigation is still needed to find the optimal coating material and to reduce the non-specific binding.

## **6.2 Application**

The CMOS-chip based printing system can be used to print particles in desired patterns on any solid material, as long as the material is electrical insulating and can be fixed in the holder. The spot density of the printing is 10,000 spots / cm<sup>2</sup>. In addition, the particles melted on the surface has no micro-bubble inside, while the conventional ink printing suffers the bubble problem. This non-bubble advantage is very important to the application of electrical circuit printing.

The synthesis and staining result shows that we can functionalize the slide surface with amino acids and other monomers, and the array density can be 10,000 spots / cm<sup>2</sup>. This functionalized surface can be applied to various fields, such as label free detection, lab on chip and solar cell.

The high-density peptide arrays anticipated to be synthesized with the printing system and applied to the proteomic research, including the protein-protein, protein-peptide, protein-DNA, protein-RNA, or protein-metal interactions. When the high-density peptide arrays can be synthesized, the spot density (10,000 spots / cm<sup>2</sup>) of the peptide array is much higher than that of conventional SPOT method (96-768 spots / cm<sup>2</sup>). Accordingly, the cost for high-throughput peptide screening with chip-printing method is 100 to 25 times lower than that of the conventional SPOT method.

## **6.3 Next Generation of the Chip-printing System**

The next generation of chip-printing system should be more automated. Besides, the particle-printing quality on the slide can also be further improved by improving the aerosol generation system.

For automation, the position sensor for chip and slide should be mounted and the particle deposition quality should be evaluated automatically. With position sensor, the process of aligning the chip with slide will be significantly simplified, since the relative position between chip and slide can be monitored and adjusted automatically. The evaluation of deposition quality is also important because the quality aerosol deposition on chip is not predictable. If the printing system can evaluate the deposition quality itself, it can

automatically decide whether it should repeat the particle deposition on chip should or not.

Redesign the system geometry is another important issue for automating the system. One geometry problem comes from the sixty PVC tubes in the aerosol system. The aerosol system needs sixty tubes to transport and recycle the aerosol, and all these sixty tubes should travel 400 mm during the printing. Hence, enough space and new geometry design are necessary for the tube motion. Another geometry problem is that the particle-recycling suction cups on the aerosol outlets can collide with the chip connector. Therefore, the suction cups or the chip connector should be redesigned for automation as well.

Improving the structure and space use of the system is another task. Although the aerosol system needs more space, there is still surplus space somewhere in the whole system. For example, a lot of space near the slide holder is unused. Therefore, the whole structure can be redesigned to optimize the space usage efficiency and make the system smaller.

The CMOS chip can also be improved. The current CMOS chip has about 16,000 pixels, so 16,000 spots can be synthesized with one CMOS chip. If the future chip has double or triple pixels, the synthesized spots can also be doubled or tripled. In addition, involving the distance sensor and position sensor into the CMOS chip can significantly help the system automation.

To improve the particle deposition quality, the aerosol generator should be improved for stable aerosol generation and homogeneous particle deposition. Now the aerosol generation is significantly influenced by the particle characteristics, the particle amount in reservoir, and the pressure of injected air. Therefore, the aerosol generation is unstable and the generation system should be fine tuned very often according to the particle amount in reservoir. In addition, the particles can block the aerosol outlet easily and make the automation of aerosol generation difficult as well. Hence, a solution for preventing the outlets from being blocked with particles should also be developed.

## References

- [ALB08] Albert T, Egler C, Jakushev S, Schuldenzucker U, Schmitt A, Brokemper O, Zabe-Kühn M, Hoffmann D, Oldenburg J, Schwaab R. *The B-cell epitope of the monoclonal anti-factorVIII antibody ESH8 characterized by peptide array analysis*. Thrombosis and Haemostasis, vol 99; 2008. pp 634-637.
- [ATH89] Atherton M, Sheppard RC, *Solid phase peptide synthesis: A practical approach (The practical approach series)*. Oxford University Press, USA, 1989.
- [BEY05] Beyer M. *Doctoral Thesis: Entwicklung und Anwendung neuartiger Trägeroberflächen zur kombinatorischen Peptidsynthese mit Aminosäure-Tonerpartikeln*. Universität Heidelberg; 2005.
- [BEY07] Beyer M, Nesterov A, Block I, König K, Felgenhauer T, Fernandez S, Leibe K, Torralba G, Hausmann M, Trunk U, Lindenstruth V, Bischoff R, Stadler V, and Breitling F. *Combinatorial synthesis of peptide arrays onto a computer chip's surface*. Science, vol. 318; 2007, pp. 1888.
- [BIA03] Bialek K, Swistowski A, Frank R. *Epitope-targeted proteome analysis: towards a large-scale automated protein-protein-interaction mapping utilizing synthetic peptide arrays*. Analytical and Bioanalytical Chemistry, vol 376; 2003. pp 1006-1013.
- [BRE08] Breitling F, Nesterov A, Stadler F, Felgenhauer F, Bischoff R. *High-density peptide arrays*. Molecular BioSystem, vol 5, 2009, pp 224-234.
- [BRE11] Breitling F, Löffler F, Schirwitz F, Cheng Y, Märkle F, König K, Felgenhauer T, Dörsam E, Bischoff R, Nesterov-Müller A. *Alternative setups for automated peptide synthesis*. Mini Reviews in Organic Chemistry, May 2011.
- [EGB] [www.egbeck.de/skripten/bkurse10.htm](http://www.egbeck.de/skripten/bkurse10.htm), Ernst-Georg Beck, 2011.
- [EIC04] Eichler J. *Rational and random strategies for the mimicry of discontinuous protein binding sites*. Protein and Peptide Letters, vol 11; 2004. pp 281-290.
- [EIC05] Eichler J. *Synthetic peptide arrays and peptide combinatorial libraries for the exploration of protein-ligand interactions and the design of protein inhibitors*. Combinatorial Chemistry & High Throughput Screening, vol 8; 2005. pp 135-143.
- [FOD91] Stephen F, Leighton R, Michael P, Lubert S, Amy L, Dennis S. *Light-Directed, Spatially Addressable Parallel Chemical Synthesis*. Science, vol 251; 1991. pp 767-773.
- [FRA92] Frank R. *Spot-Synthesis. An Easy Technique for the Positionally Addressable, Parallel Chemical Synthesis on a Membrane Support*. Tetrahedron, vol 48; 1992. pp 9217-9232.
- [FRA02-1] Frank R. *High-Density Synthetic Peptide Microarrays: Emerging Tools for Functional*. Combinatorial Chemistry & High Throughput Screening, vol 5; 2002, pp 429-440.
- [FRA02-2] Frank R. *The SPOT-synthesis technique: Synthetic peptide arrays on membrane supports – principles and applications*. Journal of Immunological Methods, vol 267; 2002. pp 13-26.

- [HOL05] Holmberg A, Blomstergren A, Nord O, Lukacs M, Lundeberg J, Uhlén M, *The biotin-streptavidin interaction can be reversibly broken using water at elevated temperatures*. *Electrophoresis*, vol 26; 2005, pp 501-510.
- [INT] <http://www.intavispeptides.com>, August 2012.
- [KNO99] Knoblauch T, Rüdiger S, Schönfeld J, Driessen J, Schneider-Mergener J, Bukau B. *Substrate specificity of the SecB chaperone*. *Journal of Biological Chemistry*, vol 274; 1999, pp 34219-34225.
- [KÖN10-1] König K, Block I, Nesterov A, Torralba G, Fernandez S, Felgenhauer T, Leibe K, Schirwitz C, Löffler F, Painke F, Wagner J, Trunk U, Bischoff R, Breitling F, Stadler V, Hausmann M, Lindenstruth V. *Programmable High Voltage CMOS Chips for Particle-based High-density Combinatorial Peptide Synthesis*. *Sensors and Actuators B: Chemical*, vol. 147; 2009. pp 418-427.
- [KÖN10-2] König K. Doctoral Thesis: *COMS-based Peptide Arrays*. Heidelberg University; 2010.
- [LEE09] Lee H, You S, Gyu Woo C, Lim K, Jun K, Choi M, *Focused Patterning of Nanoparticles by Controlling Electric Field Induced Particle Motion*. *Applied Physics Letter*, vol 94; 2009, 053104.
- [LIU03] Liu R, Enstrom A, Lam K, *Combinatorial peptide library methods for immunobiology research*, *Experimental Hematology*, vol 31, 2003, pp 11-30.
- [LÖF11] Löffler F, Wagner J, König K, Märkle F, Fernandez S, Schirwitz C, Torralba G, Hausmann M, Lindenstruth V, Bischoff R, Breitling F, and Nesterov A. *High-Precision Combinatorial Deposition of Micro Particle Patterns on a Microelectronic Chip*. *Aerosol Science and Technology*, vol 45; 2011; pp 65-74.
- [MER63] Merrifield RB. *Solid Phase Peptide Synthesis. The Synthesis of a Tetrapeptide*. *Journal of the American Chemical Society*, vol 85; 1963. pp 2149-2154.
- [MER64-1] Merrifield RB. *Solid Phase Peptide Synthesis II. The Synthesis of Bradykinin*. *Journal of the American Chemical Society*, vol 86; 1964. p 304.
- [MER64-2] Merrifield RB. *Solid Phase Peptide Synthesis III. An Improved Synthesis of Bradykinin*. *Biochemistry*, vol 3; 1964. pp 1385-1390.
- [NES07-1] Nesterov A, Löffler F, König K, Trunk U, Leibe K, Felgenhauer T, Stadler V, Bischoff R, Breitling F, Lindenstruth V, Hausmann M. *Noncontact charge measurement of moving microparticles contacting dielectric surfaces*. *Review of Scientific Instruments*, vol 78; 2007.
- [NES07-2] Nesterov A, Löffler F, König K, Trunk U, Leibe K, Felgenhauer T, Bischoff R, Breitling F, Lindenstruth V, Stadler V, Hausmann M. *Measurement of triboelectric charging of moving micro particles by means of an inductive cylindrical probe*. *Journal of Physics D: Applied Physics*, vol 40; 2007. pp 6115-6120.
- [NES08] Nesterov A, König K, Felgenhauer T, Lindenstruth V, Trunk U, Fernandez S, Hausmann M, Bischoff R, Breitling F, Stadler V. *Precise selective deposition of microparticles on electrodes of microelectronic chips*. *Review of Scientific Instruments*, vol 79; 2008.

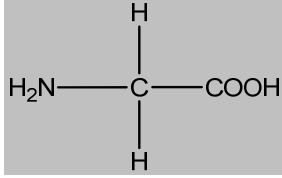
- [NES09] Nestor JJ. *The Medicinal Chemistry of Peptides*. Current Medicinal Chemistry, vol 16; 2009. pp 4399-4418.
- [NES10-1] Nesterov A, Löffler F, Cheng Y, Torralba G, König K, Hausmann M, Lindenstruth V, Stadler V, Bischoff R, Breitling F. *Characterization of Triboelectrically Charged Particles Deposited on Dielectric Surfaces*. Journal of Physics D: Applied. Physics, vol 43; 2009. pp 1-6.
- [NES10-2] Nesterov A, Dörsam E, Cheng Y, Schirwitz C, Märkle F, Löffler F, König K, Stadler V, Bischoff R, Breitling F. *Peptide arrays with a chip*, Methods in Molecular Biology, vol 669, 2010. pp 109-124.
- [OKI] [www.oki.com](http://www.oki.com), April 2012.
- [OTV08] Otvos L. *Peptide-Based Drug Design: Here and Now*. Methods in Molecular Biology, vol 494; 2008. pp 1-8.
- [PEPPE] [www.pepperprint.com](http://www.pepperprint.com), Volker Stadler, April 2012.
- [REI02] Reineke U, Ivascu C, Schlieff M, Landgraf C, Gericke S, Zahn G, Herzel H, Volkmer-Engerdt R, Schneider-Mergener J. *Identification of Distinct Antibody Epitopes and Mimotopes from a Peptide Array of 5520 Randomly Generated Sequences*. Journal of Immunological Methods, vol 267; 2002. pp 37-51.
- [SED04] Sedra A, Smith C. K, *Microelectronic Circuits (5th edition)*, Oxford University Press, 2004.
- [STA07] Stadler V, Beyer M, König K, Nesterov A, Torralba G, Lindenstruth V, Hausmann M, Bischoff R, Breitling F. *Multifunctional CMOS Microchip Coatings for Protein and Peptide Arrays*. Journal of Protein Research, vol 6; 2007. pp 3197-3202.
- [STA08-1] Stadler V, Felgenhauer T, Beyer M, Fernandez S, Leibe K, Güttler S, Gröning M, König K, Torralba G, Hausmann M, Lindenstruth V, Nesterov A, Block I, Pipkorn R, Poustka A, Bischoff R, Breitling F. *Combinatorial synthesis of peptide arrays with a laser printer*. Angewandte Chemie – International Edition, vol 47; 2008. pp 7132-7135.
- [STA08-2] Stadler V, Kirmse R, Breitling F, Ludiwig T, Bischoff R. *PEGMA/MMA copolymer graftings: generation, protein resistance, and a hydrophobic domain*. Langmuir, vol 24; 2008. pp 8151-8157,
- [UTT08] Uttamchandani M, Yao SQ. *Peptide Microarrays: Next Generation Biochips for Detection, Diagnostics and High-Throughput Screening*. Current Pharmaceutical Design, vol 14; 2008. pp 2428-2438.
- [VEC] [www.veeco.com](http://www.veeco.com), April 2012.
- [VLI10] Vlieghe P, Lisowski V, Martinez J, Khrestchatisky M. *Synthetic Therapeutic Peptides: Science and Market*. Drug Discovery Today, vol 15; 2010. pp 40-56.
- [WAG10] Wagner J, Löffler F, König K, Fernandez S, Bischoff R, Nesterov A, Breitling, F, Hausmann M, Lindenstruth V. *Quality Analysis of Selective Micro-particle Depositions on Electrically Programmable Surfaces*. Review of Scientific Instruments, vol 81; 2010.
- [YOU] [www.youmy-elec.en.alibaba.com](http://www.youmy-elec.en.alibaba.com), April 2012.



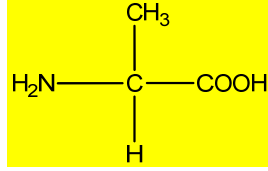
# Appendices



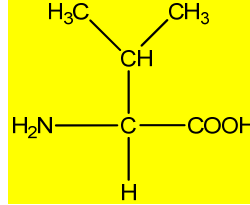
# A1. Amino Acids



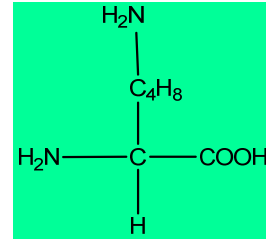
Glycine-Gly-G



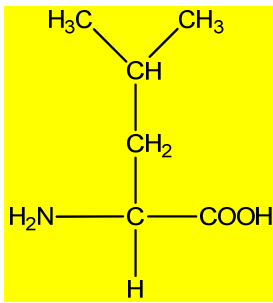
Alanine-Ala-A



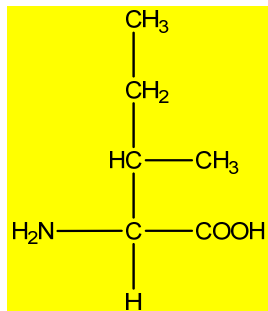
Valine-Val-V



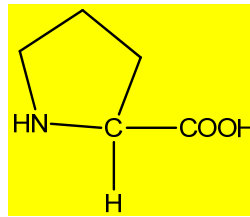
Lysin-Lsy-K



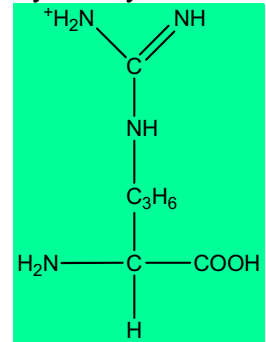
Leucine-Leu-L



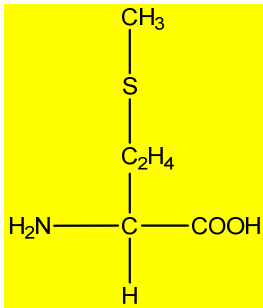
Isoleucine-Ile-I



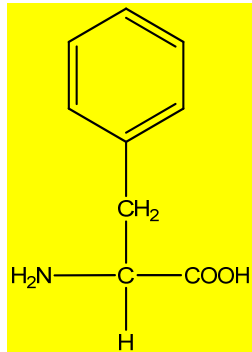
Proline-Pro-P



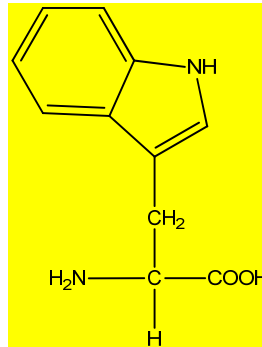
Arginine-Arg-R



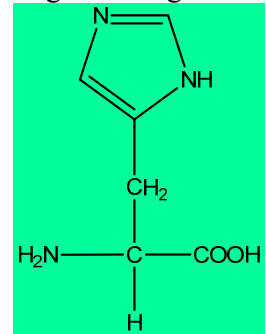
Methionine-Met-M



Phenylalanine-Phe-F



Tryptophan-Trp-W



Histidine-His-H

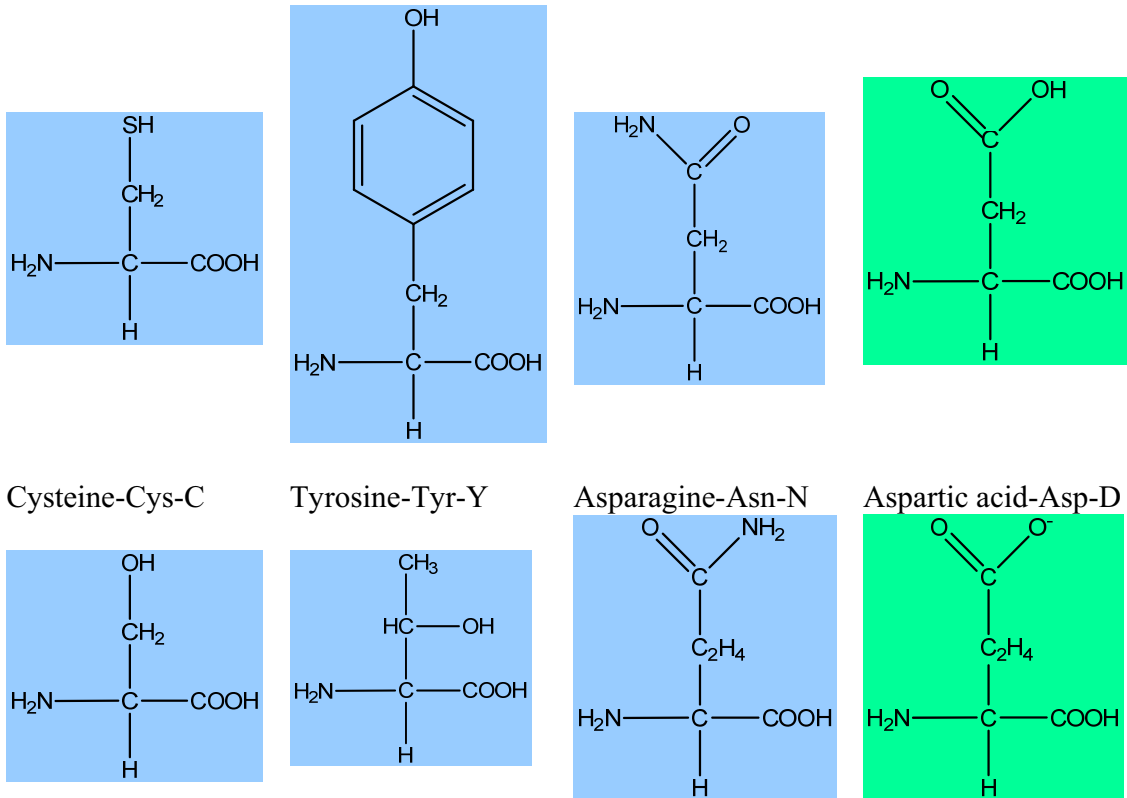


Figure A1.1: The chemical structure of 20 standard amino acids. Three-letter and one-letter codes are also given here. The color background shows different chemical properties of the amino acids. Charged polar amino acids are on green background, non-charged polar amino acids are on blue background, and non-polar amino acids are on yellow background. Glycine has lowest molecular weight and greatest flexibility in binding angles in the peptide chain.

## A2. LabVIEW Program

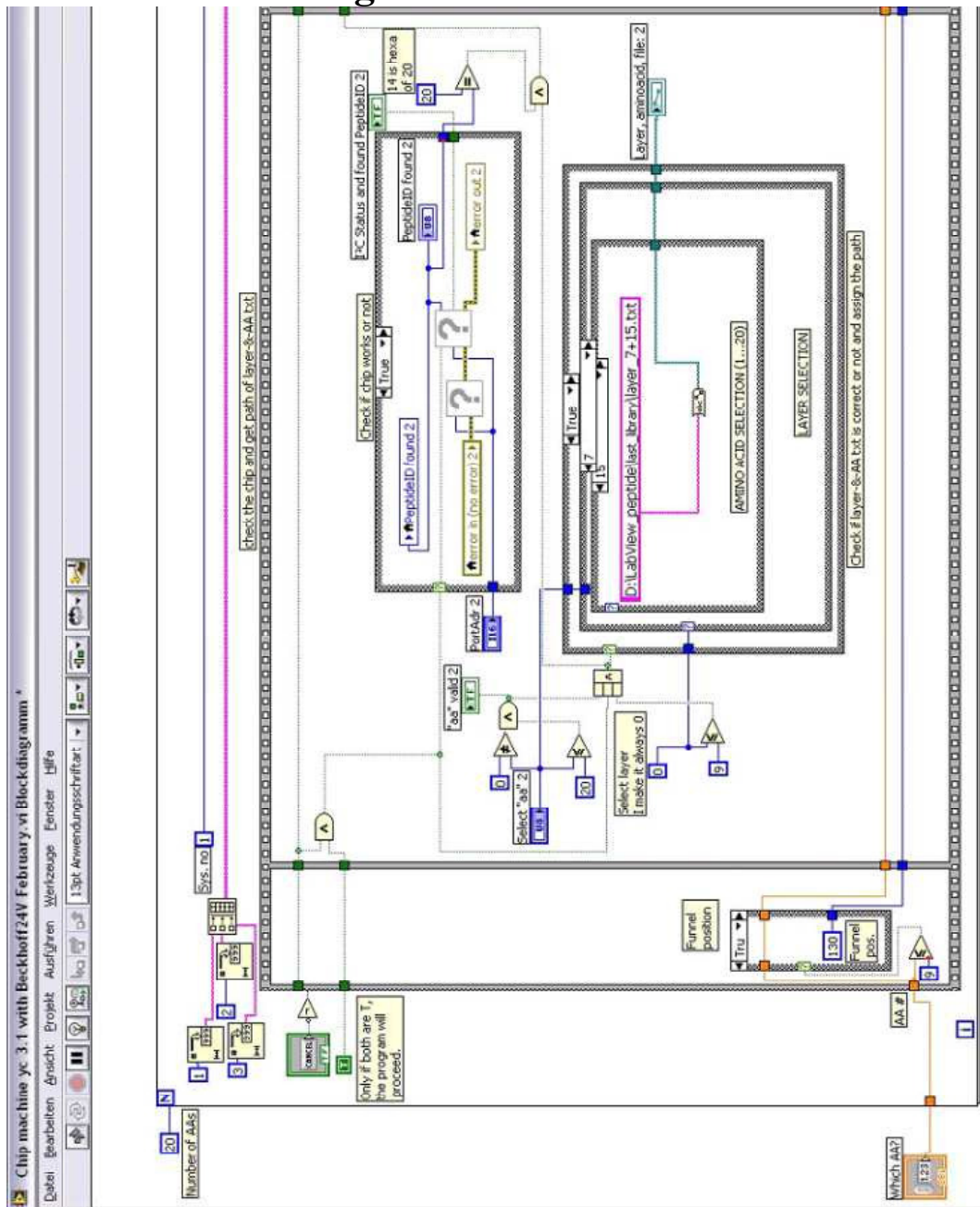


Figure A2.1-1: Main program of chip-printing system. The program is cascade structure so the commands can run one by one. The program shown here loads the printing pattern and activate the CMOS chip.

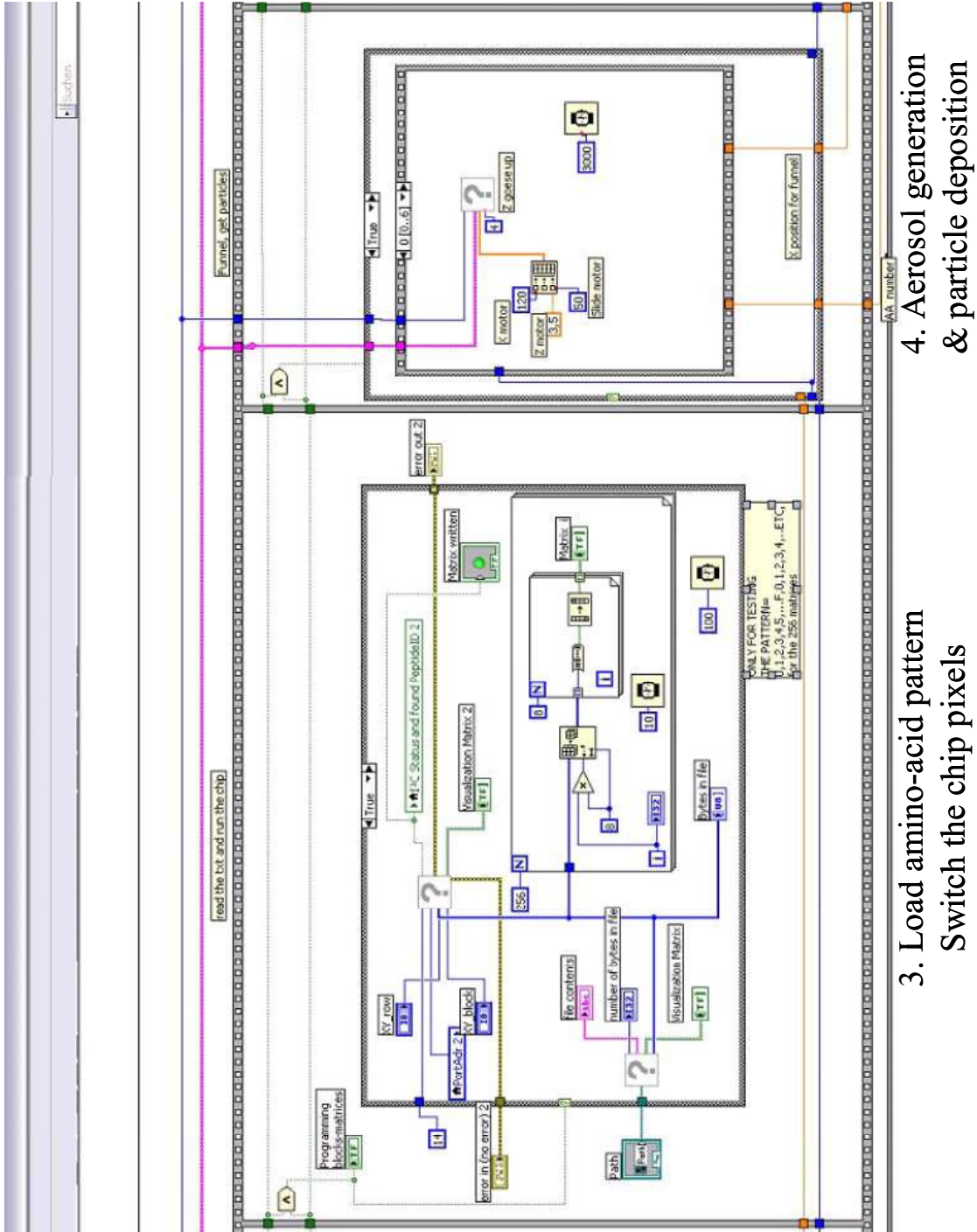


Figure A2.1-2: Main program of chip-printing system. The program is cascade structure so the commands can run one by one. The program shown here actuates the motors and runs the aerosol generation system.

4. Aerosol generation & particle deposition

3. Load amino-acid pattern Switch the chip pixels

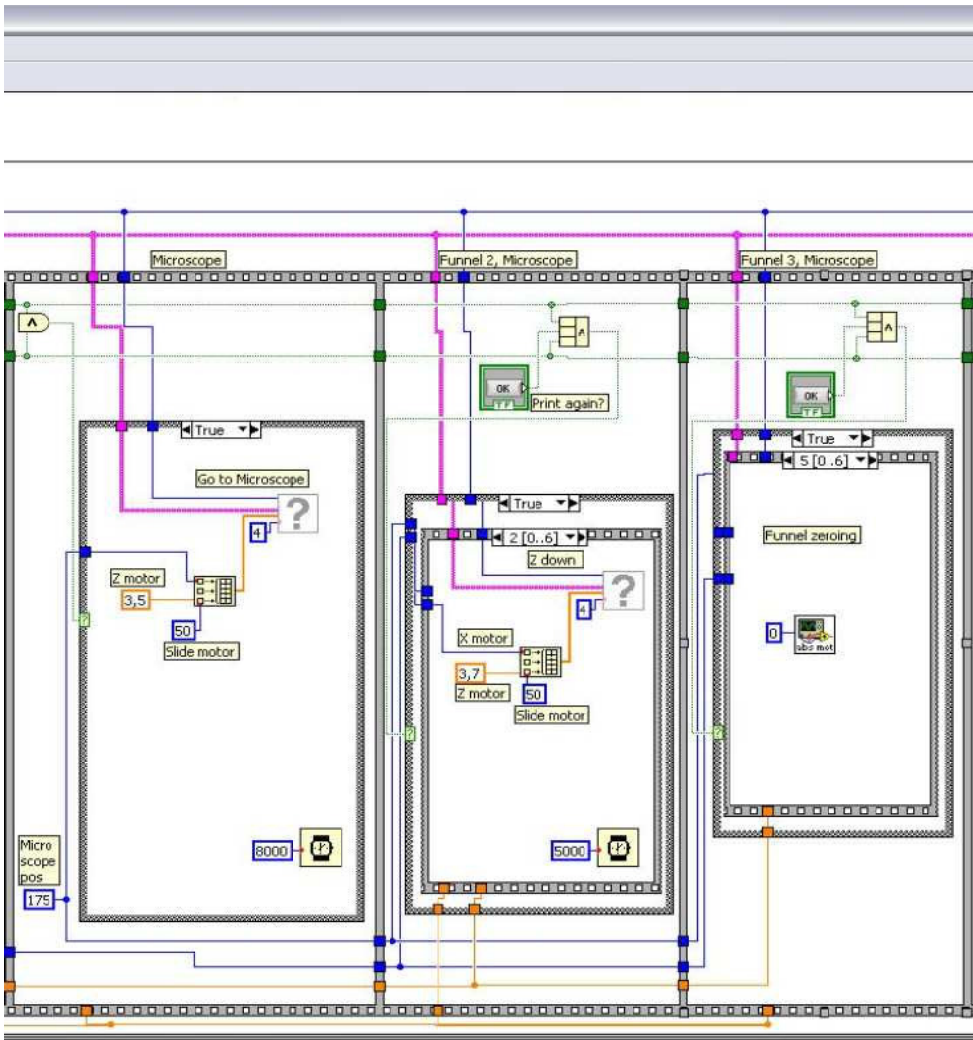
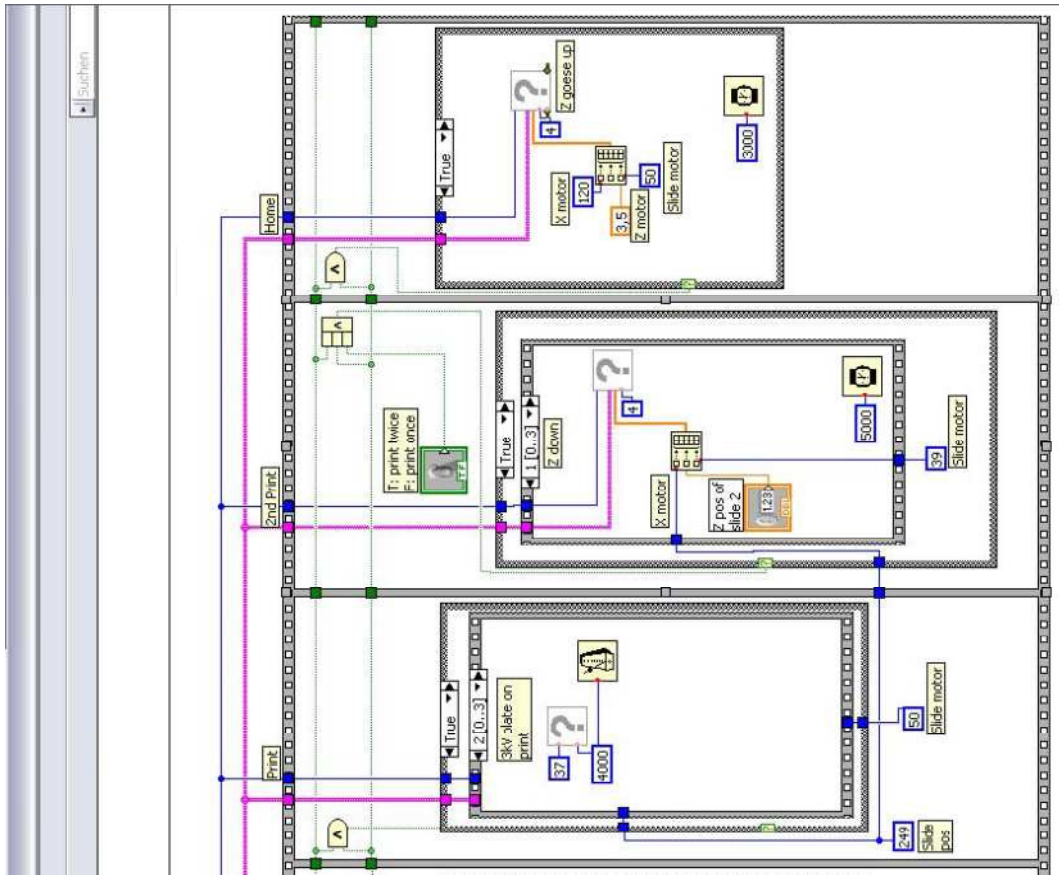


Figure A2.1-4: Main program of chip-printing system. The program shown here moves the CMOS chip to microscope to check particle deposition to see if second or third particle deposition is necessary.

5. Use microscope to check the deposition quality.
6. Deposit particles twice or three times if the deposition is bad.



7. Print the particles onto slide.      8. Go to zero position

Figure A2.1-3: Main program of chip-printing system. The program shown here moves the CMOS chip to the glass slide to print particles onto the slide, and moves the CMOS chip back to the initial position.





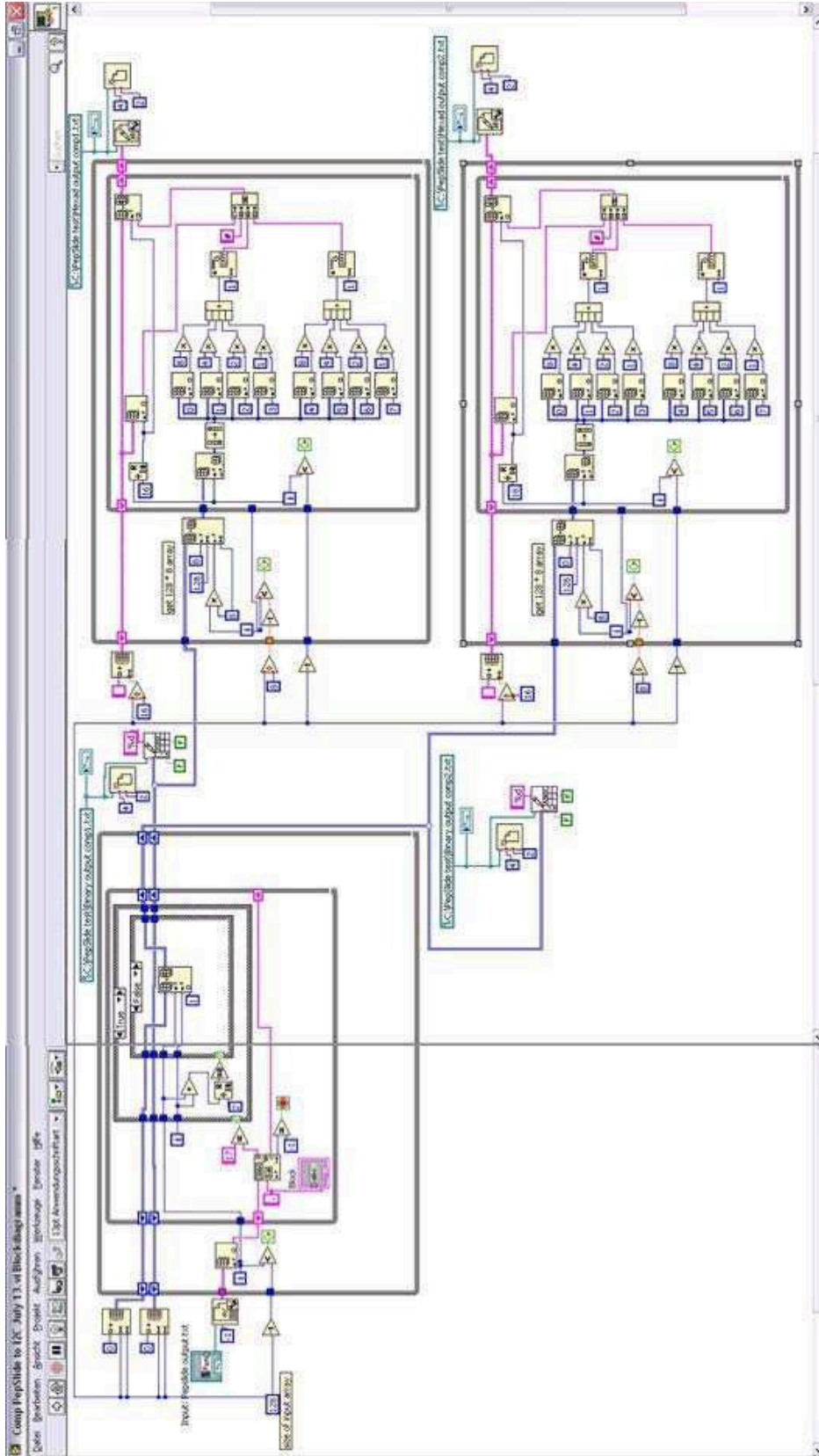


Figure A2.3: Converting program. This program loads .txt file, which describes the particle deposition pattern, and converts data type for CMOS chip program. The algorithm is described in section 3.2.4.

### A3. 3D UniGraphics Drawing of the System

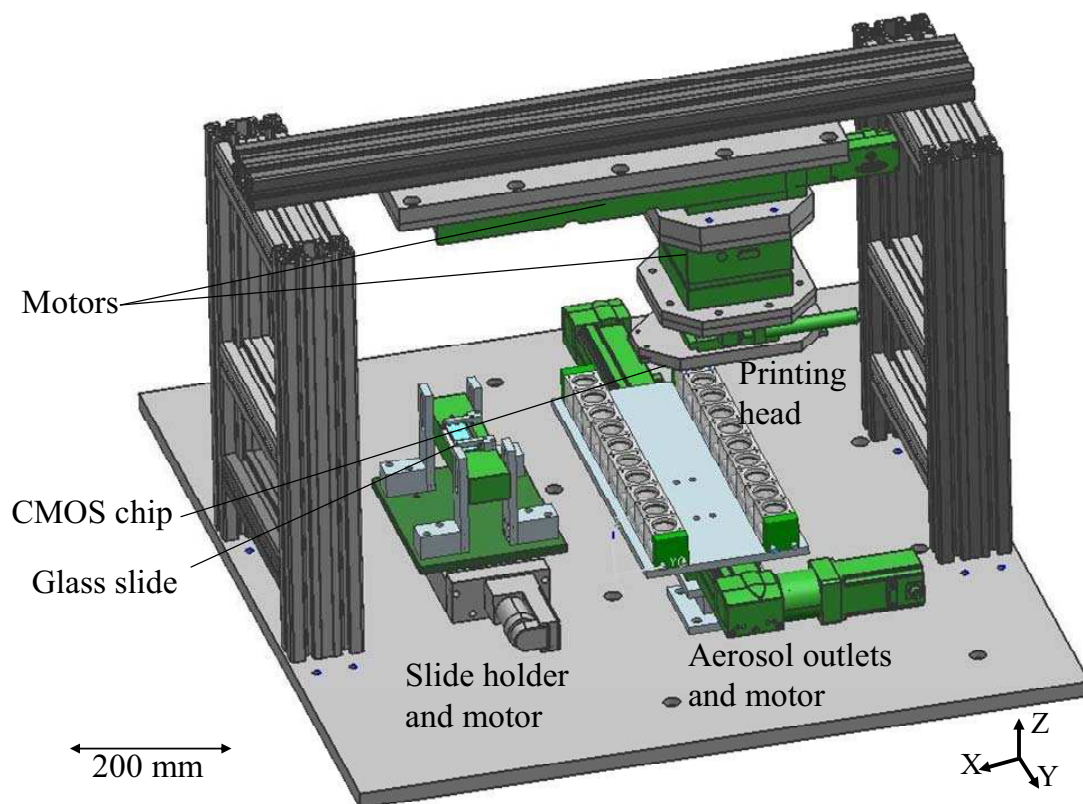


Figure A3.1: Printing system. The CMOS chip is mounted on the printing head, which can be moved in X and Z direction by the motors. The printing head also has two tilt stages to parallelize chip with slide. The aerosol outlets are moved by a motor with long travel range, so the chip can get different amino-acid particles. The glass holder is also mounted on high-precision motor so the chip can print onto different area of the slide.

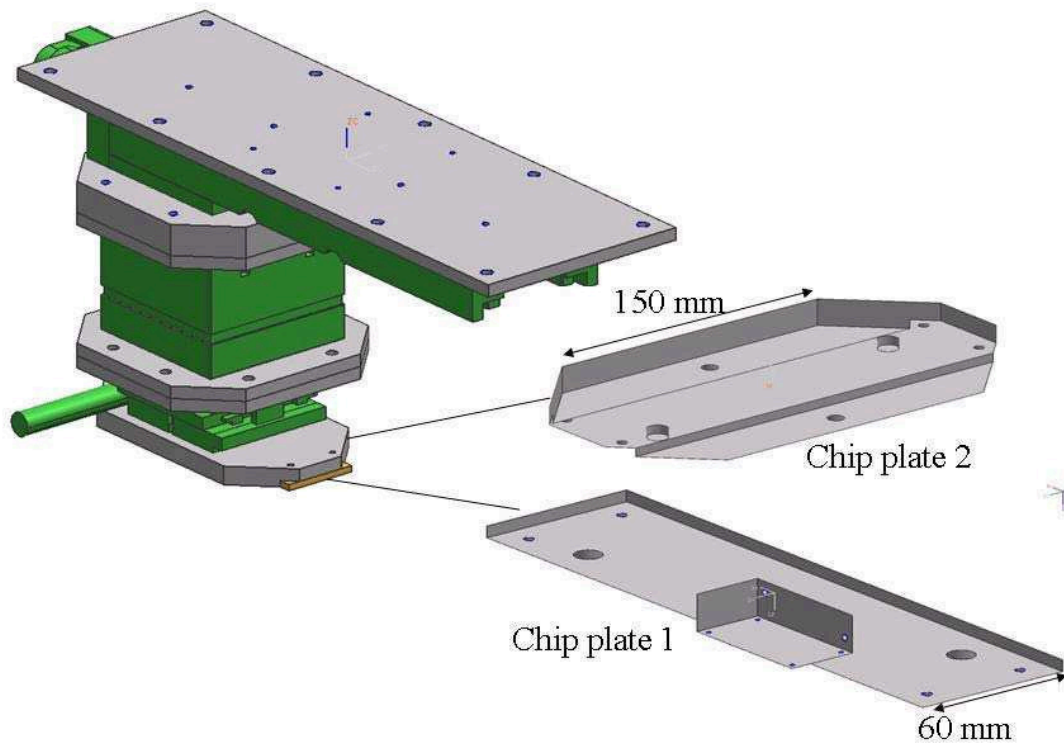


Figure A3.2: Printing head. This printing head includes two high precision motor ( $0.5 \mu\text{m}$ ) and two tilt stages, so the chip can be moved with high precision. The CMOS is fixed on Chip plate 1 with 4 screws, and the Chip plate 1 is mounted on Chip plate 2. Therefore, the Chip plate 1 can be dismantled from the printing head to replace the CMOS chip.

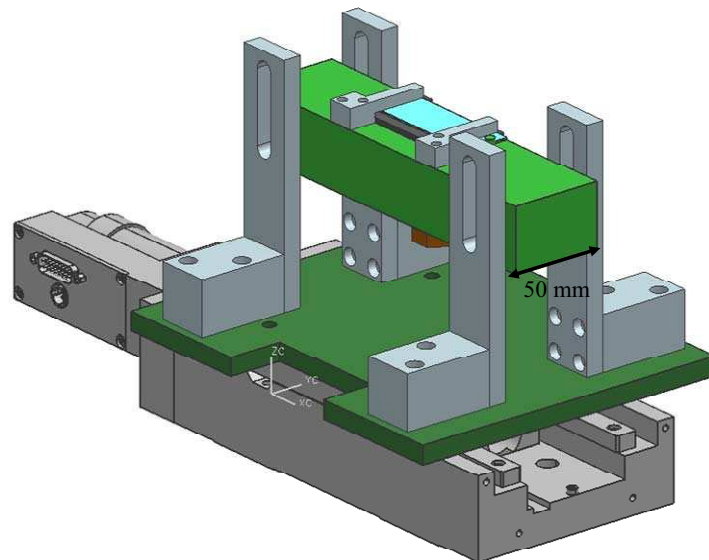


Figure A3.3: The slide holder and the motor. The slide is mounted in the slide holder so slide can be repetitively mounted in the same position. The slide motor is also high precision motor, so the chip can print particles correctly onto the slide.

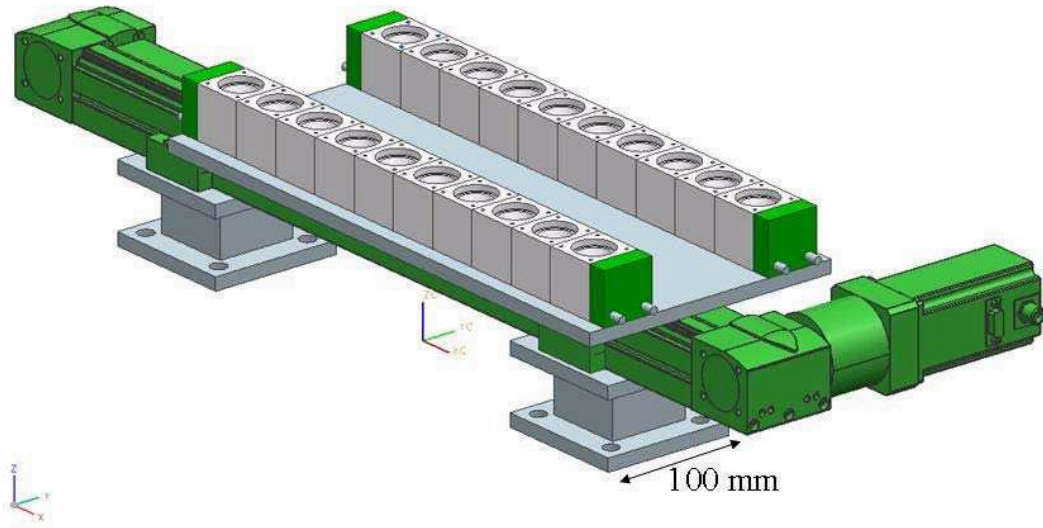


Figure A3.4: Aerosol outlets and motor. Twenty aerosol outlets are arranged into two rows. The travel range of the motor is 400 mm, so the different aerosol outlets can be moved to the CMOS chip.

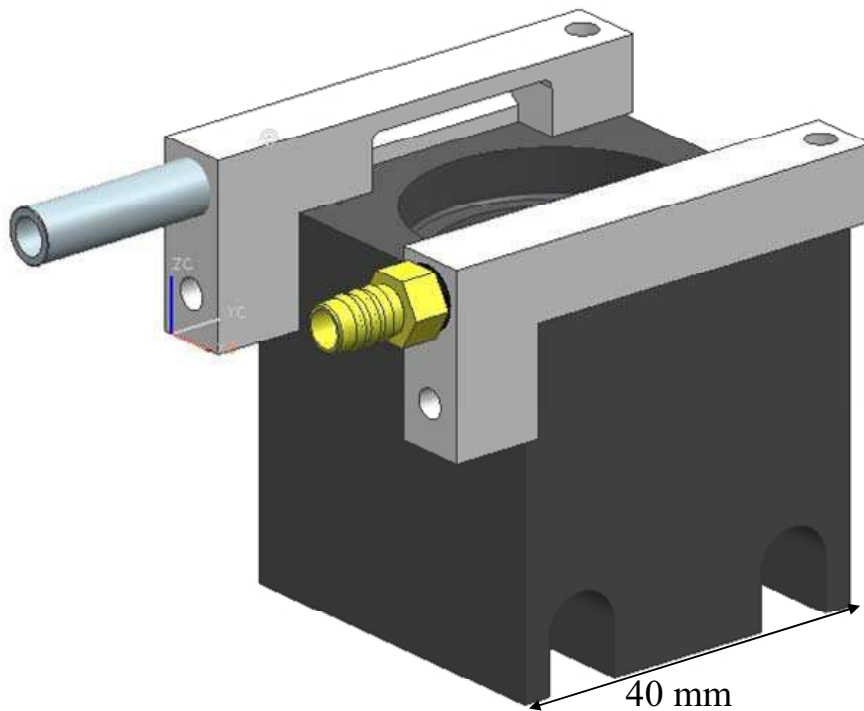
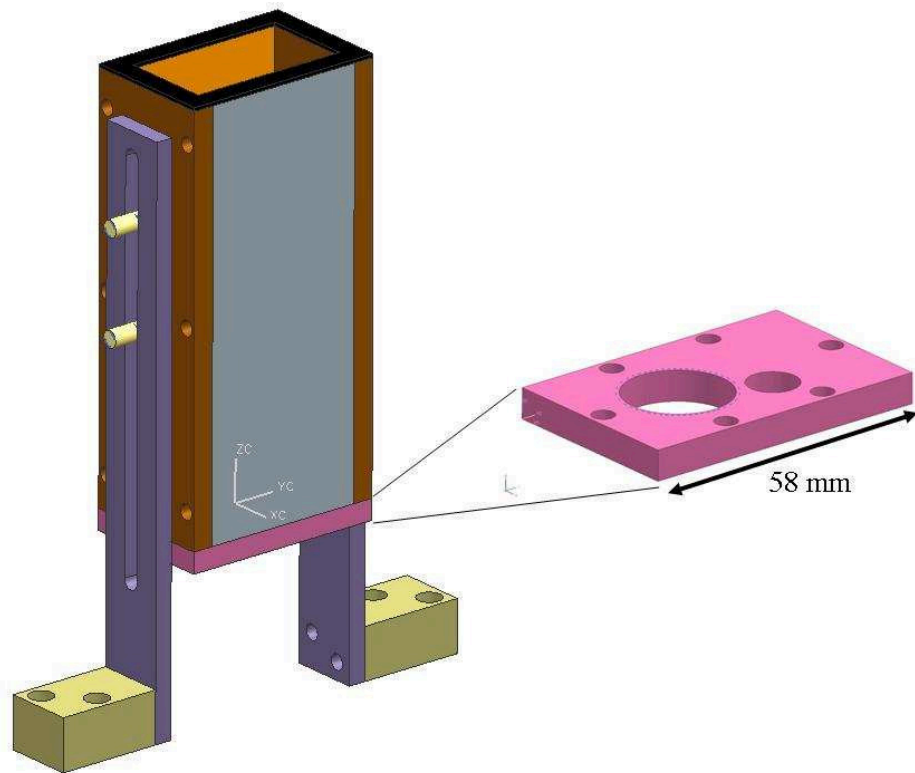
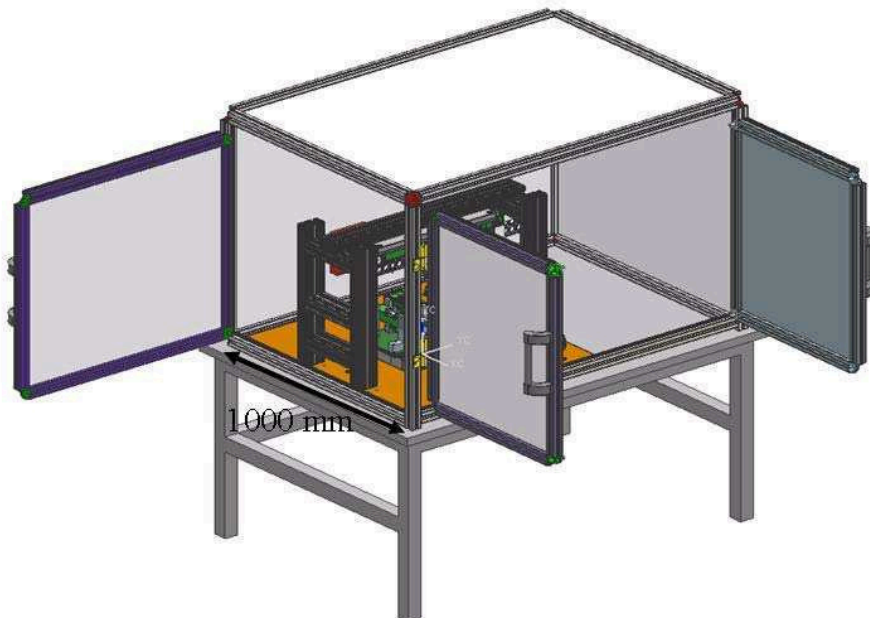


Figure A3.5: The aerosol outlet. Two suction cups are mounted on the aerosol outlet. After particle deposition, the unused aerosol is sucked by the suction cups and goes through a recycling filter to recycle the unused particles.



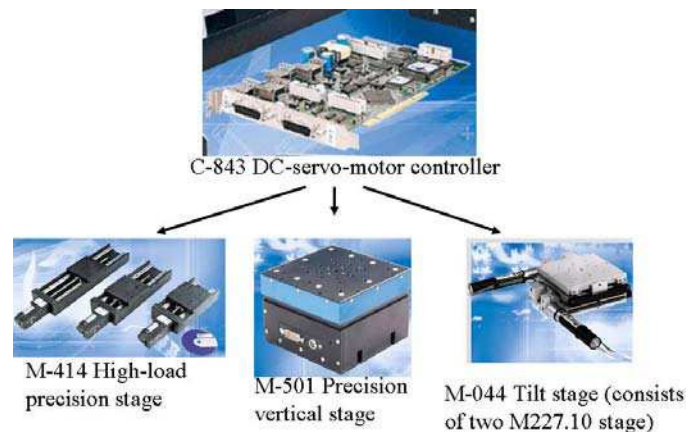
A3.6: Chip cleaner. The bottom has two holes. The small hole is for a nozzle which blows off the particles on chip with compressed air. The big hole is for the tube connecting to a vacuum generator, so the cleaner can suck the blown-off particles.



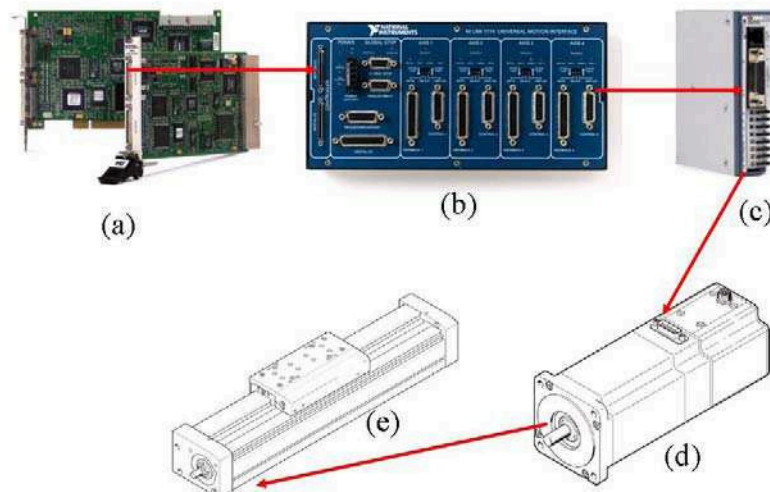
A3.7: Chip-printing system, cover, and table. The cover can be opened from the front and left side for experiments. The printing system is mounted on the left side and the aerosol system will be mounted on the right side of the table.

## A4. Motor Control Interface

To control the system motors with LabVIEW program, PCI (Peripheral Connection Interface) card, motion interface, or stepper drive are used as interfaces between computer program LabVIEW and the motors. The motors from PI (Physik Instrumente) can be simply controlled with PCI cards and PI control library for LabVIEW (A4.1). On the other hand, the Festo motor is mainly for industry application, so some control interfaces from NI (National Instruments) are used to control the Festo motor (A4.2).



A4.1: PI motor control. The PCI card from PI is plugged in the computer slot and then the user can control all the PI motors with LabVIEW or C++ program.



A4.2: Festo motor control. The Festo PCI card (a): NI PCI-7332 Stepper motion controller is plugged in the computer slot and connects to a motion interface (b): NI UNI-7772 Universal motion interface. This motion interface converts the digital commands from the PCI card and send it to the step-motor driver (c): NI P70530 Stepper drive. The driver switches 48 volt to actuate the step motor (d): Festo EMMS-ST-57-S-SE, and the motor moves the axis (e): Festo EGC-70 axis.

## A5. Production of Particles [NES10-2]

1. For the composition of amino acid particles, see section 4.1.
2. The 20 different Fmoc-protected and C-terminally activated amino acid derivatives were from Fluka:  
Fmoc-L-ALanin-OPfp;            Fmoc-L-Cys(Trt)-OPfp;            Fmoc-LAsp(OtBu)-OPfp;  
Fmoc-L-Glu(OtBu)-OPfp;            Fmoc-L-Phe-OPfp;            Fmoc-dl-Gly-OPfp;  
Fmoc-L-His(Trt)-OPfp;            Fmoc-LIle-OPfp;            Fmoc-L-Lys(tBoc)-OPfp;  
Fmoc-L-Leu-OPfp; Fmoc-L-Mest-OPfp;    Fmoc-L-Asn(Trt)-OPfp;    Fmoc-L-Pro-OPfp;  
Fmoc-L-GLn(Trt)-OPfp;            Fmoc-L-Arg(Pbf)-OPfp;            Fmoc-L-Ser(OtBu)-OPfp;  
Fmoc-L-Thr(tBu)-OPfp; Fmoc-LVal-OPfp; Fmoc-L-Trp-OPfp; Fmoc-L-Tyr(tBu)-OPfp.
3. Mix together the constituent parts of amino acid particles and solubilize by stirring in 3–4 weight equivalents of acetone (w/w). The ingredients are: Fmoc-protected OPfp -esters of the 20 different amino acids (10% w/w), either N,Ndiphenylformamide (DPF), diphenyl sulfoxide (DPSO), or dip-tolyl sulfoxide (DTSO) as “solid solvent” (25% w/w), resin (60% w/w, either polystyrene or S-LEC P LT-7552), Pyrazolone orange (4% w/w), and sodium-di(aqua)-di(2-hydroxy- 3-napthoic acido) ferrate(III) (1% w/w; see Note 2).
4. Remove the bulk of acetone for 20 min at 30°C in a distillator.
5. Remove acetone overnight in a freeze dryer.
6. Store the particle mass under nitrogen in a desiccator for months at room temperature (see Note 1).
7. Premill the particle mass with a rotating scissors mill to yield particles with an average diameter of 100–200  $\mu\text{m}$  (see Note 3).
8. Slowly feed in the resulting particles into an air jet mill. During milling, silica nanoparticles (0.05% w/w) are added (see Note 4).
9. This procedure results in particles with average diameters from 4 to 10  $\mu\text{m}$  (check with microscope).
10. For a narrow size distribution and thus uniform physical properties, remove particles beyond 32  $\mu\text{m}$  with analytical sieves (see Note 5).
11. Remove particles with a diameter  $<1 \mu\text{m}$  with a winower (see Note 5).
12. Analyze individual particle batches for narrow size distribution with a mastersizer. Starting with 100 g particle mass, a typical manufacturing run should yield 70 g amino acid particles in the size range between 4 and 20  $\mu\text{m}$ .
13. Analyze particle batches for their triboelectric charge by a Q/m meter. A typical result would yield an electric charge of approx.  $-4 \mu\text{C/g}$  of particles (Fig. 5; see Note 5).
14. Analyze particle batches for their melting behavior by dynamic difference calorimetry. The melting point should be between 70 and 75°C.



## A6. Synthesis and Staining Steps of Biotin and Amino-acid

Get slide and particle	Clean the slide with NaOH and then coat with PEGMA/MMA or APTES.
Mark on Slide	
1 <sup>st</sup> layer	
Print Gly particles on slide twice	Clean the chip afterward.
Print Ala particles on slide twice	
Melt and couple Ala and Gly	Coupling protocol (see section 5.2.3)
Capping (block residue)	Block residue protocol (see section 5.2.3)
Wash	Wash protocol
Deprotection	Deprotect / remove Fmoc protocol (see section 5.2.3)
2nd layer	
Print Gly twice	
Melt and couple Gly	Coupling protocol
Print Biotin once	
Melt and couple Biotin	Coupling protocol
Capping (block residue)	Block residue protocol:
Wash	Wash protocol (see section 5.2.3)
Deprotection	Deprotect / remove Fmoc protocol (see section 5.2.3)
Biotin and HA	
HA coupling on to Gly	(HA) activation with HOBt/HBTU
Deprotect the Fmoc on HA	Deprotect / remove Fmoc protocol
Deprotect the side groups of HA	After peptide synthesis, deprotect the side groups STP, HA antibody, biotin Gly, Ala has no side chain.
Block the surface with BSA	BSA blocking protocol (see section 5.2.3)
Staining with HA antibody and Streptavidin	Staining with fluorescence-labeled molecules.
Scanning	Odyssey scanner Resolution: 21 $\mu\text{m}$ , Scan wavelength 700~800 $\mu\text{m}$ DKFZ scanner: GenePix Resolution 5 $\mu\text{m}$ Cy3 (546 $\mu\text{m}$ ) Cy5 (647 $\mu\text{m}$ )

# Curriculum Vitae

Date of Birth: 1982.4.11

Nationality: Taiwan

E-mail: [yccheng@gmail.com](mailto:yccheng@gmail.com)

- 2008-2012 Mechanical Eng. Ph.D., German Cancer Research Center (Peptide library) / Darmstadt University of Technology  
Advisor: PD Dr. Alexander Nesterov and Prof. Edgar Dörsam  
Dissertation: “CMOS-chip based printing system for combinatorial synthesis”.
- 2007-2008 Emergency Medical Technician, Fire Department of Taipei, Obligatory Military Service
- 2006-2007 Research Assistant, Department of Physics, National Taiwan University
- 2004-2006 M. Sc. in Electrical Engineering, National Taiwan University, Taiwan  
Thesis: “The application of coded excitation on ultrasonic pulse inversion fundamental imaging”.
- 2000-2004 B. Sc. in Electrical Engineering, National Taiwan University, Taiwan
- 1997-2000 Kaohsiung Municipal Kaohsiung Senior High School, Taiwan
- 1994-1997 Kaohsiung Municipal WuFu Junior High School, Taiwan
- 1988-1994 Municipal KuangHua Primary School, Kaohsiung City, Taiwan

Heidelberg, August 2012